University Hospital Ulm, Institute of Experimental Cancer Research

Director: Prof. Dr. Christian Buske

Dissecting the Role of Lymphoid Enhancer Factor 1 (LEF1) in Acute Myeloid Leukemia

Dissertation submitted in partial fulfillment of the requirements for the degree of "Doctor rerum naturalium" (Dr. rer. nat.) of the International Graduate School in Molecular Medicine Ulm

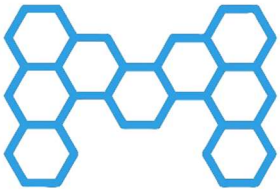

International Graduate School
in Molecular Medicine Ulm

Kristin Feder,

Heilbronn

2019

CEMMA
cellular and molecular mechanisms in aging

Dean:	Prof. Dr. Thomas Wirth
Chairman IGradU:	Prof. Dr. Michael Kühl
First supervisor:	Prof. Dr. Christian Buske
Second supervisor:	Prof. Dr. Lars Bullinger
Third supervisor:	PD Dr. Michael Fiegl
External reviewer:	PD Dr. Irmela Jeremias
Day doctorate awarded:	05.08.2019

Results gained in my thesis have been published in the following publication:

Kristin Feder, Katrin Edmaier-Schröger, Vijay Rawat, Nicole Kirsten, Klaus Metzeler, Johann Kraus, Konstanze Döhner, Hartmut Döhner, Hans Kestler, Michaela Feuring-Buske, and Christian Buske, *Differences in expression and function of LEF1 isoforms in normal versus leukemic hematopoiesis*, Leukemia, accepted for publication on 06.08.2019.

Table of Contents

Abbreviations

5-FU	5-Fluorouracil
7-AAD	7-Aminoactinomycin
AD	Activation Domain
ALL	Acute Lymphoid Leukemia
AML	Acute Myeloid Leukemia
AP-1	Activator Protein 1
APC	Adenomatous Polyposis Coli
Bl6	mouse strain C57Bl/6J x C3H/HeJ
BLBD	β-catenin/LEF-1 binding domain
BM	Bone Marrow
BMP2	Bone Morphogenetic Protein 2
BMT	Bone Marrow Transplantation
BSAP	B-cell Specific Activator Protein
βTRCP	β-transducing repeat-containing protein
Ca	Calcium
CAD	Context-dependent Activation Domain
CamKII	Calcium/calmodulin-dependent protein Kinase II
CBF	Core Binding Factor
CCND1	Cyclin D1
CD	Cluster of Differentiation
cDNA	copy DNA
CEBPα	CCAAT/enhancer-binding protein alpha
CFC	Colony-Forming Cell

CFU-S	Colony-Forming Unit Spleen
CK1	Casein Kinase-1
CLL	Chronic Lymphoid Leukemia
CLP	Common Lymphoid Progenitor
CML	Chronic Myeloid Leukemia
CMP	Common Myeloid Progenitor
CN	Cytogenetically Normal
CO_2	Carbon Dioxide
CRU	Competitive Repopulation Unit
Ct	Cycle Threshold
CTBP	C-terminal binding protein
ddH2O	distilled and demineralized water
DKK1	Dickkopf 1
DMEM	Dulbecco's Modified Eagle Medium
DMSO	Dimethyl Sulfoxide
DNA	Deoxyribonucleic Acid
DNase	Deoxyribonuclease
ΔNLEF1	N-terminally deleted Lymphoid Enhancer Factor 1
dNTPs	Deoxynucleotides
DPBS	Dulbecco's Phosphate Buffered Saline
DPT	$CD4^+CD8^+$ Double Positive Thymocytes
DSMZ	Deutsche Sammlung von Mikroorganismen und Zellkulturen
DVL	Dishevelled
e.g.	"exempli gratia" (it.) - for example
EDTA	Ethylenediaminetetraacetic Acid

ETO	Eight Twenty-One
Ets1	v-ets erythroblastosis virus E26 oncogene homolog 1
FAB	French-American-British
FACS	Fluorescence Activated Cell Sorting
FBS	Fetal Bovine Serum
FDA	Food and Drug Administration
FLT3	Fms Like Tyrosine Kinase 3
FSC	Forward Scatter
Fzd	Frizzled
g	Relative Centrifugal Force
G-CSF	Granulocyte Colony-Stimulating Factor
GFP	Green Fluorescent Protein
GM-CSF	Granulocyte-Macrophage Colony-Stimulating Factor
GMP	Granulocyte Macrophage Progenitor
GRG/TLE	Groucho/Transducin-like enhancer protein
GSK3β	Glycogen Synthase Kinase-3 β
Gy	Gray (radiation unit)
HCSL1	Hematopoietic Cell-Specific Lyn substrate 1
HDAC	Histone Deacetylase
HEPES	4-(2-HydroxyEthyl)-1-PiperazineEthaneSulfonic acid
HHR	Hydrophobic Heptad Repeat
HSC	Hematopoietic Stem Cell
i.p.	intraperitoneally
i.v.	intravenously
IC50	Half-maximal Inhibitory Concentration

ICAT	Inhibitor of β-Catenin and Tcf-4
IL-3/6	Interleukin-3/6
IMDM	Iscove's Modified Dulbecco's Medium
Inv(16)	Inversion of chromosome 16
IP	Immunoprecipitation
IP3	Inositol triphosphate
JNK1	c-Jun N-terminal Kinase 1
KD	Knockdown
LEF1/Lef1	Lymphoid Enhancer Factor 1
LEF1WT	long isoform of LEF1
LGS	Legless
LMPP	Lymphoid-primed Multipotent Progenitor
LN	Liquid Nitrogen
LP	Leukemic Progenitor
LRP5/6	Lipoprotein Related Protein 5/6
LSC	Leukemic Stem Cell
LT	Long-term
MACS	Magnetic Activated Cell Sorting
MAPK	Ras/Raf/Mitogen-Activated Protein Kinase
mDC	myeloid Dendritic Cells
MEP	Megakaryocyte-Erythroid Progenitor
MgCl2	Magnesium Chloride
MPO	Myeloperoxidase
mRNA	Messenger RNA
mSin3	SIN3 transcription regulator

MTGR1	Myeloid Translocation Gene-Related protein 1
MYND-ZF	Myeloid, Nervy, and DEAF-1 zinc finger domain
n.a.	not available
n.d.	not detectable
NF-AT	Nuclear Factor Associated with T cells
NF-κB	Nuclear Factor kappa-light-chain-enhancer of activated B cells
NHR	Nervy Homology Region
NLK	Nemo-Like Kinase
NLS	Nuclear Localization Signal
NMT	Nuclear Matrix Targeting Signal
NPM1	Nucleophosmin 1
NSG	mouse strain NOD.Cg-Prkdc<scid>Il2rg<tm1Wjl>/SzJ
o/n	overnight
p	short arm of a chromosome
PAX5	Paired Box 5
PCP	Planar Cell Polarity
pDC	plasmacytoid Dendritic Cell
Pep	mouse strain C57Bl/6Ly-Pep3b x C3H/HeJ
PKC	Protein Kinase C
PLC	Phospholipase C
PP2A	Protein Phosphatase 2A
PS	Penicillin/Streptomycin
PYGO	Pygopus
q	long arm of a chromosome
qRT-PCR	quantitative Real Time Polymerase Chain Reaction

RBC	Red Blood Cell
RHD	Runt Homology Domain
RNA	Ribonucleic Acid
RNase	Ribonuclease
ROCK	RHO-associated Coiled-coil-containing protein Kinase 1
rpm	Revolutions per Minute
RPMI	Roswell Park Memorial Institute
RT	Room Temperature
RUNX1	Runt-related transcription factor 1 (=AML1)
RUNX1T1	RUNX1 Translocation Partner 1 (=ETO)
SCF	Stem Cell Factor
SDS-PAGE	Sodium Dodecyl Sulfate Polyacryl Gel Electrophoresis
sFRP	selected Frizzled Protein
shRNA	short hairpin RNA
SMRT	Silencing Mediator of Retinoic acid and Thyroid hormone
SSC	Sideward Scatter
ST	Short-term
t(15;17)	Translocation of chromosomes 8 and 21, leading to the PML-RARA fusion gene
t(8;21)	Translocation of chromosomes 8 and 21, leading to the AML1-ETO fusion gene
TAF110	TATA-box-Associated Factor 110
TAK1	TGFβ-Activated Kinase 1
TAT	Transactivator of Transcription
TBP	TATA Binding Protein

TCF1	Transcription Factor 1
TCGA	The Cancer Genome Atlas
TEMED	Tetramethylethylenediamine
UTR	Untranslated Region
VCM	Virus Containing Medium
VWRPY	recognition motif for the Groucho/TLE family
WB	Western Blot
WBC	White Blood Cell
WHO	World Health Organization
WRE	Wnt Responsive Elements
YFP	Yellow Fluorescent Protein
ZF	Zinc Finger domain

1. Introduction

1.1. Hematopoiesis

Hematopoiesis describes the complex processes of generation, differentiation and maturation, leading to different functional blood cells. These cells circulate through our blood and fulfill different tasks ranging from roles in the immune system to response to injuries. Not only the blood cells are essential for a proper functioning organism, but also the blood plasma, which belongs to the circulatory system. Through the blood, not only the blood cells are transported to their destination, but also vitamins, hormones, glucose and minerals. In general, about 36-50% of the blood consists of blood cells. The major amount of these cells are erythrocytes, which are responsible for oxygen transport from the lung to the different organs. A small portion of cells are white blood cells, which are crucial for the immune system and thrombocytes, which are involved in wound healing.

The formation of all blood cells occurs in a hierarchical system. All blood cells originate from hematopoietic stem cells (HSC), which reside in the bone marrow (BM). HSCs are rare but able to self-renew and to differentiate into all lineages step by step, leading to the generation of approximately 10^{12} new blood cells per day [79]. HSCs can be further subdivided into long-term (LT) HSCs and short-term (ST) HSCs. LT-HSCs are able to self-renew for the whole lifetime of the organism, have the ability to avoid telomere shortening effectively [1, 107] and give rise to ST-HSCs. ST-HSCs, which have limited self-renewal capacity, further can give rise to multipotent progenitor cells (MPP), which are briefly self-renewing [76]. MPPs can differentiate in lymphoid-primed multipotent progenitors (LMPP), common myeloid (CMP) or common lymphoid progenitors (CLP) (s. Figure 1).

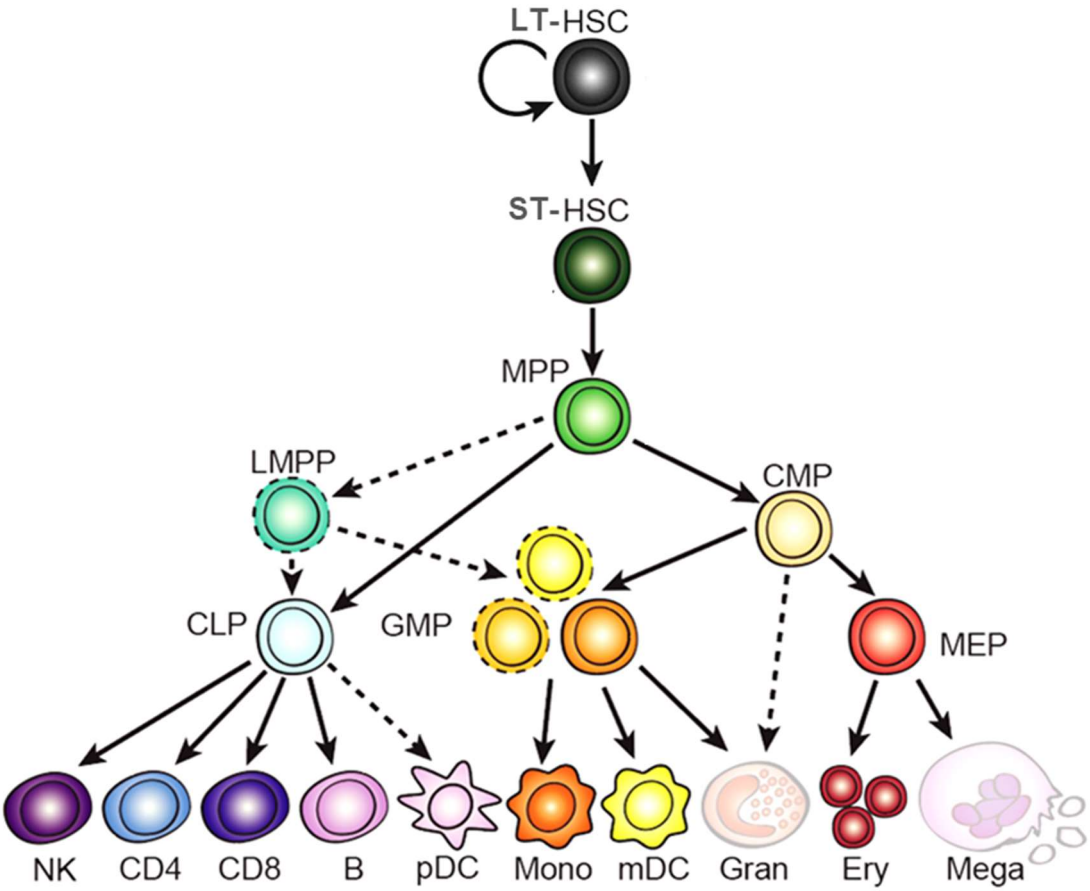

Figure 1: The hematopoietic hierarchy (adapted from [60], software and associated documentation files distributed under the MIT Licence, Copyright (c) 2017 Caleb Lareau). LT-HSC: long-term hematopoietic stem cell; ST-HSC: short-term hematopoietic stem cell; MPP: multipotent progenitor cell; LMPP: lymphoid-primed multipotent progenitor; CMP: common myeloid progenitor; CLP: common lymphoid progenitor; GMP: granulocyte-monocyte progenitor; MEP: megakaryocyte-erythroid progenitor; NK: natural killer cell; CD4/CD8: T cell with CD4 or CD8 surface marker, B: B cell; pDC: plasmacytoid dendritic cell; Mono: monocyte; mDC: myeloid dendritic cell; Gran: granulocyte, Ery: erythrocyte; Mega: megakaryocyte.

LMPPs further differentiate into CLPs, which give rise to natural killer (NK) cells, T-lymphocytes with CD4 or CD8 surface markers, B-lymphocytes and dendritic cells. LMPPs and CMPs can differentiate into granulocyte-monocyte progenitors (GMP), which give rise to monocytes, dendritic cells and granulocytes. CMPs are able to differentiate into megakaryocyte-erythroid progenitors (MEPs), which further differentiate into erythrocytes and megakaryocytes.

The different mature blood cells can be distinguished not only from the progenitor cells they originate from, but also according to their function. The most well-known function of blood may be the transport of oxygen and carbon dioxide through erythrocytes. This process is dependent on hemoglobin, which is present in all

erythrocytes and has a high affinity to oxygen [58]. Erythrocytes, compared to most other blood cells, do not contain a nucleus and are not independently motile in the blood. White blood cells on the other hand have these properties. The big group of white blood cells consists of granulocytes, monocytes and lymphocytes, which all take part in immune response. In general, granulocytes are guided to sites of tissue damage and infection by chemotaxis, where they can perform phagocytosis of e.g. bacteria and parasites. Monocytes are phagocytic towards infectious agents and larger particles, but cannot act against bacteria as granulocytes. The main focus of B and T lymphocytes is the defense against foreign proteins, antigens and whole cells [32].

Taken together, hematopoiesis is a very complex process which needs to be tightly regulated in order to function properly and respond in cases of disease, injury and daily turnover. Major signaling pathways regulating hematopoiesis are the canonical and non-canonical Wnt signaling. These pathways are required for embryonic and normal hematopoietic stem cell self-renewal and differentiation and lymphopoiesis. A dysregulation of Wnt will perturb the normal hematopoiesis and is often found in leukemia.

1.2. Acute Myeloid Leukemia

There are many diseases known to originate from a malfunctioning hematopoietic system, with leukemia being among the most well-known ones. Among the most prominent types of blood cancer are myeloma, lymphoma and leukemia. Leukemia is further subdivided into four different forms, dependent on which part of the hematopoiesis is perturbed –the myeloid or the lymphoid- and whether it is an acute or a chronic form. Here, the focus is on acute myeloid leukemia (AML), which is the most common myeloid leukemia and mostly occurs with advanced age; more than 50% of the diseased patients is older than 70 years at the time of diagnosis [54]. Symptoms usually are anemia, fever and infections due to declined immune system, and bleeding due to thrombocytopenia.

Formerly, AMLs were classified according to the French-American-British (FAB) classification, which is performed according to the characteristics and amount of blast cells found in the bone marrow. According to the maturation grade of blasts,

patients are grouped in the subtypes M0 to M7 [14]. This system does not classify patients with regard to genetic factors affecting the prognosis. The more recent AML classification including molecular characteristics is the World Health Organization (WHO) classification. Now, patients can be further classified e.g. according to genetic abnormalities, AML with myelodysplasia-related changes, disease with relation to previous radiation and chemotherapy, as well as AMLs, which are not otherwise specified. This more detailed classification allows the assigning of patients to favorable and unfavorable outcomes (s. Table 1).

Table 1: WHO classification of AML, prognosis and corresponding FAB classification [2, 20, 106].

WHO classification	**Prognosis**	**FAB classification**
AML with recurrent genetic abnormalities		
t(8;21), *AML1-ETO* fusion gene	favorable	M2
inv(16) or t(16;16)	favorable	M4eo
t(15;17), *PML-RARα* and variants	favorable	M3
MLL abnormalities	unfavorable	
t(9;11)		
t(6;9)	unfavorable	
inv(3) or t(3;3)	unfavorable	
t(1;22)		
t(9;22), *BCR-ABL*	unfavorable	
NPM1 mutation	favorable	
NPM1 mutation and *FLT3-ITD*		
CEBPα mutation	favorable	
-5 or del(5q)		
-7		
abn(17p)		
AML with multilineage dysplasia		
following MDS or MDS/MPD		
without antecedent MDS or MPD, with dysplasia at least		
50% of cells in two or more myeloid lineages		
AML and MDS, therapy related		

alkylating agents/radiation-related		
topoisomerase 2 inhibitor-related		
others		
AML, not otherwise categorized		
minimally differentiated		M1
without maturation		M0
with maturation		
acute myelomonocytic leukemia		M4
acute monoblastic/monocytic leukemia		M5
acute erythroid leukemia		M6
acute megakaryoblastic leukemia		M7
acute basophilic leukemia		
acute panmyelosis with myelofibrosis		
myeloid sarcoma		

Usually patients with translocation between chromosomes 8 and 21 (t(8;21)), inversion of chromosome 16 (inv(16)) and translocation of chromosomes 15 and 17 (t(15;17)) belong to the group of favorable genetic abnormalities with better treatment outcome. Amongst these genetic changes, t(8;21) is the most common translocation in AML, leading to the Acute Myeloid Leukemia 1 – Eight Twenty-One (AML1-ETO) fusion gene in the patients. Amongst genetic changes characterized as unfavorable, there are deletions in chromosomes 5 or 7, translocation or inversion of chromosome 3 and translocations between chromosomes 6 and 9 [106].

Not all AML blasts are in a proliferative state and only a subset of AML cells are clonogenic, indicating the presence of a hierarchical structure similar to normal hematopoiesis. On the top of this malignant hematopoiesis the leukemic stem cells (LSC) are located, which are able to self-renew and differentiate to a certain extent [13, 44] (s. Figure 2).

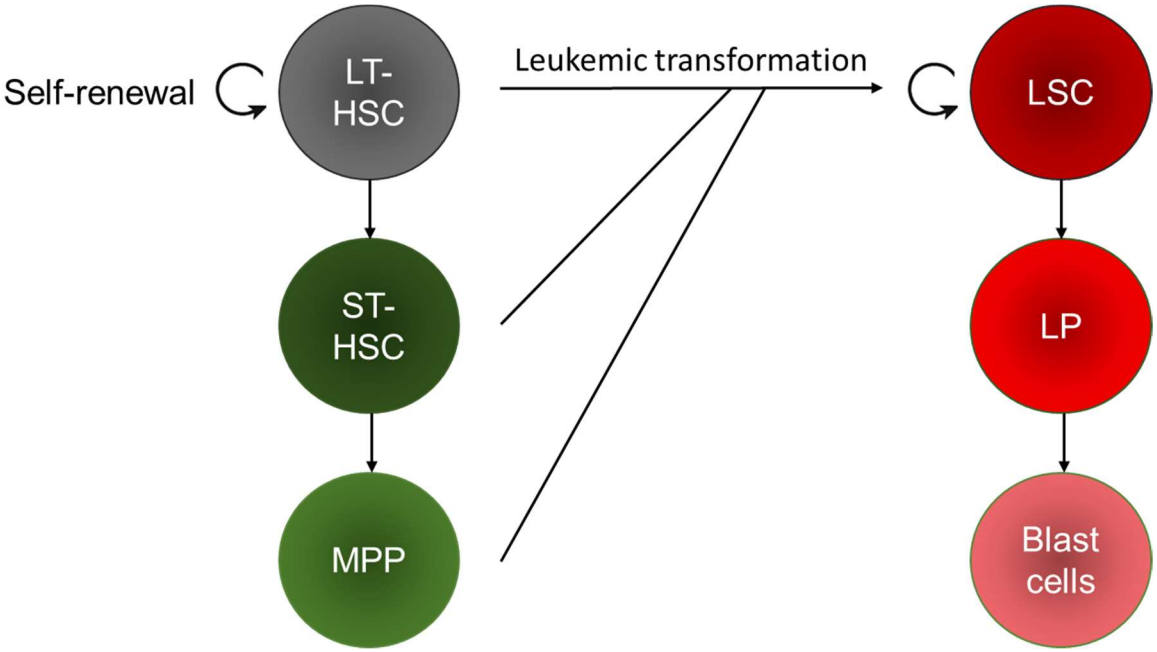

Figure 2: Leukemic transformation of long-term (LT), short-term (ST) hematopoietic stem cells (HSCs) or multipotent myeloid progenitors (MPPs) lead to the formation of a leukemic stem cell (LSC). LSCs are able to self-renew and differentiate into leukemic progenitors (LP) and further into blast cells.

They reside within the same location as healthy HSCs, are able to self-renew as healthy HSCs and differentiate into blast cells. Since treatment of this LSC population is difficult, but crucial for long-term treatment success, is it important to find ways to target this population specifically. Usually a relapse after chemotherapy is due to a fraction of LSCs, that was not sufficiently targeted. Thus, the development of novel treatment concepts targeting LSCs requires characterization of druggable differences between normal HSCs and LSCs.

Deregulated signaling pathways are possible targets for treatment strategies as e.g. treatment of AML with fms like tyrosine kinase 3 (FLT3) mutation through application of Midostaurin [94, 95], which was recently approved by the Food and Drug Administration (FDA). Another pathway, which is deregulated in AML and other cancers is Wnt signaling. So far, there are no treatments approved specifically targeting this pathway, but deregulation of this pathway or associated factors can generate an Achilles heel in AML, which is discussed in this thesis.

1.3. AML1-ETO positive AML

As already mentioned, the most frequent fusion gene occurring in AML is *AML1-ETO*, which arises from the translocation of chromosome 8, harboring the *ETO* gene and chromosome 21, harboring the *AML1* gene (s. Figure 3).

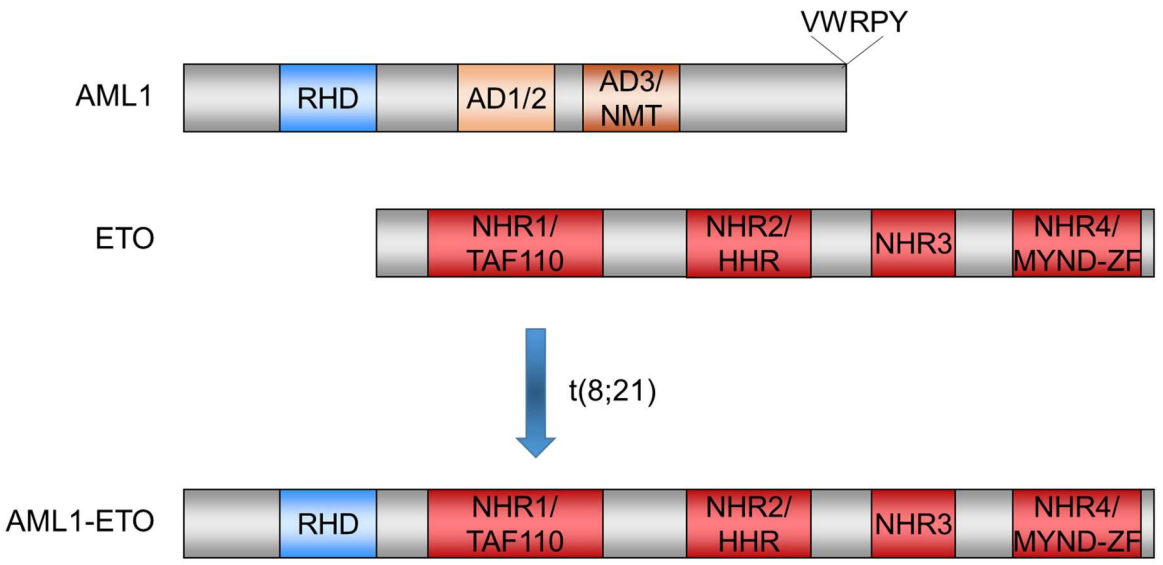

Figure 3: The fusion gene *AML1-ETO* arising from translocation (8;21) of *AML1* and *ETO*. RHD: runt homology domain, AD: activation domain, NMT: nuclear matrix targeting signal, VWRPY: recognition motif for the Groucho/TLE family, TAF110: TATA-box-associated factor 110, NHR: Nervy homology region, HHR: hydrophobic heptad repeats, MYND-ZF: myeloid, Nervy, and DEAF-1 zinc finger domain.

The *AML1* gene, also known as *RUNX1*, contains 12 exons, encodes the α subunit of the core binding factor (CBF) and forms the active transcriptional heterodimer together with its β subunit [49]. CBFβ is homologous to the Big Brother and Brother proteins in *Drosophila Melanogaster* and increases the DNA binding ability of AML1 [35], but has not been shown so far to bind to DNA or cofactors on its own. AML1 is a transcription factor which contains a runt homology domain (RHD) [70] for DNA binding and a nuclear localization signal [64] at the N terminus, whereas the C-terminal domain of AML1 is responsible for its action as transcriptional regulator [71]. Here, three activation domains are located, which can be phosphorylated through mitogen activated protein kinase (MAPK) signaling [100]. Through the VWRPY motif on the C-terminus the Groucho/TLE family of transcriptional co-repressors are able to recognize AML1 [5] and repress AML1 induced transactivation [47]. In general, AML1 is in need of cofactors to effectively induce transcription activation. Often, the formation of ternary DNA-protein-complexes is

necessary, e.g. via recruitment and binding of v-ets erythroblastosis virus E26 oncogene homolog 1 (Ets1) [33]. The formation of this ternary complex can be facilitated by the DNA bending protein TCF/LEF. Classical downstream targets of AML1 are usually involved in hematopoietic differentiation, including cytokines as interleukin-3 (IL3) [68] and granulocyte-macrophage colony stimulating factor (GM-CSF) [97], myeloperoxidase [7] and the T cell receptor β chain [17, 33, 52].

The *AML1-ETO* fusion gene consists of the RHD domain from the *AML1* gene, which is responsible for its DNA binding, and almost the total *ETO* sequence. *ETO* itself was unknown before its identification as part of the fusion gene arising from the (8;21) translocation [24]. The *ETO* gene consists of 13 exons and is expressed in progenitor cells as AML1, in myeloid and erythroid cells, but not in more differentiated leukocytes [25]. This indicates a role for ETO in blood development, but not at the level of more differentiated cells [63]. ETO contains several Nervy homology regions (NHR) with different features. There are shared similarities with the TATA-box-associated factor 110 (TAF110), heptad repeat of hydrophobic amino acids (HHR) and the myeloid, Nervy, and DEAF1 zinc finger domain (MYND-ZF). So far, ETO was not found to have DNA binding abilities even though it contains a NLS and the zinc finger domain, but being able to perform protein-protein interactions through its NHR domains [19]. Most of the activity assigned to the ETO protein was actually found by investigation of the fusion gene, but on the whole ETO is described as a co-repressor. Further support of this hypothesis was found, as ETO directly binds to the complex consisting of human nuclear receptor co-repressor (N-CoR), histone deactelyase (HDAC) and SIN3 transcription regulator family member A (mSin3A) [110]. ETO also directly binds to the silencing mediator of retinoic acid and thyroid hormone receptors (SMRT) [18].

Taken together the fusion protein AML1-ETO contains the DNA binding ability of AML1 and the repressing HDR domains of ETO (s. Figure 4).

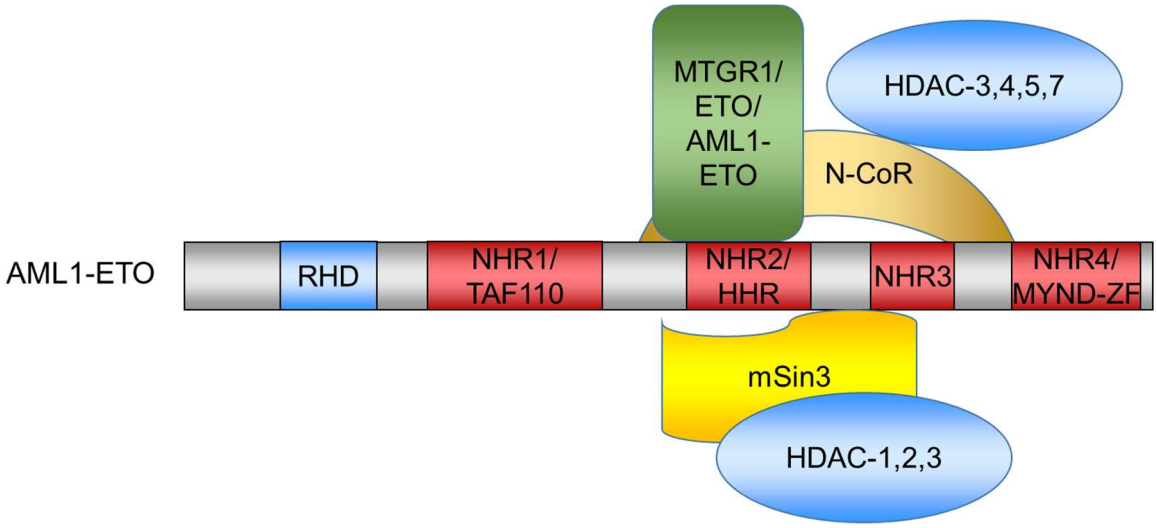

Figure 4: The AML1-ETO fusion protein and its different binding partners. AML1: acute myeloid leukemia 1, RHD: runt homologous domain, TAF110: TATA-box-associated factor 110, HHR: hydrophobic heptad repeats, ND: Nervy domain, ZF: zinc finger domain, MTGR1: myeloid translocation gene-related protein 1, ETO: eight twenty-one, N-CoR: nuclear receptor co-repressor, HDAC: histone deactelyase, mSin3: SIN3 transcription regulator.

The fusion protein itself has a size of 752 amino acids, which can be detected by Western Blot at 95kDa [85]. It could be shown that the fusion of *AML1* to *ETO* does not inhibit the ability of AML1 to dimerize with CBFβ [70], but rather led to more effective dimerization [99], leading to competitive inhibition of normal AML1. This could be shown with the example of GM-CSF promoter activation: even a 25fold higher expression of AML1 than AML1-ETO could not overcome the repressive function of the fusion protein, GM-CSF expression was still below baseline activity [28]. AML1-ETO is not only competing with AML1 for the dimerization with CBFβ, but also is able to repress AML1 target gene expression by recruitment of histone deactetylases, thereby replacing AML1 complexes containing co-activators [63]. This finding goes hand in hand with the fact, that in AML harboring the t(8;21), AML1 induced myeloid differentiation is blocked [22].

Taken together, the fusion protein AML1-ETO is able to counteract the natural function of AML1, since it shows a higher affinity to the CBFβ and is able to repress AML1 target gene expression of histone deacetylation due to fusion to ETO.

1.4. Wnt Signaling

Wnt pathways are crucial for most processes in the human body and deregulation can lead to major dysfunctions in cells up to cancer [116]. Wnt signaling is based on binding of the different Wnt proteins onto Frizzled (Fzd) receptors on the cell. Wnt ligands comprise a large family of secreted, hydrophobic glycoproteins that control a variety of developmental and adult processes in all metazoan organisms [72] and have a size of around 40kDa [98]. Wnt signaling starts in Wnt protein secreting cells after stimulus. Here, the O-acyltransferase porcupine performs lipid modification of Wnt proteins in the endoplasmatic reticulum [96, 113] and afterwards the Wnt ligands are transported to the plasma membrane through Wntless/Evi/Sprinter [10, 11, 36]. Because of the hydrophobicity of the secreted Wnt proteins, they usually act on nearby cells.

In general, Wnt signaling can be further subdivided in canonical and non-canonical Wnt signaling. Depending on which *WNT* gene is activated, one or the other pathway is triggered. Wnt ligands that activate the canonical Wnt signaling are Wnt1, Wnt2, Wnt3, Wnt8a, Wnt8b, Wnt10a and Wnt10b [51, 67], whereas Wnt4, Wnt5a and Wnt11 were shown to be involved in the non-canonical Wnt signaling [3, 38].

1.4.1. Canonical Wnt Signaling

The canonical Wnt signaling is a very complex signaling pathway involved in many processes, ranging from embryonal development to hematopoiesis and the immune system. In hematopoiesis, canonical Wnt signaling is e.g. involved in differentiation of HSCs, cell proliferation and cell survival. Different functions are dependent on the on and off status of the Wnt signaling (s. Figure 5).

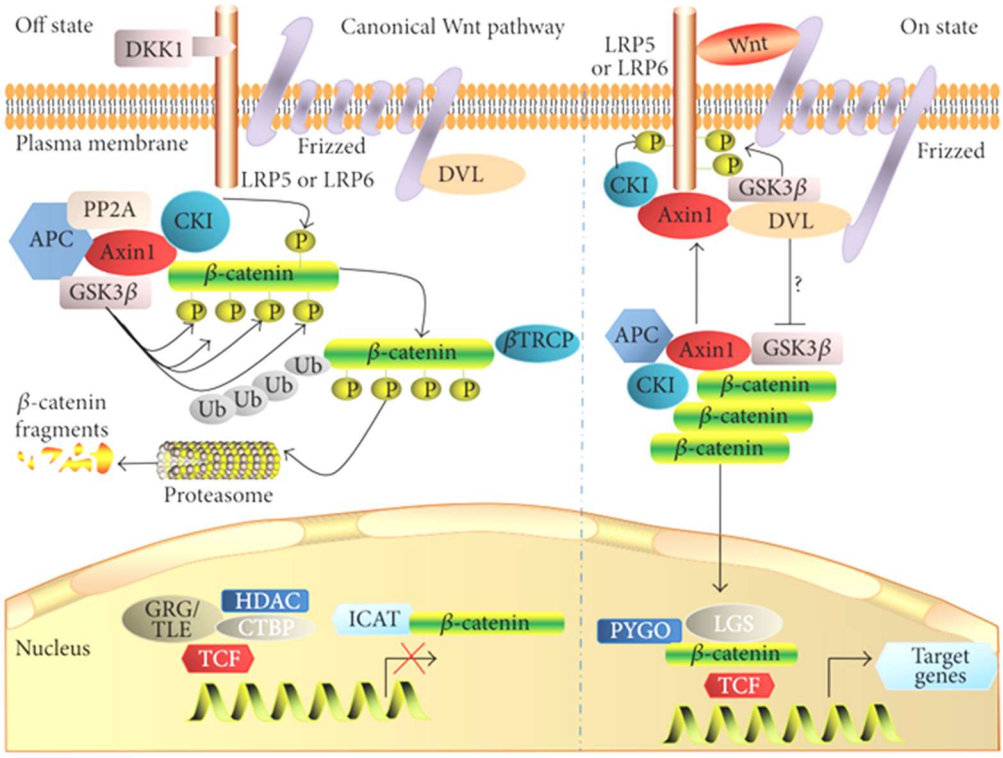

Figure 5: The canonical Wnt signaling pathway in its “off” and “on” state (see [88], CC BY 4.0, https://creativecommons.org/licenses/by/4.0/). DKK1: Dickkopf 1, DVL: Dishevelled; LRP5/6: lipoprotein related protein 5/6; PP24: protein phosphatase 2A; APC: adenomatous polyposis coli; CK1: casein kinase-1; GSK3β: glycogen synthase kinase-3 β; βTRCP: β-transducing repeat-containing protein; HDAC: histone deacetylase; GRG/TLE: Groucho/Transducin-like enhancer protein; CTBP: C-terminal binding protein; TCF: transcription factor; ICAT: inhibitor of β-catenin and Tcf-4; PYGO: Pygopus; LGS: Legless.

In the off state, β-catenin is bound to its multiprotein destruction complex consisting of the tumor suppressors Axin and adenomatous polyposis coli (APC), the Ser/Thr kinases glycogen synthase kinase-3 (GSK3) and casein kinase-1 (CK1), protein phosphatase 2A (PP2A), and the E3-ubiquitin ligase β-TrCP [92]. β-catenin gets phosphorylated near the N-terminus, ubiquitinylated and degraded by the proteasome. The transcriptional co-repressor Groucho/Transducin-like enhancer protein (GRG/TLE) keeps interacting with histone deacetylase (HDAC) and C-terminal binding protein (CTBP) and the inhibitor of β-catenin and Tcf4 (ICAT) keeps bound to nuclear β-catenin. In this case, there is no expression of canonical Wnt downstream targets. For the on-state a WNT ligand binds to the lipoprotein related protein LRP6 or LRP5 and Fzd, which are transmembrane proteins. This Wnt-Fzd-LRP6 complex recruits the scaffolding protein Dishevelled (DVL), resulting in LRP6 phosphorylation and its activation. Afterwards, the activated complex leads to recruitment of the destruction complex to the receptors, resulting in inhibition of

Axin-mediated phosphorylation of β-catenin. The released and stabilized β-catenin translocates into the nucleus, where it usually binds to the transcription factor lymphoid-enhancer factor 1 (LEF1) or other proteins from the TCF family of transcription factors to activate Wnt target gene expression.

1.4.2. Non-canonical Wnt Signaling

As mentioned before, activation of a Wnt pathway by Wnt4, Wnt5a or Wnt11 usually leads to activation of the non-canonical Wnt signaling, which can be further sub-divided into the Wnt/Calcium ($Ca2^+$) and the Wnt/planar cell polarity (PCP) pathway (s. Figure 6).

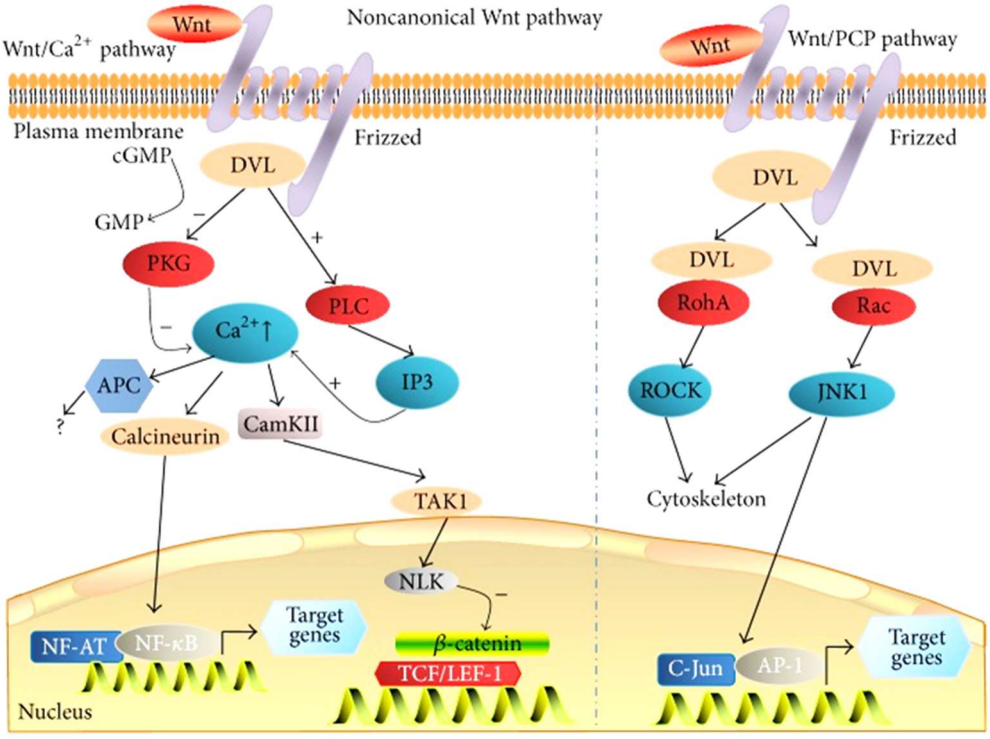

Figure 6: The non-canonical Wnt signaling pathways Wnt/$Ca2^+$ and Wnt/PCP (see [88], CC BY 4.0, https://creativecommons.org/licenses/by/4.0/). DVL: Dishevelled; PKC: protein kinase C; PLC: phospholipase-3; IP3: inositol triphosphate; APC: adenomatous polyposis coli; CamKII: calcium/calmodulin-dependent protein kinase II; TAK1: TGFβ-activated kinase 1; NLK: Nemo-like kinase; NF-AT: nuclear factor associated with T cells; NF-κB: nuclear factor kappa-light-chain-enhancer of activated B cells; TCF/LEF1: transcription factor/lymphoid-enhancer factor 1; PCP: planar cell polarity; ROCK: RHO-associated coiled-coil-containing protein kinase 1; JNK1: c-Jun N-terminal kinase 1; AP-1: activator protein 1.

Here, the co-receptors LRP6 or LRP5 is not needed. The respective Wnt ligands binds to Fzd and DSV is recruited. In the Wnt/PCP pathway this leads to activation of small GTPases such as Rac, Rho and the c-Jun N-terminal kinase 1 (JNK1). The result is actin polymerization and cytoskeletal modifications [37]. In case of the Wnt/$Ca2^{+}$ pathway, activation of DSV leads to increased activation of Phospholipase-C (PLC) and inhibition of Protein Kinase C (PKC), resulting in higher Calcium levels inside the cell. Activation of Wnt/$Ca2^{+}$ is e.g. necessary for embryonic development [115].

1.4.3. Deregulated Wnt signaling in t(8;21) leukemia

Expression of AML1-ETO alone is not sufficient to induce any disease [56], so there is a need of an additional hit. Deregulated Wnt signaling is a phenomenon known to occur in many cancers and also AML; specifically, fusion proteins were already shown to effectively activate this signaling cascade [77]. After overexpression of AML1-ETO the levels of γ-catenin were significantly increased, leading to stabilization of β-catenin [73]. Not only cell lines overexpressing the fusion protein, but also AML1-ETO positive primary samples showed high levels of γ-catenin expression. Activation of γ-catenin was mediated by the HHR and MYND-ZF domains of AML1-ETO. Higher levels of γ-catenin/LEF1 and β-catenin/LEF1 complexes could be determined, leading to enhanced LEF1 target gene expression, increased clonogenic growth and induced a rapidly fatal disease in the murine model. Since *AML1-ETO* positive cells showed strongly reduced clonogenic potential after electroporation with a dominant negative TCF [77], it is safe to say that members of the TCF family play a crucial role in t(8;21) leukemia.

1.5. Lymphoid-Enhancer Factor 1

A major transcription factor of the Wnt signaling is LEF1, which is part of the LEF/TCF family of transcription factors. This LEF/TCF family consists of 4 members: TCF7, LEF1, TCF7L1, and TCF7L2. The full-length isoforms of these members contain several functional domains, which are conserved throughout various metazoan organisms. This includes a DNA-binding domain, which recognizes the

Wnt response elements (WRE) [6, 105] and a conserved N-terminal β-catenin interaction domain [12].

The long LEF1 isoform (LEF1WT), which has activity in the canonical Wnt signaling, contains a N-terminal β-catenin binding site, a context-dependent activation domain (CAD) and a DNA-binding domain near the C-terminus. There also exists another isoform of LEF1, lacking the β-catenin binding domain (s. Figure 7). Since the β-catenin binding domain is located at the N-terminus, this isoform is called ΔNLEF1.

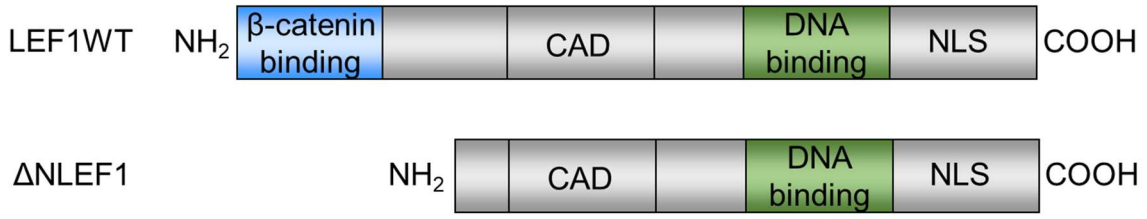

Figure 7: Schematic presentation of the LEF1WT and ΔNLEF1 isoforms. CAD: context-dependent activation domain; NLS: nuclear localization signal.

So far, the function of ΔNLEF1 was less investigated than the function of the canonical LEF1 isoform and has mainly been described as a dominant negative isoform of LEF1WT, which is transcribed from an intronic alternate promoter. The LEF1 gene spans 12 exons and the LEF1WT protein has a size of 54kDa [112]. The alternate promoter is located within the second intron of the LEF1 gene and transcription from this promoter leads to the production of a protein lacking the first 113 amino acids with a size of 38kDa [45, 62].

ΔNLef1 was found to be expressed during late osteoblast differentiation, where it induces the expression of osteocalcin and type 1 collagen, resulting in increased bone formation rates in ΔNLef1 transgenic mice [43]. ΔNLef1 expression was shown to be regulated indirectly by bone morphogenetic protein 2 (BMP2) and Wnt3a [42], direct regulation of the alternative promoter was found to be performed via Runx2 [42], which on the other hand is directly regulated by expression of the long isoform of Lef1 [50]. The effect of ΔNLef1 to activate gene expression is tissue dependent, since the short isoform is able to be activated by constitutive β-catenin expression via the residues 150-175 in mesenchymal cell lines, but not in the human leukemic cell line Jurkat and murine EL4 lymphoma cells [43].

In colon cancer cells overexpression of ΔNLEF1 significantly reduced proliferation, led to an increase of cells in the G0/G1 phase of the cell cycle and increased

apoptosis. In addition, migration of cancerous cells was shown to be reduced, inhibited the growth of colon carcinoma *in vivo* and angiogenesis of the tumors was decreased [111].

Dr. Katrin Edmaier from our institute analyzed the role of both isoforms in the mouse system: she demonstrated, that ΔNLef1 has the same activity as Lef1WT in murine progenitor and short-term repopulating cells, but clearly reduced activity at the level of long-term repopulating cells. Exclusive expression of LEF1 in its short isoform was found in most immature HSCs, which are characterized as $CD34^{-}CD38^{-}CD93^{high}$ [4], indicating a role for this short isoform at the top of the hematopoietic hierarchy.

The function of LEF1WT on the other hand is intensively investigated. It was found in our institute, that deregulated Lef1 expression induces AML in mice [80] with a long latency, which is propagated by a LSC with lymphoid characteristics. In addition, it could be found that Lef1 is essential for normal hematopoietic stem and progenitor cell function [21]. After knockdown of Lef1 the properties of clonogenic progenitor, short-term repopulating cells and also long-term repopulating cells were reduced significantly. The action of Lef1 at the level of short-term and long-term repopulating cells was found to be depending on the DNA-binding abilities of Lef1 [21].

It was already shown, that in ALL and AML cases LEF1 is usually expressed as the long isoform [112]. Analysis of LEF1 isoform expression was also performed in our hands in a cohort of primary AML cases and additionally in functionally validated

LSCs, revealing that these cells nearly exclusively express the long isoform of LEF1 (s. Figure 8).

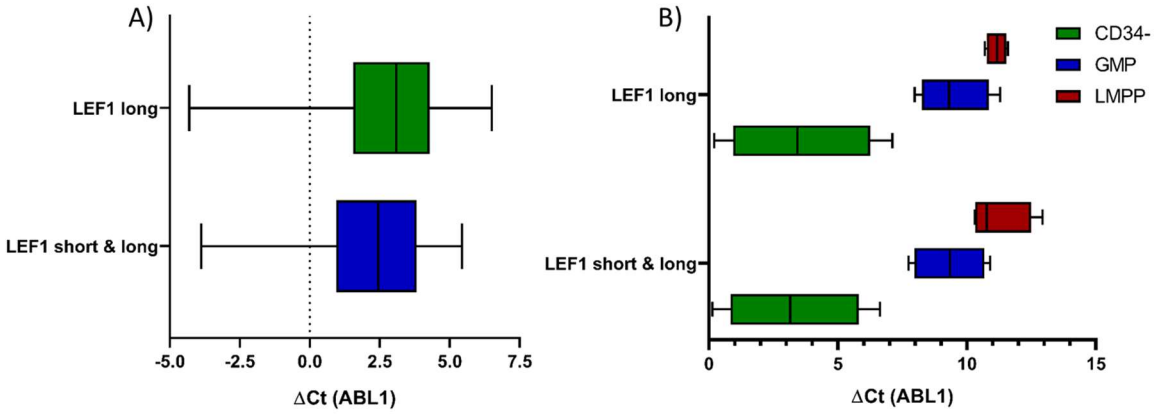

Figure 8: qRT-PCR analysis of LEF1 isoform expression in 100 CN-AML patient samples (A) and functionally validated LSC populations and CD34- cells (B) (according to [26]).

Since it was found, that AML bulk cells as well as AML LSCs express exclusively the long isoform and HSCs only the short, this therapeutic window was investigated in this thesis using different approaches to inhibit LEF1-β-catenin binding.

1.5.1. Roles of Lymphoid Enhancer Factor 1 in Hematopoiesis

As mentioned before, LEF1 is a major transcription factor of Wnt signaling, which plays roles in different steps of hematopoiesis. Within the hematopoietic hierarchy it was shown to be highest expressed in T-lymphocytes, but relatively low in HSCs (s. Figure 9).

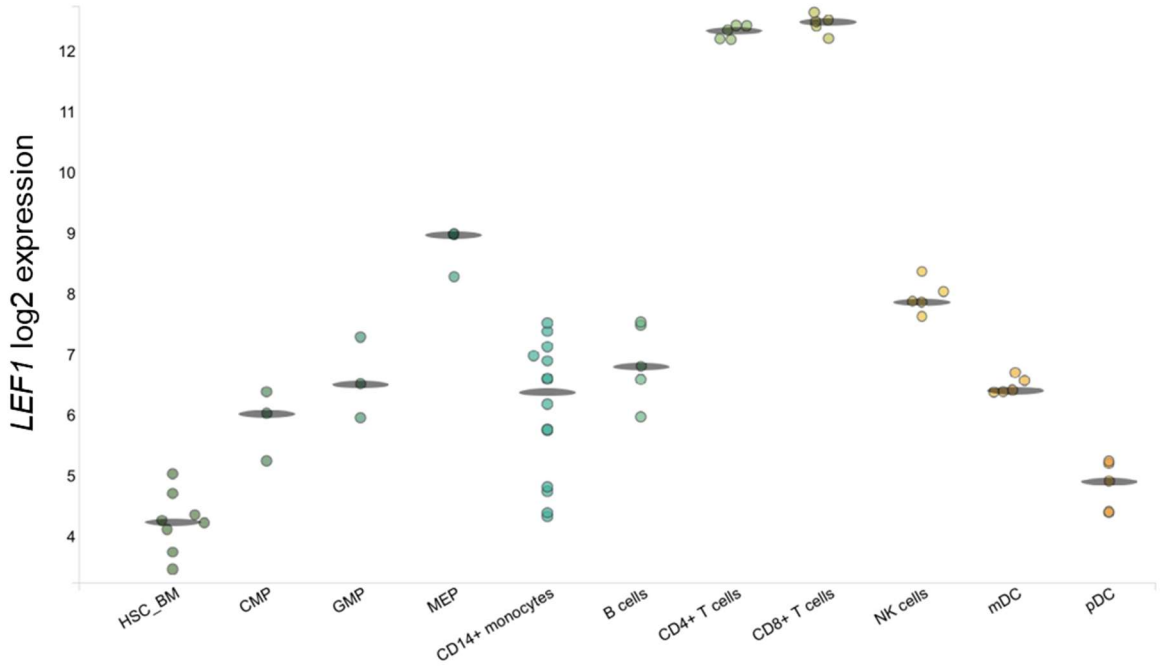

Figure 9: LEF1 expression within the hematopoietic populations [8] (BloodSpot, Normal human hematopoiesis, HemaExplorer dataset, subset 221558_s1, accessed on 02.03.2019). HSC_BM: hematopoietic stem cells from bone marrow; CMP: common myeloid progenitor; GMP: granulocyte-monocyte progenitor; MEP: megakaryocyte-erythroid progenitor; NK cells: natural killer cells; mDC: myeloid dendritic cells; pDC: plasmacytoid dendritic cell.

Within T-lymphocytes, LEF1 and TCF1 are crucially involved in cell fate decision and differentiation, since Lef1 deficiency led to severe early T cell developmental block and embryonic lethality [93]. In T-lymphocyte cell fate decision, Lef1 is involved in silencing of the *Cd4* gene, leading to formation of $CD8^+$ T cells out of $CD4^+CD8^+$ double positive thymocytes (DPT) [93]. LEF1 is also crucial for pro-B cell development, but not further differentiation of B cells [82]. Here, Lef1-deficient mice exhibit defects in pro-B cell proliferation and survival *in vitro* and *in vivo* through aberrant levels of fas and c-myc. For the transdifferentiation of pre-B cells into macrophages, suppression of Lef1 is crucial for CCAAT/enhancer-binding protein alpha (CEBPα) induction of the monocytic phenotype [83]. CEBPα induction leads to expression of the micro RNAs (miR) miR-34a and miR-223, which target the 3'UTR of Lef1. LEF1 was also found to be involved in granulopoiesis through interaction with the hematopoietic cell-specific Lyn substrate 1 (HCSL1) [91] and in natural killer T cell development together with transcription factor 1 (TCF1) [15] (s. Figure 10).

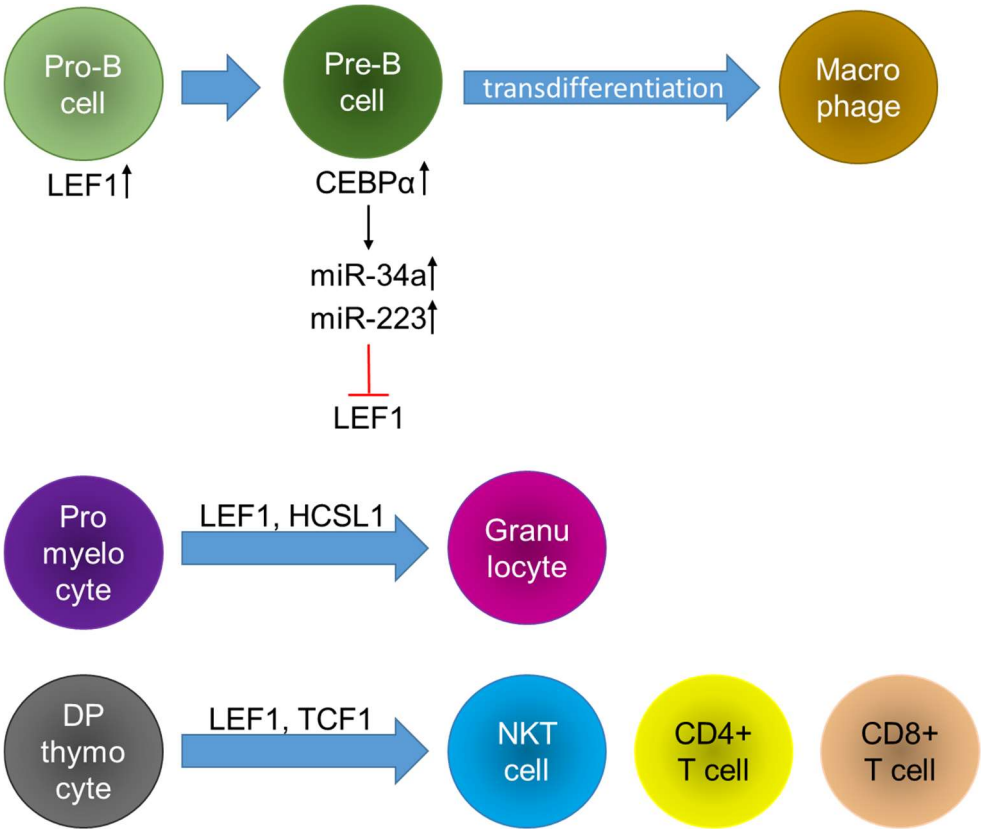

Figure 10: The roles of LEF1 in hematopoiesis. The expression of LEF1 together with other factors determines cell fate decision and differentiation. CEBPα: CCAAT/enhancer-binding protein alpha, HCSL1: hematopoietic cell-specific Lyn substrate 1, DP: $CD4^+$ $CD8^+$ double positive, TCF1: transcription factor 1, NKT cell: natural killer T cell.

Taken together a tight regulation of Wnt signaling and of its major transcription factor LEF1 is essential for normal hematopoiesis.

1.5.2. Roles of Lymphoid Enhancer Factor 1 in Leukemia

Proper regulation of Wnt signaling and its major transcription factor LEF1 is essential for healthy hematopoiesis. High expression levels of Lef1, leading to enhanced Wnt signaling, was found in different types of leukemia, including AML, ALL, CML and CLL. The hypothesis, that elevated Lef1 expression is a key factor in leukemia was supported by the finding of our group, that constitutive Lef1 expression leads to induction of AML in mice [80] without the necessity to co-express other leukemogenic factors in this model. However, in our model overexpression of Lef1 in the murine bone marrow transplantation (BMT) model induced an AML with a latency of around one year and only in a fraction of transplanted mice. In addition, methylation of Wnt inhibitors, including the selected

frizzled proteins sFRP1, sFRP2, sFRP4 and sFRP5, as well as Dickkopf 1 and 3, could be confirmed in 64% of primary AML patient samples [104]. Our group could also demonstrate that in patients with cytogenetically normal (CN) AML high LEF1 is a favorable prognostic marker [69], which could be confirmed also for AML with intermediate cytogenetic risk and FLT3-ITD AML [30].

As mentioned before, high LEF1 expression was also found in other kinds of leukemia. In ALL a general upregulation of Wnt genes upon methylation of Wnt inhibitors was found, including LEF1 [84]. This high LEF1 expression was later identified as a predictor of unfavorable outcome in adult patients with B-precursor ALL [59], but a favorable marker for childhood ALL [48]. An upregulation of Lef1 was also found in CML, leading to a deregulation of Wnt [87]. In CLL high expression of LEF1 is associated with poor survival and disease progression [23, 114] and the survival of malignant cells was shown to be dependent on LEF1 expression [39, 101].

Taken together, a role of abnormal Wnt signaling and Lef1 expression was found in different types of leukemia including AML. Expression levels of LEF1 were associated as prognostic marker in AML and other leukemia, indicating functional relevance of expression levels of this transcriptional mediator of WNT signaling.

1.6. Aim of this Thesis

AML is the most frequent acute leukemia in adults and is still associated with a high mortality despite intensive chemotherapy and approaches such as allogeneic transplantation. Thus, there is still an urgent need for innovative treatment options. One prerequisite is a better understanding of the biology of AML. In our institute we were able to show, that aberrant expression of Lef1 leads to the induction of AML in mice and that orderly expression of Lef1 was shown to be relevant in maintaining normal progenitor and hematopoietic stem cell function.

The aim of this thesis was to understand differences in expression of LEF1 isoforms between normal and AML stem cells and based on this to explore the possibility to target AML cells by interfering with the binding of LEF1 to β-catenin. A second goal was to identify factors which collaborate with LEF1 to induce AML as LEF1 alone is

only able to induce AML after long latency and only in a part of transplanted mice in a murine bone marrow transplantation model.

2. Material

2.1. Antibodies

Table 2: List of antibodies used for FACS, Immunoprecipitation and Western Blot

Antibody	Purpose	Color	Company
anti-human CD2	FACS	FITC	BD Biosciences, San Jose, CA, USA
anti-human CD3	FACS	APC efluor 780	Thermo Fisher Scientific, Waltham, Massachusetts, USA
anti-human CD11b	FACS	PE	BD Biosciences, San Jose, CA, USA
anti-human CD14	FACS	APC	Thermo Fisher Scientific, Waltham, Massachusetts, USA
anti-human CD15	FACS	FITC	BD Biosciences, San Jose, CA, USA
anti-human CD16	FACS	PE	BD Biosciences, San Jose, CA, USA
anti-human CD19	FACS	PE-Cy7	Thermo Fisher Scientific, Waltham, Massachusetts, USA
anti-human CD34	FACS	APC, FITC	BD Biosciences, San Jose, CA, USA
anti-human CD34	FACS	PE	Miltenyi Biotec GmbH, Bergisch Gladbach, Germany
anti-human CD38	FACS	APC, PE	BD Biosciences, San Jose, CA, USA
anti-human CD45RA	FACS	PE, PerCP-Cy5.5	BD Biosciences, San Jose, CA, USA
anti-human CD49f	FACS	FITC	BD Biosciences, San Jose, CA, USA
anti-human CD56	FACS	APC	Thermo Fisher Scientific, Waltham, Massachusetts, USA

anti-human CD90	FACS	Biotin	Thermo Fisher Scientific, Waltham, Massachusetts, USA
anti-human CD93	FACS	FITC	BD Biosciences, San Jose, CA, USA
anti-human CD110	FACS	APC	BD Biosciences, San Jose, CA, USA
anti-human CD123	FACS	PE-Cy7	Thermo Fisher Scientific, Waltham, Massachusetts, USA
anti-mouse CD4	FACS	PE	BD Biosciences, San Jose, CA, USA
anti-mouse CD8	FACS	APC	BD Biosciences, San Jose, CA, USA
anti-mouse CD19	FACS	PE	Thermo Fisher Scientific, Waltham, Massachusetts, USA
anti-mouse B220	FACS	APC	Thermo Fisher Scientific, Waltham, Massachusetts, USA
anti-mouse cKit	FACS	PerCP-Cy5.5	Thermo Fisher Scientific, Waltham, Massachusetts, USA
anti-mouse Sca1	FACS	PE-Cy7	BD Biosciences, San Jose, CA, USA
anti-mouse Gr1	FACS	AF700	Thermo Fisher Scientific, Waltham, Massachusetts, USA
anti-mouse Mac1	FACS	efluor 450	Thermo Fisher Scientific, Waltham, Massachusetts, USA
anti-mouse CD16/32	FACS	none	Biolegend, San Diego, USA
Streptavidin anti Biotin	FACS	APC efluor 780	Thermo Fisher Scientific, Waltham, Massachusetts, USA
anti-human LEF1 (C18A7)	IP, WB		Cellsignal, Danvers, Massachusetts, United States
anti-human β-catenin	WB		BD Biosciences, San Jose, CA, USA
mouse anti-rabbit IgG light chain HRP	WB		Santa Cruz Biotechnologies, Dallas, USA

goat anti-mouse IgG HRP	WB		Santa Cruz Biotechnologies, Dallas, USA
rabbit IgG, polyclonal	IP		Abcam, Cambridge, United Kingdom

2.2. Cell lines and primary cells

Table 3: List of acute myeloid leukemia cell lines, human primary samples, murine cells and their culture conditions

Cell Type	Origin	Culture Medium
AML cell line OCI-AML3	DSMZ	RPMI, 20% FBS, 1% PS
AML cell line SKNO1	DSMZ	RPMI, 10% FBS, 1% PS, 10 ng/ml GM-CSF
AML cell line THP1	DSMZ	RPMI, 10% FBS, 1% PS
Cell line 293T	DSMZ	DMEM, 10% FBS, 1% PS
Cell line 293T LentiX	DSMZ	DMEM, 10% FBS, 1% PS
Cell line Phoenix Ampho	DSMZ	DMEM, 10% FBS, 1% PS
Primary Patient Material	in house	IMDM, 10% FBS, 100ng/ml Flt3, 100ng/ml SF, 20ng/ml IL3, 20ng/ml IL6, 20ng/ml G-CSF
Cord Blood Cells	Frauenklinik Ulm	IMDM, 10% FBS, 100ng/ml Flt3, 100ng/ml SF, 20ng/ml IL3, 20ng/ml IL6, 20ng/ml G-CSF
murine 5-FU bone marrow cells	in house	DMEM, 15% FBS, 1% PS, 6ng/ml IL-3, 10ng/ml IL-6, 50ng/ml SCF

Table 4: List of primary CN-AML samples and their characteristics

BioID	CEBPα	NPM1	FLt3ITD	FLT3TKD	age	gender	karyotype
2198	WT	mut type A	neg	WT	51	w	46,XX[20]
2209	WT	mut type A	pos > 0,05 and >0,7	WT	71	m	46,XY[20]
2377	WT	mut I/WT	neg	WT	78	w	46,XX[13]
2720	WT	mut type A	pos > 0,05 and < 0,7	WT	82	m	45,X,-Y[16] 46,XY[4]
2721	WT	mut type A	pos > 0,05 and >0,7	WT	62	w	46,XX[20]
5282	neg	mut type A	pos >0,05 and > 0,7	WT	68	f	46,XX[20]

2.3. Chemicals

Table 5: List of chemicals

Chemical	Company
Ampicillin	AppliChem GmbH, Darmstadt, Germany
APS	AppliChem GmbH, Darmstadt, Germany
Bromphenol Blue	Merck, NJ, USA
BSA	SERVA Electrophoresis GmbH, Heidelberg, Germany
$CaCl_2$	AppliChem GmbH, Darmstadt, Germany
EDTA	AppliChem GmbH, Darmstadt, Germany
Giemsa	Merck, NJ, USA
Glycine	Sigma-Aldrich, Taufkirchen, Germany
HEPES	Sigma-Aldrich, Taufkirchen, Germany
Luria Broth	Carl Roth GmbH & Co. K, Karlsruhe, Germany
LB Agar	Carl Roth GmbH & Co. K, Karlsruhe, Germany
May-Gruenwald	Merck, NJ, USA
Milk powder	Carl Roth GmbH & Co. K, Karlsruhe, Germany

$Na_2HPO_4x2H_2O$	AppliChem GmbH, Darmstadt, Germany
SDS	AppliChem GmbH, Darmstadt, Germany
Tris-HCl	Sigma-Aldrich, Taufkirchen, Germany

2.4. Consumables

Table 6: List of consumables

Consumables	Company
0,45µm filter	Millipore, Billerica, MA, USA
1,5ml Eppendorf tube	Eppendorf, Hamburg, Germany
2ml Eppendorf tube	Eppendorf, Hamburg, Germany
40µm cell strainer	Thermo Fisher Scientific, Waltham, Massachusetts, USA
5ml Polystyrene round-bottom tube with cell strainer cap	BD Biosciences, Heidelberg, Germany
5ml Polystyrene round-bottom tube with normal cap	BD Biosciences, Heidelberg, Germany
5ml Syringe	B. Braun Melsungen AG, Melsungen, Germany
10cm corning dish	Stemcell Technologies, Köln, Germany
15cm corning dish	Sarstedt, Nürnberg, Germany
10cm suspension cell dish	Sarstedt, Nürnberg, Germany
13ml round bottom tube	Sarstedt, Nürnberg, Germany
15ml Falcon tube	BD Biosciences, Heidelberg, Germany
50ml Falcon tube	BD Biosciences, Heidelberg, Germany
500mL Vacuum Filter/Storage Bottle System	Sigma-Aldrich, Taufkirchen, Germany
Blunt-end needle	Stemcell Technologies, Köln, Germany
Cytospin Filter Paper	Tharmac, Waldsolms, Germany
Drigalski spatula	Carl Roth GmbH & Co. K, Karlsruhe, Germany
Inoculation loop	Carl Roth GmbH & Co. K, Karlsruhe, Germany

MicroAmp Fast optical 96-well reaction plate, 0,1ml	Applied Biosystems, Foster City, CA, USA
MicroAmp Optical Adhesive Film	Applied Biosystems, Foster City, CA, USA
NC-Slide A8™	ChemoMetec Kaiserslautern, Germany
SERVAgel precast vertical gel, 8-16% gradient	SERVA, Heidelberg, Germany
Suspension cell culture plate, 6-well	Sarstedt, Nürnberg, Germany
Suspension cell culture plate, 48-well	Sarstedt, Nürnberg, Germany
Suspension cell culture plate, 96-well	Sarstedt, Nürnberg, Germany
Suspension cell culture flask T25	Sarstedt, Nürnberg, Germany
Suspension cell culture flask T75	Sarstedt, Nürnberg, Germany

2.5. Cytokines

Table 7: List of human and murine cytokines used for cultivation

Cytokine	Company
human FLT3	Immunotools, Friesoythe, Germany
human G-CSF	Immunotools, Friesoythe, Germany
human GM-CSF	Immunotools, Friesoythe, Germany
human IL-3	Immunotools, Friesoythe, Germany
human IL-6	Immunotools, Friesoythe, Germany
human SCF	Immunotools, Friesoythe, Germany
murine IL-3	Immunotools, Friesoythe, Germany
murine IL-6	Immunotools, Friesoythe, Germany
murine SCF	Immunotools, Friesoythe, Germany

2.6. Inhibitors

Table 8: List of LEF1-β-catenin inhibitors

Inhibitor	Company
Calphostin C	Tocris Bioscience, Bristol, United Kingdom

Cercosporin	Abcam, Cambridge, United Kingdom
active peptide TAT-NLS-BLBD-6	Genscript, NJ, USA
control peptide TAT-NLS-BLBD-6m	Genscript, NJ, USA

2.7. Instruments

Table 9: List of instruments

Instrument	Company
BD LSRFortessa™	BD Biosciences, Heidelberg, Germany
Cytospin 4 centrifuge	Thermo Fisher Scientific, Waltham, Massachusetts, USA
Eppendorf 5810R centrifuge	Eppendorf, Hamburg, Germany
Eppendorf 5415R centrifuge	Eppendorf, Hamburg, Germany
Eppendorf Minispin centrifuge	Eppendorf, Hamburg, Germany
Fusion FX7 Spectra, Property of the Department of Dermatology, University Hospital Ulm, Germany	Vilber Lourmat, Eberhardzell, Germany
Galaxy 170S Incubator	New Brunswick Scientific, Edison, NY, USA
Hemacytometer/Neubauer improved	LO LaborOptik, Friedrichsdorf, Germany
HemaVet® 950	Drew Scientific, Waterbury, CT, USA
Heraeus Incubator	Thermo Fisher Scientific, Waltham, Massachusetts, USA
MACS® manual Separator QuadroMACS®	Miltenyi Biotec GmbH, Bergisch Gladbach, Germany
Magnetic Stirrer MR Hei-Standard	Heidolph Instruments GmbH & CO. KG, Schwabach, Germany
NanoDrop® Spectrophotometer ND-1000	Thermo Fisher Scientific, Waltham, Massachusetts, USA
Nikon Eclipse Ti	Nikon, Minato, Japan
Nucleocounter (only for testing)	ChemoMetec Kaiserslautern, Germany
Overhead-Shaker SU1010	Sunlab, Leipzig, Germany

peqSTAR 96 Universal Gradient	PEQLAB Biotechnology GmbH, Erlangen, Germany
Powersource 300V	VWR, Darmstadt, Germany
Special accuracy weighing machine CPA6235	Sartorius, Göttingen, Germany
Taqman 7900HT Fast real-time PCR system	Applied Biosystems, Foster City, CA, USA
Thermocycler	VWR, Darmstadt, Germany
Ultrasonic Homogenizer UW2070, Property of the Department of Dermatology, University Hospital Ulm, Germany	Bandelin Electronic GmbH, Berlin, Germany
Ultrasonic Powersource HD2070, Property of the Department of Dermatology, University Hospital Ulm, Germany	Bandelin Electronic GmbH, Berlin, Germany
Vac-Man®	Promega, Madison, WI, USA
Vacuum Eluator™	Promega, Madison, WI, USA
Vacuum Pump 2522Z-02	Welch, Fürstenfeldbruck, Germany

2.8. Kits

Table 10: List of Kits

Kit	Company
Annexin V APC/FITC Kit	BD Biosciences, San Jose, CA, USA
BrdU Flow Kit APC	BD Biosciences, San Jose, CA, USA
Arcturus PicoPure RNA Kit	Thermo Fisher Scientific, Waltham, Massachusetts, USA
Direct-Zol RNA Miniprep	Zymo Research Europe GmbH, Freiburg, Germany
DNase I	Qiagen, Venlo, Netherlands
Human CD3 Microbeads	Miltenyi Biotec GmbH, Bergisch Gladbach, Germany

Human CD19 Microbeads	Miltenyi Biotec GmbH, Bergisch Gladbach, Germany
Human CD34 enrichment Kit	Miltenyi Biotec GmbH, Bergisch Gladbach, Germany
Human lineage depletion Kit	Miltenyi Biotec GmbH, Bergisch Gladbach, Germany
Pierce™ classic magnetic IP/Co-IP Kit	Thermo Fisher Scientific, Waltham, Massachusetts, USA
PureYield™ Plasmid MaxiPrep Kit	Promega, Madison, WI, USA
PrimeScript 1st strand cDNA Synthesis Kit	Clontech Laboratories, Mountain View, CA, USA
RNase inhibitor	Qiagen, Venlo, Netherlands
RNeasy Micro Kit	Qiagen, Venlo, Netherlands
Sensiscript RT Kit	Qiagen, Venlo, Netherlands
Qiashredder	Qiagen, Venlo, Netherlands

2.9. Media and Buffers

Table 11: List of media used for cultivation of cells

Media	Company
DMEM High Glucose (4.5 g/l)	Thermo Fisher Scientific, Waltham, Massachusetts, USA
Dulbecco's PBS (1X DPBS)	Thermo Fisher Scientific, Waltham, Massachusetts, USA
FBS	Capricorn Scientific, Ebsdorfergrund, Germany
IMDM	Thermo Fisher Scientific, Waltham, Massachusetts, USA
RPMI 1640	Thermo Fisher Scientific, Waltham, Massachusetts, USA

Table 12: List of media used for bacteria cultivation

Bacteria medium & plates	
LB medium	25g Luria Broth ad 1l with $_{dd}H2O$
LB agar	40g LB Agar ad 1l with $_{dd}H2O$

Table 13: List of buffers prepared for SDS-PAGE and Western Blot

SDS-PAGE & Western Blot	
10x Electrophoresis buffer	30g Tris-HCl (0.25 M)
	144g Glycine (1.92 M)
	10g SDS (0.1 %)
	ad 1l with $_{dd}H2O$
10x Transfer buffer	30g Tris-HCl (0.25 M)
	144.1g Glycine (1.92 M)
	ad 1l with $_{dd}H2O$
1X Transfer buffer	100ml 10x Transfer buffer
	100ml Methanol
	ad 1l with $_{dd}H2O$
10% APS	1g Ammonium persulfate
	ad 1l $_{dd}H2O$
10% SDS	50g SDS
	ad 500ml with $_{dd}H2O$
6X Laemmli buffer	5ml Glycerol (50%)
	1.2g SDS (12%)
	3.8ml 1M Tris-HCl (0.38M)
	pH 6.8 with HCl
	100mg Bromphenol Blue (1%)
	600µl β-Mercaptoethanol (6%)
	ad 10ml with $_{dd}H2O$
TBS-T	100ml 10X TBS
	1ml Tween 20
	ad 1l with $_{dd}H2O$
Blocking buffer	2.5g milk powder

	ad 50ml with TBS-T

Table 14: List of buffers prepared for cell culture, MACS and lentiviral transduction

Buffers used in cell culture	
Thawing buffer	IMDM
	10% FBS
	DNase I
Freezing buffer	FBS
	10% DMSO
MACS buffer	1X DPBS, 500ml
	2mM EDTA
	2.5ml FBS
2X HBS buffer	280mM NaCl
	10nM KCl
	1.5mM Na2HPO4
	12mM Dextrose
	50mM HEPES
	pH to 7.15

Table 15: Recipe of 4% formalin used for fixing of murine tissue samples

Formalin for murine samples	
4% Formalin	100ml 40% formaldehyde
	4g $NaH_2PO4 * H_2O$
	6.5g $Na_2HPO4 * 2H_2O$
	ad 1l with $_{dd}H2O$

2.10. Mouse Strains

Table 16: List of mouse strains, use of the different strains and the respective irradiation intensity

Mouse Strain	Acronym	Purpose	Irradiation [cGy]
C57Bl/6J x C3H/HeJ	Bl6	Donor of BM cells stimulated with 5-FU, Transplantation of retrovirally transduced 5-FU BM	1200
C57Bl/6Ly-Pep3b x C3H/HeJ	Pep	Donor of BM cells stimulated with 5-FU, Transplantation of retrovirally transduced 5-FU BM	1200
NOD.Cg-Prkdc<scid> Il2rg<tm1Wjl>/SzJ	NSG	Transplantation of Primary Samples and Cell Lines	325

2.11. Plasmids

Table 17: List of plasmids used for lentiviral and retroviral transfection

Plasmid	Insert	Color	Virus	purpose	Obtained from
MIG	AML1-ETO	GFP	Retroviral	overexpression of AML1-ETO	in house
MIY	Lef1WT	YFP	Retroviral	overexpression of Lef1WT	in house
pCDH	LEF1WT	RFP	Lentiviral	overexpression of LEF1WT	in house, cloning by Genscript
pGIPZ	shLEF1	BFP	Lentiviral	Knockdown of LEF1	AG Lüder-Meyer, University Hospital Ulm
pGIPZ	scrambled	BFP	Lentiviral	Non-targeting control vector	AG Lüder-Meyer, University Hospital Ulm

psPAX2	none	none	Lentiviral	helper plasmid for VCM production	in house
pMD2.G	none	none	Lentiviral	helper plasmid for VCM production	in house

2.12. Primers

Table 18: List of primers used for cDNA synthesis and qRT-PCR analysis via taqman

primer	purpose	company
random nonamers	cDNA synthesis	Sigma Aldrich, Taufkirchen, Germany
human CCND1, Hs00765553_m1	qRT-PCR	Thermo Fisher Scientific, Waltham, Massachusetts, USA
human C-MYC, Hs00153408_m1	qRT-PCR	Thermo Fisher Scientific, Waltham, Massachusetts, USA
human GAPDH, Hs02786624_g1	qRT-PCR	Thermo Fisher Scientific, Waltham, Massachusetts, USA
human LEF1 long & short, Hs01547250_m1	qRT-PCR	Thermo Fisher Scientific, Waltham, Massachusetts, USA
human LEF1 long, Hs00212390_m1	qRT-PCR	Thermo Fisher Scientific, Waltham, Massachusetts, USA
human RUNX1-RUNX1T1, Hs03024752_ft	qRT-PCR	Thermo Fisher Scientific, Waltham, Massachusetts, USA
human TBP	qRT-PCR	Thermo Fisher Scientific, Waltham, Massachusetts, USA
murine Hprt, Mm01545399_m1	qRT-PCR	Thermo Fisher Scientific, Waltham, Massachusetts, USA
murine Lef1 long & short, Mm00550265_m1	qRT-PCR	Thermo Fisher Scientific, Waltham, Massachusetts, USA

murine Lef1 long, Mm01310389_m1	qRT-PCR	Thermo Fisher Scientific, Waltham, Massachusetts, USA

2.13. Reagents

Table 19: List of reagents

Reagent	Company
$CaCl_2$	in house
Cell Dissociation Buffer (Gibco)	Thermo Fisher Scientific, Waltham, Massachusetts, USA
DEPC-treated water	Biosystems/Ambion, Austin, TX, USA
$_{dd}H20$	in house
DMSO	Sigma-Aldrich, Taufkirchen, Germany
ECL™ Western Blotting Analysis System	GE Healthcare Life Sciences, Amersham, UK
ECL™ Prime Western Blotting System	GE Healthcare Life Sciences, Amersham, UK
EDTA	Merck, Darmstadt, Germany
Ethanol (99.5%)	Sigma-Aldrich, Taufkirchen, Germany
Glycerol	Sigma-Aldrich, Taufkirchen, Germany
Immersion oil	Sigma-Aldrich, Taufkirchen, Germany
Isopropanol	Sigma-Aldrich, Taufkirchen, Germany
Methylcellulose H4330	Stemcell Technologies, Köln, Germany
Methylcellulose H4434	Stemcell Technologies, Köln, Germany
Methylcellulose M3434	Stemcell Technologies, Köln, Germany
Penicillin/Streptomycin	PAN Biotechnologies, Aidenbach, Germany
Polybrene	Sigma-Aldrich, Taufkirchen, Germany
RetroNectin® GMP grade	Clontech Laboratories, Mountain View, CA, USA

TaqMan® Universal PCR Master Mix, No AmpErase® UNG	Applied Biosystems, Foster City, CA,USA
TBS (10x)	Thermo Fisher Scientific, Waltham, Massachusetts, USA
TEMED	AppliChem GmbH, Darmstadt, Germany
TRIzol® Reagent	Invitrogen, Carlsbad, CA, USA
Trypan blue	Invitrogen, Carlsbad, CA, USA
Trypsin-EDTA	PAN Biotechnologies, Aidenbach, Germany
Tween 20	Sigma-Aldrich, Taufkirchen, Germany
SuperSignal™ West Femto Maximum Sensitivity Substrate	Thermo Fisher Scientific, Waltham, Massachusetts, USA
Stripping Buffer	Thermo Fisher Scientific, Waltham, Massachusetts, USA

3. Methods

3.1. Freezing and Thawing of Mammalian Cells

Mammalian cells were usually stored in liquid nitrogen (LN) or -80°C freezers. Cell lines were thawed in a 37°C water bath, the cell suspension washed with 1X DPBS and after centrifugation at 1500rpm for 5min the supernatant was discarded and the cells were taken into culture with the respective media. For primary patient samples and cord blood (valid ethics votes present), the thawing needed to be performed more carefully to prevent clumping of the sample. Here, the samples were thawed in a 37°C water bath until only a small piece of frozen sample was left, then the cells were washed with thawing buffer. This thawing buffer consists of the culture medium supplemented with DNase I to prevent free DNA, which originates from busted cells due to the thawing process, from forming clumps with the cells. The cells are cultured at 37°C and 5% CO_2 in an incubator.

To freeze cells, cells from culture were washed with 1X DPBS and then mixed with freezing buffer and aliquoted into CryoTubes. For short-term storage, the cells were stored in a –80°C freezer, for long-term storage the cells were transferred into liquid nitrogen storage containers after a minimum of 3 days at -80°C.

3.2. Cell Count

Cell counting was performed by manual counting with the hemacytometer (Neubauer chamber) or counting via Vi-Cell cell counting machine. Cells from experimental mice as well as primary patient samples and cord blood were counted by HemaVet.

The Vi-Cell is able to count cells within a minimum of 300µl cell suspension. After mixing the cells with trypan blue, analysis of photos of multiple cross-sections in the counting chamber give the size, amount and percentage of total and living cells. In case of low number of cells, the cells were counted manually using the Neubauer chamber. Here, a small amount of cells was mixed with trypan blue and the living cells were counted under the light microscope. The cell concentration is calculated as followed:

$$\frac{cells}{ml} = \frac{cells(counted)}{quadrants(counted)} * dilution\ factor * 10000$$

Cells from experimental mice as well as primary patient samples and cord blood were counted using the Hemavet machine. Per counting 30µl of cell suspension were used. The Hemavet distinguishes between different cell types and gives i.a. red blood cell (RBC) and white blood cell (WBC) counts.

3.3. RNA Extraction

Extraction of ribonucleic acid (RNA) was performed using different methods. The Direct-zol Miniprep Kit or RNeasy Micro Kit were used for standard RNA extraction of samples with high amounts of cells. To increase the RNA concentration, before extraction the cell lysates were first frozen at -80°C, thawed on ice and then run through Qiashredder columns in order to further disrupt the cells. RNA from primary AML samples and cord blood, especially the sorted subpopulations from cord blood, was extracted using the Arcturus PicoPure RNA Kit. The extractions were performed according to the manufacturer's protocols. Briefly, the cells were lysed in the respective lysis buffers, the lysates were mixed with Ethanol followed by several washing steps to ensure high purity of RNA. DNase treatment was performed to digest remaining DNA, which could later in the qRT-PCR possibly falsify the results. In the end, the RNA was eluted in 10-50µl nuclease-free water. RNA concentrations were determined using the NanoDrop® Spectrophotometer ND-1000.

3.4. DNase I Treatment

For RNA extraction methods using columns, the RNase-free DNase Set was used on columns during the extraction process. Here, the DNase was dissolved in nuclease-free water, diluted in RDD buffer and applied to the columns, followed by incubation at room temperature (RT) for 15min. After a washing step the RNA extraction was completed.

3.5. cDNA Synthesis

For gene expression analysis by TaqMan the mRNA needed to be transcribed into copy deoxyribonucleic acid (cDNA). Synthesis of cDNA of cell lines was performed

using the PrimeScript RT-PCR Kit. The desired amounts of RNA were diluted with nuclease-free water and mixed with the 5X PrimeScript buffer, random hexamers and the PrimeScript enzyme. After an incubation at 37°C for 15min, followed by inactivation of the enzyme at 85°C, the cDNA was ready to use. In case of RNA from primary patient samples and cord blood with high concentrations, the PrimeScript RT-PCR Kit was used, for very low concentrations cDNA synthesis was performed using the Sensiscript RT Kit. Here, the maximal amount of RNA per reverse transcription was 50ng. The RNA was mixed with the 10X buffer, dNTPs, RNase inhibitor I, reverse transcriptase and random nonamers. The suitable program for this cDNA synthesis included a reverse transcription step of 60min at 37°C. cDNA of all samples was either analyzed directly by qRT-PCR or stored at -20°C until further use.

3.6. TaqMan qRT-PCR

Analysis of gene expression was performed with quantitative real-time polymerase chain reaction (qRT-PCR), measuring the amount of cDNA using fluorescent primers and the TaqMan 7900HT system. These taqman probes anneal to the single strands of the DNA. In the beginning a quencher suppresses the fluorescent activity of the fluorophore. Once the polymerization reaches the site of the taqman probe, displacement and cleavage of the fluorophore takes place. This fluorescence is measured by the machine, the amount of produced PCR product correlates with the fluorescence intensity.

Usually the composition per well was 10µl 2x Universal OCR MasterMix No AmpErase UNG, 8µl PCR-grade H_2O, 1µl primer and 1µl cDNA. In some cases, the concentration of the RNA for cDNA synthesis was very low, so the composition was adjusted. The maximum amount of cDNA used per well was ¼ of the total volume. For very precious samples as the sorted cord blood subpopulations the volume per well was reduced to 10µl to use less sample, the amounts of reagents were adjusted accordingly. The analysis was performed in 96 well plates, sealed with optical films. The settings in the SDS2.4 software were as followed: ΔΔCt with 96 well layout, 45 cycles. Each program started with 10min at 95°C, then 45x cycles with 15s at 95°C and 60s at 60°C. Afterwards the raw data was analyzed with the RQ Manager 1.2.1 software: the respective housekeeping was set, threshold was fixed to 0.2. From the

raw Ct values, Average ΔCt and ΔΔCt values are calculated. To compare samples to one another, fold expression was calculated with the following formula: $fold\ expression = 2^{-\Delta\Delta Ct}$. Multiplication of the fold expression with 100 gives the expression respective to the control in %.

3.7. Transformation of Heat-Competent E. coli

To multiply a given amount of plasmids heat-sensitive E. coli bacteria type DH5α were used. The heat shock competent cells were produced in house and stored in aliquots at -80°C. Per plasmid 30µl cells were used and mixed gently with 1µl of plasmid solution. The bacteria were incubated on ice for 30min, then heat-shocked at 42°C for 45s and put back on ice for 2min. Afterwards 500µl SOC media was added to the bacteria, followed by incubation for 1h at 37°C and 300rpm. 100-200µl of the cell suspension were plated per ampicillin-containing agar plate and incubated at 37°C overnight (o/n) in a dry incubator. The next morning single colonies were picked and put into LB medium for maxi preparation.

3.8. Plasmid Isolation

After successful inoculation of 100-250ml LB medium containing the antibiotic for selection of the plasmid carrying bacteria, plasmid isolation was performed using the MaxiPrep Kit according to the manufacturers “Promega Quick” protocol. Briefly, the bacteria were pelleted, lysed and the DNA containing supernatant was run through clearing and binding columns by vacuum application. After removal of endotoxins and washing of the column, the plasmids were eluted in nuclease-free water. The concentration of plasmid DNA was analyzed using the NanoDrop® Spectrophotometer ND-1000. The samples were sent for sequencing to LGC to confirm presence and correct direction of the desired inserts.

3.9. Glycerol Stock

After obtaining the confirmation that the plasmids function as desired, glycerol stocks of the respective bacteria solution were prepared. Here, 500µl bacteria suspension was mixed with 500µl Glycerol and stored in CryoTubes at -80°C. For

the following MaxiPrep of the same vectors the LB media was inoculated with few bacteria cells scraped off from the glycerol stock.

3.10. LEF1-β-Catenin Binding Inhibition

The inhibition of LEF1 binding to β-catenin was performed using different methods. The small-molecule inhibitors Calphostin C and Cercosporin were applied, as well as the TAT-NLS-BLBD-6 synthetic peptide.

Calphostin C and Cercosporin both are PKC inhibitors, which were identified as effective LEF1-β-catenin binding inhibitors. Since Calphostin C and Cercosporin were dissolved in DMSO, DMSO was used as solvent control for the experimental arms. For *in vitro* assays and *in vivo* readouts of *in vitro* experiments concentrations between 1nM and 1mM were used. Treatment of living cells with the compounds to inhibit LEF1-β-catenin binding for the Co-Immunoprecipitation (Co-IP) was not possible, since the compounds were shown to induce Caspase activity *in vitro*, which would lead to degradation of β-catenin and falsify the result [31]. Because of this, protein lysates were treated directly with 100µM of the compounds.

The synthetic peptides TAT-NLS-BLBD-6 (active) and TAT-NLS-BLBD-6m (control) were synthesized by Genscript. The peptides consist of a part of the transactivator of transcription (TAT) protein for cellular import, a nuclear localization signal (NLS) for nuclear import and a part of the binding sequence of LEF1 to β-catenin (BLBD-6) or a mutated non-targeting control sequence (BLBD-6m). Both peptides were dissolved in 1X DPBS to a stock concentration of 2mM, 1X DPBS was used as solvent control for the respective experimental arms. Because of the short half-life of the peptides, concentrations of 100µM and 200µM were used to ensure a detectable effect in the assays.

3.11. IC50 calculation

The half-maximal inhibitory concentrations (IC50) of Calphostin C and Cercosporin were determined by treatment of OCI-AML3, SKNO1 and THP1 with log10 concentrations ranging from 1nM to 1mM versus DMSO. Cell counts were performed in technical duplicates per biological replicate. The number of viable cells was normalized to the DMSO treated cells, converted into probit values and plotted

versus the concentration. A linear line was plotted to the data points, only extreme outliers were excluded and the resulting x-axis intercept equaled the IC50 value.

3.12. Protein Extraction

To confirm the presence of distinct proteins in the cells, sodium dodecyl sulfate polyacrylamide gel electrophoresis (SDS-PAGE) followed by Western Blot (WB) was performed. Protein was extracted IP lysis buffer, since most of the lysates were further used for Co-Immunoprecipitation. Each sample was washed properly with 1X DPBS to avoid the presence of FBS in the protein lysate. Before adding the lysis buffer to the sample, it was substituted with protease inhibitor (100X), phosphatase inhibitor cocktail 1/3 (100X) and phosphatase inhibitor cocktail 2 (100X) to avoid protein degradation. After suspension of the pellet in lysis buffer, the samples were incubated on ice for 30min, followed by three freeze-thaw cycles with LN and thawing on ice. The samples were sonicated using the ultrasonic homogenizer located in the Institute of Dermatology, since the IP lysis buffer may not disrupt all nuclei by itself. The sonication was performed three times with 20% intensity and 15s per pulse. To extract the pure protein, centrifugation was performed for 15min at 4°C with 16.000rpm. The protein containing supernatant was transferred into a new tube and the concentration was measured using the BioRad Protein assay. The lysates were used directly for SDS-PAGE or IP or stored at -80°C until further use.

3.13. Determination of Protein Concentration

To determine the concentration of the protein lysates the BioRad Protein Assay was used. Briefly, the samples were diluted in $_{dd}H_2O$ and the Bradford reagent was added. After 10min incubation the samples were measured with the BioPhotometer at 595nm. To determine the concentration of the samples a BSA standard and blank samples were also analyzed. These values were used to create a standard curve. The equation used to calculate the concentration of the samples was as followed:

$$c(sample) = \frac{value(sample) - y\ intercept(standard)}{slope\ (standard)}$$

3.14. Co-Immunoprecipitation

To detect binding partners of proteins via SDS-PAGE and WB, Co-IP was performed. In this thesis the binding of LEF1 to β-catenin was of interest, especially the loss of binding after application of methods inhibiting LEF1-β-catenin binding. Co-IP was performed with the Pierce magnetic Co-IP Kit. The input material per IP was increased to 3mg protein compared to the standard protocol, which was treated in a total volume of 200µl for 24h at 4°C with 100µM of either of the compounds versus DMSO. Afterwards the immunocomplex was formed o/n with 20µg LEF1 antibody per sample versus the same amount of rabbit IgG at 4°C on an overhead-shaker. The next day, magnetic beads were washed and added to the samples, followed by 1h incubation at RT on an overhead-shaker. The samples were washed several times with the IP lysis/wash buffer and $_{dd}H_2O$ and eluted by low pH elution in a final volume of 60µl.

3.15. SDS-PAGE

With SDS-PAGE the proteins in a sample are separated according to their size and charge. The electrophoresis was performed using ready-made gradient gels 8-16%. The samples were prepared using 6x Laemmli buffer and incubated at 95°C for 10min to denature the proteins. After loading the samples together with a ladder, the gels were first run at 80V for 30min until the samples passed the stacking gel, afterwards for further 1.5 – 2h at 120V until the blue Laemmli buffer band reached the bottom of the gel to ensure optimal separation. The gels were taken out of the cassettes and blotted on membranes using the wet blot method.

3.16. Western Blot

Proteins from SDS-PAGE gels were blotted onto a PVDF membrane to detect specific proteins via antibodies. For this thesis only o/n wet transfers were performed to ensure complete transfer of proteins of all sizes. After activation of the PVDF membrane for 10s in 100% Methanol, the gels were layered in cassettes with the membrane, Whatman papers and the sponges (s. Figure 11).

Figure 11: Western Blot setup for o/n wet transfer.

The cassette was put in a Western Blot (WB) container filled with 1X transfer buffer and run at 30V in the cold room o/n on a magnetic stirrer. After successful transfer the membranes were blocked for at least 1h at RT with 5% milk TBS-T on a shaker. After blocking the membranes were sealed in films together with the primary antibodies in 5% milk TBS-T. The concentration of the primary antibodies varied from 1:200 for LEF1 to 1:500 for β-catenin. Incubation with the primary antibodies was usually performed o/n at 4°C on a shaker to ensure more specific binding. Afterwards the membranes were washed properly with TBS-T to remove unspecifically bound antibodies, followed by incubation with the respective secondary HRP-conjugated antibodies (diluted 1:2000 with 5% milk TBS-T) at RT for 1.5h on a shaker. The membranes were washed again with TBS-T and the bands were detected using the ECL, ECL prime or SuperSignal™ reagent and the Fusion FX-7 located in the Institute of Dermatology. To detect changes in LEF1 and β-catenin band intensities for the Co-IP after treatment with the inhibitors, band intensities were compared using the ImageJ software.

3.17. Lentiviral Transfection

To create a virus containing medium (VCM) from lentiviral plasmids, which could be used to transduce e.g. leukemic cell lines, transfection of 293T LentiX was performed. This transfection was performed using the Calcium Chloride method. Since lentiviruses are also able to infect humans, all lentiviral infections were performed in the S2 lab with S2 lab coats, gloves and face masks worn at all times while working with viruses. The 293T LentiX cells were cultured in such a way, that they reach 50% confluence at the day of transfection. Per transfection of a 10cm dish of 293T LentiX cells two tubes were prepared as followed: tube 1 contained 20µg DNA of interest, 10µg psPAX2 helper plasmid, 5µg pMD2.G helper plasmid and 88µl 2M $CaCl_2$ ad 700µl $_{dd}H_2O$, tube 2 contained 700µl 2XHBS buffer with pH

7.15. The HBS buffer was bubbled with a 2ml pipette and the DNA mixture was added dropwise, followed by an incubation for 30min at RT. Meanwhile the medium on the 293T LentiX cells was changed to 9ml, then the transfection mixture was added dropwise. In the next morning the medium was changed to 3ml fresh medium and 24h and 48h later the VCM was collected. Here, the VCM was filtered using 0,45µm syringe filters before aliquoting to remove any non-viral particles in the VCM. The VCM was used directly or stored at -80°C until further use. Lentiviral VCM was produced to perform shRNA mediated LEF1 knockdown in AML cell lines.

3.18. Retroviral Transfection

To create VCM from retroviral plasmids the Lipofectamine LTX method was used on Phoenix Ampho cells. Usually retroviruses are produced using Phoenix Eco cells, but in this case, the VCM was more potent when using Phoenix Ampho for VCM production. Since viruses created with Phoenix Ampho cells are able to also infect humans, all experiments including retroviruses were performed with the same standards as for lentiviruses. For the Lipofectamine LTX method the medium of adherent cells had to be changed to antibiotic-free medium at the last splitting procedure before the transfection. The Phoenix Ampho cells were cultured in such a way that they reached 50% confluence at the day of transfection. Per transfection two tubes were prepared as followed: tube 1 contained 24µg of the retroviral construct of interest, 20µl PLUS reagent, filled up to 125ml with OptiMEM, tube 2 contained 30µl Lipofectamine LTX and 95µl OptiMEM. The mixture in tube 1 was added to tube 2 with bubbling and after 5min incubation at RT the mixture was added dropwise to the Phoenix Ampho cells. In the next morning the medium was changed to 3ml and 24h and 48h later the VCM was collected. As for the lentivirus, the VCM was filtered through a 0,45µm syringe filter and aliquoted. The VCM was used directly or stored at -80°C until further use.

To produce a potent protein lysate for Co-IP of LEF1 and β-catenin, 293T HEK cells were transfected directly with constructs overexpressing LEF1WT using the Lipofectamine LTX method as mentioned above, 48h after transfection the cells were sacrificed for protein extraction.

3.19. Transduction

Cell lines for lentiviral transduction were plated in 6-well plates, each 2mio cells per well in 3ml medium. To improve the transduction efficacy, 1µl polybrene solution was added per ml medium. Afterwards 0,5-1ml VCM was added to the cells. After 48h incubation at 37°C in the incubator, the cells were washed and put into culture again with polybrene. 48h to 72h after transduction the cells were sorted via FACS.

To transduce cells with retrovirus, transfection was performed with the help of the RetroNectin® reagent. 6-well plates were incubated with the reagent for at least 2h at RT or o/n at 4°C, blocked with 4% sterile BSA solution and rinsed with 1X DPBS. The virus was added to the wells and centrifuged at 2500rpm for 45min at 4°C, afterwards the cells with respective media and cytokines were added to the wells. After incubation with the virus for 48h the cells were taken from the wells using Cell Dissociation Buffer and Cell Scrapers. The cells were either sorted or used directly for bone marrow transplantation assays, which enables transplantation without use of additional helper cells. Retroviral VCM was used to transduce 5-FU stimulated murine BM cells with AML1-ETO and Lef1WT overexpression constructs.

3.20. Magnetic Activated Cell Sorting (MACS)

Human lineage depletion, $CD34^+$ cell enrichment and depletion of CD3 and CD19 was performed using the respective microbeads. Degassed MACS buffer was prepared by supplementing 1X DPBS with 2mM EDTA and 0,5% FBS. The buffer was filtered using a Vacuum Filter/Storage Bottle System with 0,22µm pore size and 33.2cm² CA membrane and degassed with the help a vacuum pump.

The cells for enrichment/depletion were thawed, washed and counted. According to the number of cells, the volume of MACS buffer, beads and blocking reagent was adjusted. Incubation of the cells with the beads was performed at 4°C for 30min. Afterwards the cells were washed and enrichment/depletion was performed in LS columns. After each MACS application the quality of enrichment/depletion was monitored by fluorescence-activated cell sorting (FACS).

3.21. Fluorescence-Activated Cell Sorting

The successfully transduced cells were sorted out of the cell suspension via FACS, since these cells co-express a fluorescent protein along with the protein of interest. After choosing the correct population according to size and granularity in forward scatter (FSC) and sideward scatter (SSC), the cells containing the fluorescent protein were identified and sorted. These cells were kept in culture for at least one day to recover from the sorting stress and then used for *in vitro* and *in vivo* assays. FACS was also used to analyze cells after Annexin V or BrdU staining. Furthermore, engrafted and diseased mice were characterized by FACS through surface marker staining.

3.22. Sorting of Hematopoietic Subpopulations

Expression of LEF1 isoforms throughout the hematopoietic hierarchy was analyzed. For this, two to three cord blood samples were pooled per experiment to ensure sufficient amount of $CD34^-$ and $CD34^+$ HSCs for sample processing and sorting. The subpopulations were sorted with the following procedure:

- $CD34^-CD38^-CD93^{high}$: Lineage depletion followed by CD34 depletion, gating for Lin^-, $CD34^-$, $CD38^-$, $CD45RA^-$, $CD93^{high}$
- $CD34^+$ HSCs: CD34 enrichment or $CD34^+$ cells from $CD34^-CD38^-CD93^{high}$, gating for Lin^-, $CD34^+$, $CD38^-$, $CD45RA^-$, then sorting the four populations as $CD49f^{-/+}$ and $CD90^{-/+}$
- MPPs: CD34 enrichment, gating for $CD34^+$, $CD38^-$, $CD45RA^-$, $CD90^-$
- LMPPs: CD34 enrichment, gating for $CD34^+$, $CD38^-$, $CD45RA^+$, $CD90^-$
- CMPs: CD34 enrichment, gating for $CD34^+$, $CD38^+$, $CD45RA^-$, $CD110^-$
- GMPs: CD34 enrichment, gating for $CD34^+$, $CD38^+$, $CD45RA^+$, $CD110^-$
- T cells: out of Lin^+ cells left over from the HSCs, gating for $CD2^+$, $CD3^+$, $CD16^+$, $CD19^-$, $CD56^+$
- B cells: out of Lin^+ cells left over from the HSCs, gating for $CD2^+$, $CD3^-$, $CD16^-$, $CD19^+$, $CD56^-$
- NK cells: out of Lin^+ cells left over from the HSCs, gating for $CD2^+$, $CD3^-$, $CD16^+$, $CD19^-$, $CD56^+$
- Dendritic cells: out of Lin^+ cells left over from the HSCs, gating for $CD123^+$, $CD11b^+$, $CD14^-$, $CD15^-$, $CD16^+$

- Macrophages: out of Lin^+ cells left over from the HSCs, gating for $CD123^-$, $CD11b^+$, $CD14^+$, $CD15^+$, $CD16^+$
- Granulocytes: out of Lin^+ cells left over from the HSCs, gating for $CD123^+$, $CD11b^+$, $CD14^+$, $CD15^+$, $CD16^+$

The sorted cells were further processed for qRT-PCR using the Arcturus PicoPure RNA extraction and Sensiscript cDNA synthesis Kits.

3.23. Proliferation Assay

After sorting of positively transduced cells or after performing LEF1-β-catenin binding inhibition, a certain number of cells was kept in culture to determine the changes in proliferation compared to the control cells. At d0 per experimental arm 200.000 cells were plated in 5ml medium. The cells were counted every 1-2 days for 3-8 days depending on the experimental design. Counting was performed using the Vi-Cell or hemacytometer.

3.24. Colony-Forming Cell (CFC) Assay

To further analyze the changes induced through LEF1 knockdown or LEF1-β-catenin binding inhibition, the colony-forming potential of the cells was tested. Each experimental arm was plated in duplicates and 300-660.000 cells were used, depending on the cell type. CFCs of leukemic cell lines was performed with 1000 cells per plate or the d0 equivalent, using H4330 methylcellulose and 6 well plates. Since SKNO1 cells do not form colonies, CFC assays were not performed for this cell line. For $CD34^+$ cord blood cells, 100 cells were plated per well in H4434. Primary patient samples were plated in H4434, using 220.000 cells per well. Murine bone marrow cells overexpressing AML1-ETO, Lef1WT or both were plated in M3434 methylcellulose, plating 500 cells per well. The colonies were counted after incubation at 37°C in the incubator for 14 days for human material, murine CFCs were counted after 7 days and re-plated twice.

3.25. Annexin V Apoptosis Assay

Knockdown and treatment of certain genes and proteins may have anti-proliferative effects. To further define, whether this effect is due to apoptosis, the Annexin V apoptosis assay was performed according to the manufacturers protocol. Annexin V usually binds to early apoptotic cells, showing the respective antigen on the surface. The co-staining with 7-Aminoactinomycin (7-AAD) is used to determine late apoptotic and necrotic cells, since it intercalated with the DNA. Briefly, the cells were washed and suspended in 1X Binding Buffer. Afterwards Annexin V APC and 7-AAD were added to the samples. Single color controls and a dead cell control were used at every analysis to set the gates properly.

3.26. BrdU Cell Cycle Assay

The anti-proliferative effect of knockdown and treatment may also affect the cell cycle of the cells. To determine whether the effect is due to changes in the cell cycle, BrdU cell cycle staining was performed according to the manufacturers protocol. Here, the cells were starved for 16h with RPMI medium containing only 1% FBS to synchronize the cells. Afterwards the cells cycled for 24h in normal culture medium while application of the compounds or peptides. The cells were treated with the BrdU reagent for 30min, fixed and permeabilized. The anti-BrdU antibody was added, total DNA staining was performed using 7-AAD. The stained cells were analyzed for their distribution in G0/G1, S and G2/M phases. In case of compound treated cells cell cycle analysis was measured using the Nucleocounter NC-250, which was available at our institute. Cell cycle staining was performed according to the two-step cell cycle analysis protocol using NC-Slide A8™ slides. First, the cells were washed with 1X DPBS and suspended in lysis buffer (solution 10) supplemented with DAPI, followed by incubation at 37°C for 5min. Afterwards the stabilization buffer (solution 11) was added and the samples were loaded on the slides. The cells could be distinguished in their cell cycle status dependent on their DNA signal intensity using the NucleoView™ NC-250 software.

3.27. Mouse Experiments

For different purposes different mouse strains were used. Valid applications for all mentioned mouse strains and purposes were present (application numbers 1159, 1304, 1353, 1366). Transplantation of cell lines, primary patient and cord blood cells was done in NOD.Cg-Prkdc<scid>Il2rg <tm1Wjl>/SzJ (NSG) mice. These mice were sub-lethally irradiated with 3.25Gy and treated intraperitoneally (i.p.) with IvIG 24h prior to transplantation. Overexpression of Lef1 and AML1-ETO was done on 5-FU BM taken from donor C57Bl/6Ly-Pep3bxC3H/HeJ (Pep) or C57Bl/6JxC3H/HeJ (Bl6) mice and re-transplanted into Pep or Bl6 mice. Before transplantation the Pep and Bl6 mice were lethally irradiated with 12Gy. Transplantation of cells was always performed intravenously (i.v.). Mice transplanted with AML and $CD34^+$ CB cells were sacrificed 14 weeks after transplantation to ensure long-term engraftment. All other mice were sacrificed once severely diseased.

The mice were prepared according to the following procedure: The mice were sacrificed using CO_2 followed by cervical dislocation. The bones of legs and the hips were taken out, as well as the spleen. Peripheral blood (PB) was extracted from the heart with a syringe prepared with EDTA to prevent coagulation. The spleen was weighed on a special accuracy weighing machine. For mice which were planned to be sent for histopathological analysis each half of the spleen and one femur was stored in 4% formalin, as well as the rest of the mouse. BM cells were extracted from the bones by crushing and washing with the help of a 40µm cell strainer. A single cell suspension was obtained from the spleen by pressing the organ through a 40µM cell strainer with the help of a syringe plunger. All cell suspensions and the pure PB were analyzed using the HemaVet. For experiments where the blast cell count was relevant, cytospin of bone marrow cells was performed. Per mouse two slides with each 150.000 WBCs were produced, as well as two blood smears. Engraftment analysis was performed in BM, samples from mice transplanted with primary patient samples were stained for human CD45, CD13 and CD33 or CD45, CD15, CD19, CD20 and CD33 in case of transplantation with $CD34^+$ CB cells. Analysis of engraftment of AML1-ETO and Lef1WT was performed according to the fluorescent signal of the vector, in addition the following CD markers were stained and analyzed via FACS to further determine the kind of leukemia: B220, CD4, CD8, CD19, cKit, G1, Mac1, Sca1.

Comparison of WBC counts, RBC counts and spleen size of diseased mice transplanted with 5-FU BM co-expressing AML1-ETO and Lef1WT to the corresponding values of healthy mice was performed. Here, the healthy C57BL/6J standard values were obtained from the Jax website [102].

3.28. Counting of Blasts in Murine Bone Marrow Cytospins

To determine, whether the mice were diseased with leukemia, the bone marrow cytospins were stained using May-Gruenwald-Giemsa staining. The slides were stained with May-Gruenwald reagent for 3min, washed for 5min in tap water and then stained for 1h in Giemsa solution. The slides were washed twice for 5min in tap water and then air dried. Blast counting was performed using the Nikon Eclipse Ti microscope with 100X magnification and immersion oil. Per slide, 50-100 cells were counted depending on the quality of the sample and the percentage of blasts was monitored.

3.29. Statistical Analysis

Statistical significances were calculated using the GraphPad Prism 7 software. This software was also used to create all graphs. The performed tests depended on the experiment and are noted in the respective legends. The alpha value used for calculations was always 0,05, significance was achieved when * = $p \leq 0.05$, ** = $p < 0.01$, *** = $p < 0.001$, **** = $p < 0,0001$.

4. Results

4.1. Analysis of LEF1 Expression and its Knockdown in AML Cell Lines

Expression of LEF1 was shown to be important for several AML cells [75, 90]. The AML cell lines chosen for further experiments for this thesis were OCI-AML3 as cell line with normal karyotype, SKNO1 harboring the AML1-ETO fusion gene and THP1 as MLL-AF9 fusion gene positive cell line and fast readout in the murine xenograft model. All cell lines were analyzed for their LEF1 expression (s. Figure 12).

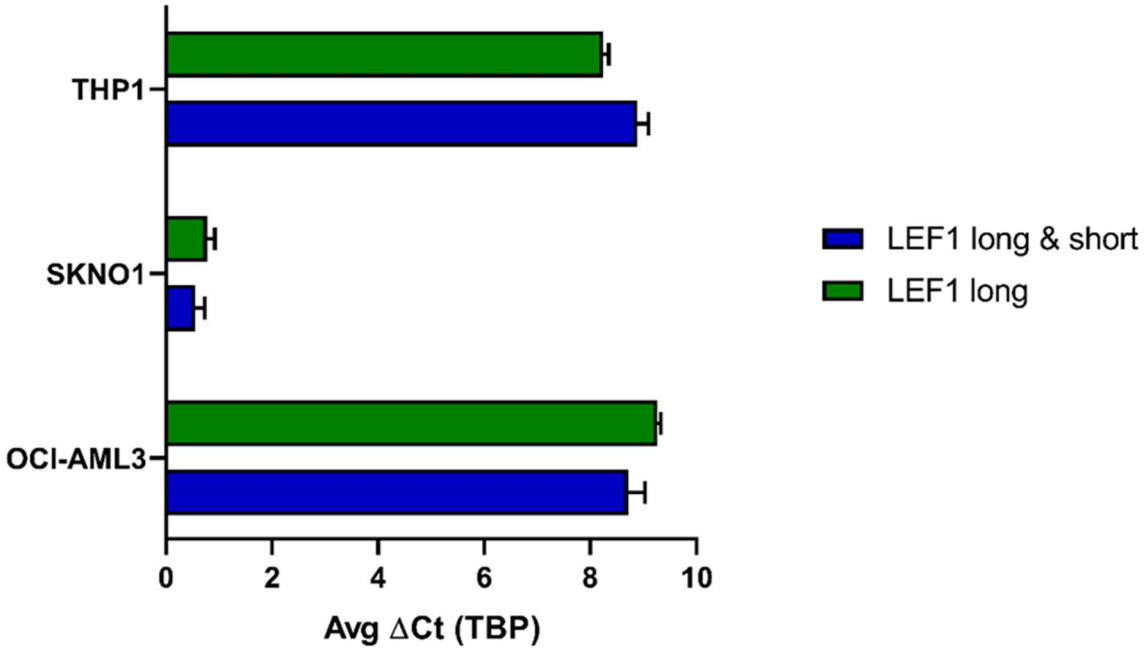

Figure 12: Expression analysis of LEF1 isoforms by qRT-PCR in the AML cell lines OCI-AML3, SKNO1 and THP1, n=3, values shown as mean + SEM after normalization to the housekeeping gene TBP (according to [26]). The expression is shown as Avg ΔCt, meaning the higher the value the lower is the expression.

The overall expression of LEF1 was lower in OCI-AML3 and THP1, but higher in SKNO1, since a lower Avg ΔCt values always indicates higher expression. In all three cell lines LEF1 was exclusively expressed as the long isoform. To confirm the importance of orderly LEF1 expression in the AML cell lines used in this thesis, shRNA mediated knockdown was performed (s. Figure 13).

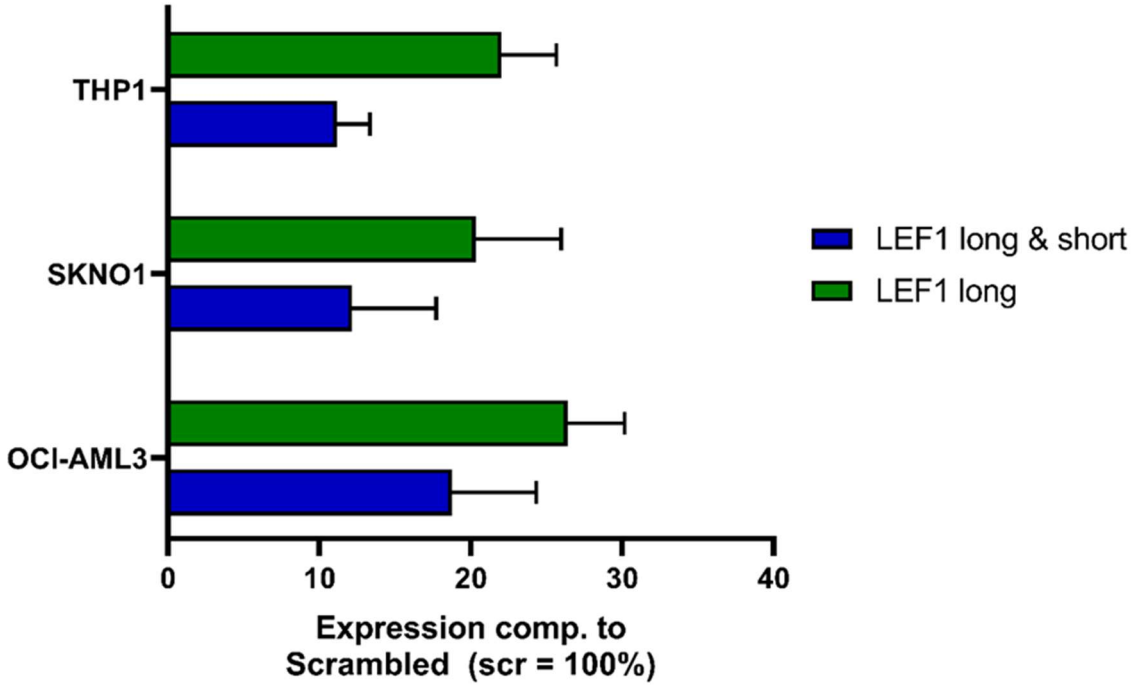

Figure 13: Analysis of LEF1 expression by qRT-PCR after shRNA mediated knockdown in OCI-AML3, SKNO1 and THP1, n=3, values shown as mean +SEM.

The knockdown reduced the expression of LEF1 in all three cell lines. The expression of both LEF1 isoforms was reduced to 18,75% (± 7,87%) in OCI-AML3, 12,15% (± 7,88%) in SKNO1 and 11,16% (± 3,11%) in THP1. The expression of the long isoform was reduced to 26,4% (± 5,34%) in OCI-AML3, 20,32% (± 8,02%) in SKNO1 and 22,03% (± 5,13%) in THP1.

To determine the role of LEF1 for these cell lines, proliferative and colony-forming capacities were tested after knockdown (s. Figures 14 and 15).

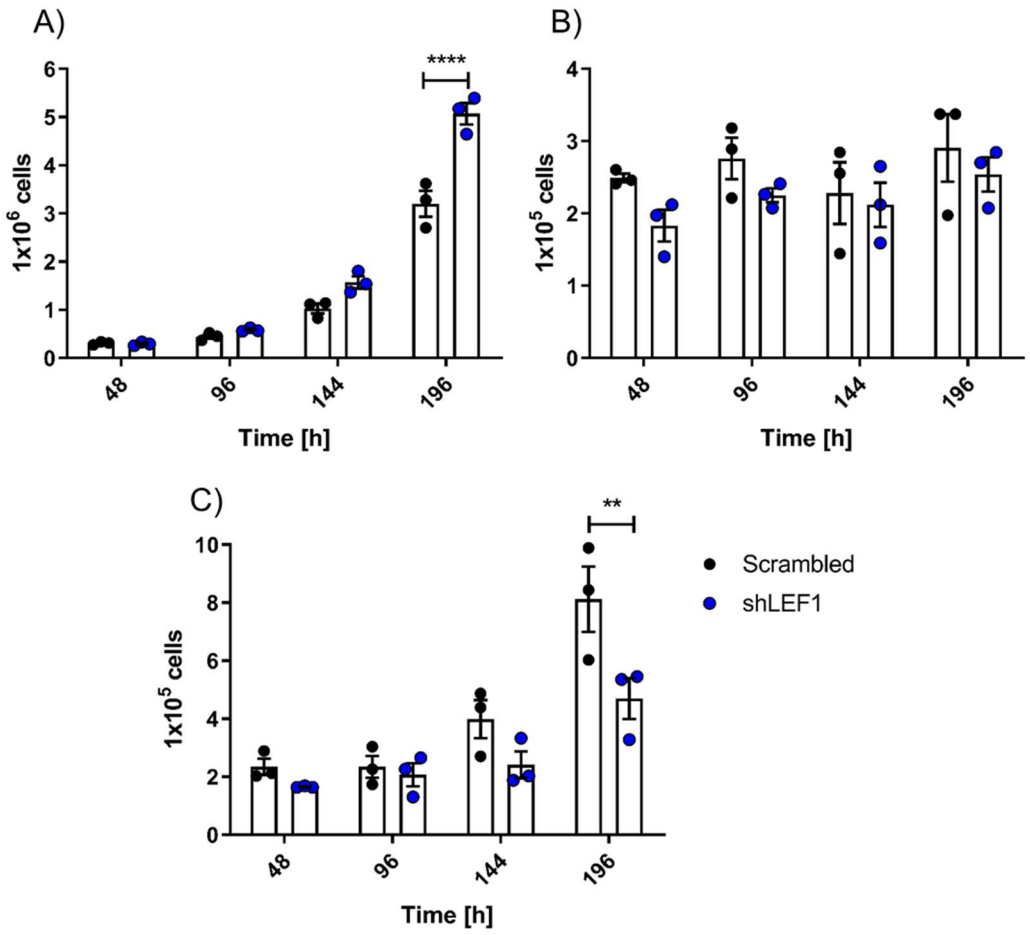

Figure 14: Proliferation of OCI-AML3 (A), SKNO1 (B) and THP1 (C) after shRNA mediated knockdown of LEF1, n=3, values shown as mean + SEM. Significances were calculated using Dunnett's multiple comparisons test, p<0,01 = **, p<0,0001 = ****.

The changes in proliferative potential of the cells lines after knockdown were very heterogeneous. In case of OCI-AML3, knockdown of LEF1 did not reduce the proliferation, but rather enhanced it significantly after 196h (p<0,0001). SKNO1 cells did not grow in culture after sorting, but slightly reduced proliferation of LEF1 knockdown SKNO1 cells versus the Scrambled control is visible as a trend. For THP1 a significant reduction in proliferative potential was found after 196h (p<0,001).

The effects of LEF1 knockdown on the colony-forming capacity was analyzed in the CFC assay (s. Figure 15).

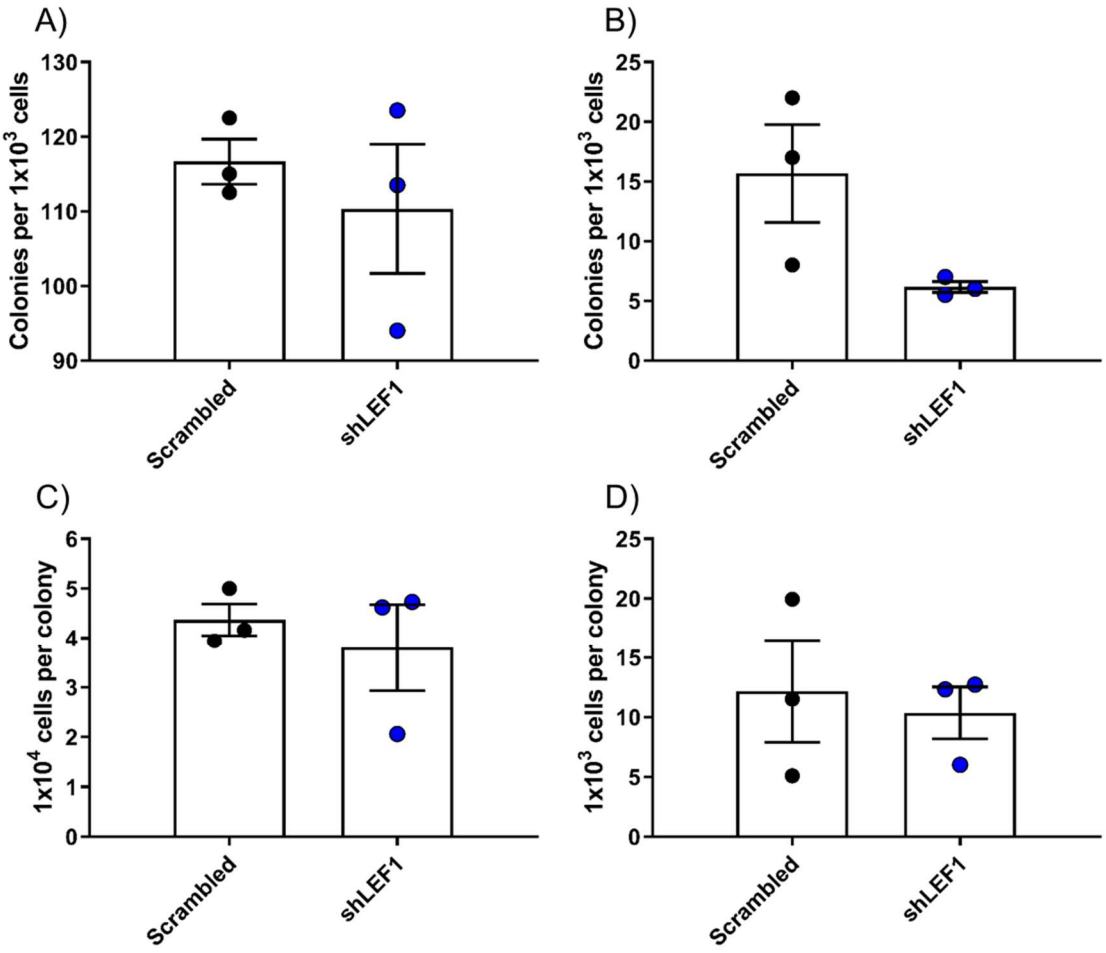

Figure 15: Colony-forming potential of OCI-AML3 (A) and THP1 (B) and cells per colony of OCI-AML3 (C) and THP1 (D) after shRNA mediated knockdown of LEF1, n=3, values shown as mean + SEM.

Here, no significant reduction of colony-forming potential was found for neither OCI-AML3 nor THP1, but in case of THP1 a reduced colony-forming potential in the LEF1 knockdown cells is noticeable as a trend. For both cell lines, the number of cells per colony was not significantly changed after LEF1 knockdown.

To further determine, whether the effect of the knockdown on proliferative potential was due to increased apoptosis or changes in the cell cycle, both possibilities were tested. Analysis of apoptosis was performed by Annexin V staining (s. Figure 16).

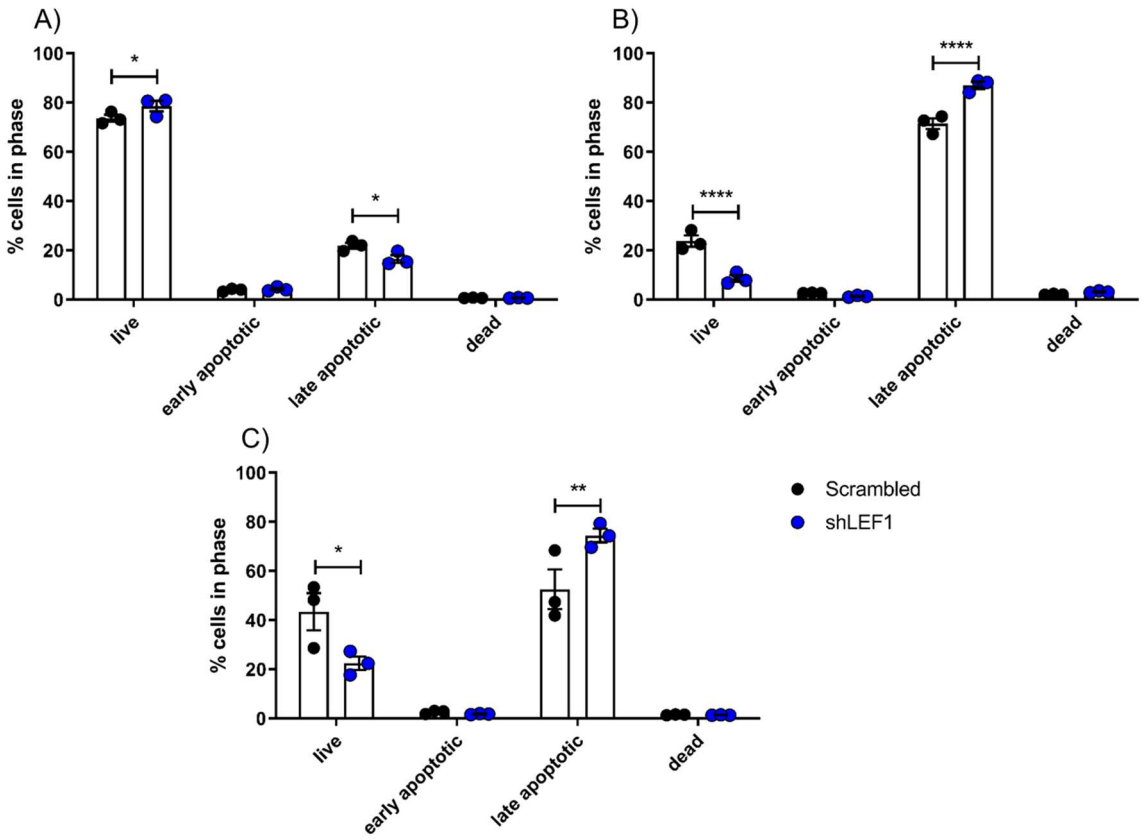

Figure 16: Apoptosis assay of OCI-AML3 (A), SKNO1 (B) and THP1 (C) after knockdown of LEF1, n=3, values shown as mean + SEM. Significances were calculated using Tukey's multiple comparisons test, p<0,05 = *, p<0,01 = **, p<0,0001 = ****.

The knockdown led to significantly increased levels of late apoptotic cells for SKNO1 rising from 71,43% (±1,97%) to 87,03% (±2,09%) (p<0,0001) and for THP1 from 52,57% (±11,42%) to 74,40% (±3,96%) (p<0,01). The portion of living cells significantly dropped from 23,77% (±3,23%) to 8,53% (±1,86%) for SKNO1 (p<0,0001) and from 43,40% (±10,68%) to 22,47 (±3,92%) for THP1 (p<0,05). For these both cell lines, no significant changes were detected in early apoptotic and dead cells in the LEF1 knockdown cells versus the scrambled control. In case of OCI-AML3 cells the effect was adverse, the portion of living cells was increased (p<0,05) and the portion of late apoptotic cells (p<0,05) was decreased. This confirmed that the reduction in proliferative and colony forming potential of the THP1 cell line was at least partly due to increased apoptosis.

To determine the effect of LEF1 knockdown on the cell cycle, BrdU staining was performed (s. Figure 17).

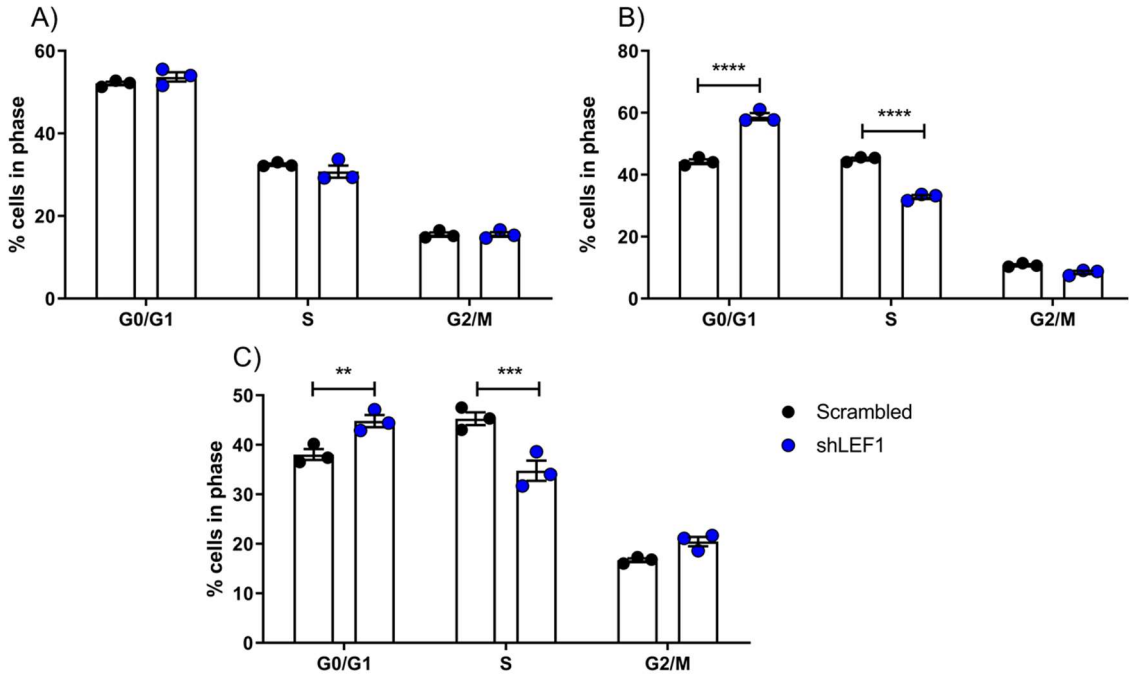

Figure 17: Cell cycle assay of OCI-AML3 (A), SKNO1 (B) and THP1 (C) after knockdown of LEF1, n=3, values shown as mean + SEM. Significances were calculated using Tukey's multiple comparisons test, p<0,05 = *, p<0,01 = **, p<0,001 = ***, p<0,0001 = ****.

Here, no significant changes were found for the OCI-AML3 cell line. In case of SKNO1 and THP1, the portion of cells in G0/G1 phase was significantly increased and the portion of cells in S phase significantly decreased. To be exact, in SKNO1 the portion of cells in G0/G1 phase increased from 44,21% (±1,10%) to 58,77% (±1,57%) (p<0,0001) in the LEF1 knockdown cells, whereas the S phase decreased from 45,01% (±1,27%) to 32,79% (±0,88%) (p<0,0001). In THP1 cells the rate of cells in G0/G1 phase rose from 38,04% (±1,56%) to 44,80% (±1,76%) (p<0,01) and percentage of cells in S phase dropped from 45,45% (±5,60%) to 34,75% (±2,84%) (p<0,001) in the LEF1 knockdown cells. Overall, cycling of the cells was found to be inhibited due to a reduced transition of cells from G0/G1 to S phase.

Knockdown of LEF1 in THP1 and SKNO1 reduced their proliferative potential, apoptosis was enhanced and the cell cycling was perturbed. Taken together, orderly LEF1 expression and with this intact Wnt signaling is essential for proper function of these AML cell lines.

4.2. Most Immature CD34$^-$ Human HSCs Exclusively Express the Short Isoform of LEF1 in Contrast to Leukemic Samples

To get insight in the LEF1 isoform expression pattern throughout the whole hematopoietic hierarchy, HSC populations ranging from most immature CD34$^-$ to HSC populations containing also MPPs were sorted out of human cord blood together with more differentiated cells, ranging from progenitor cells to terminally differentiated cells (s. Figure 18).

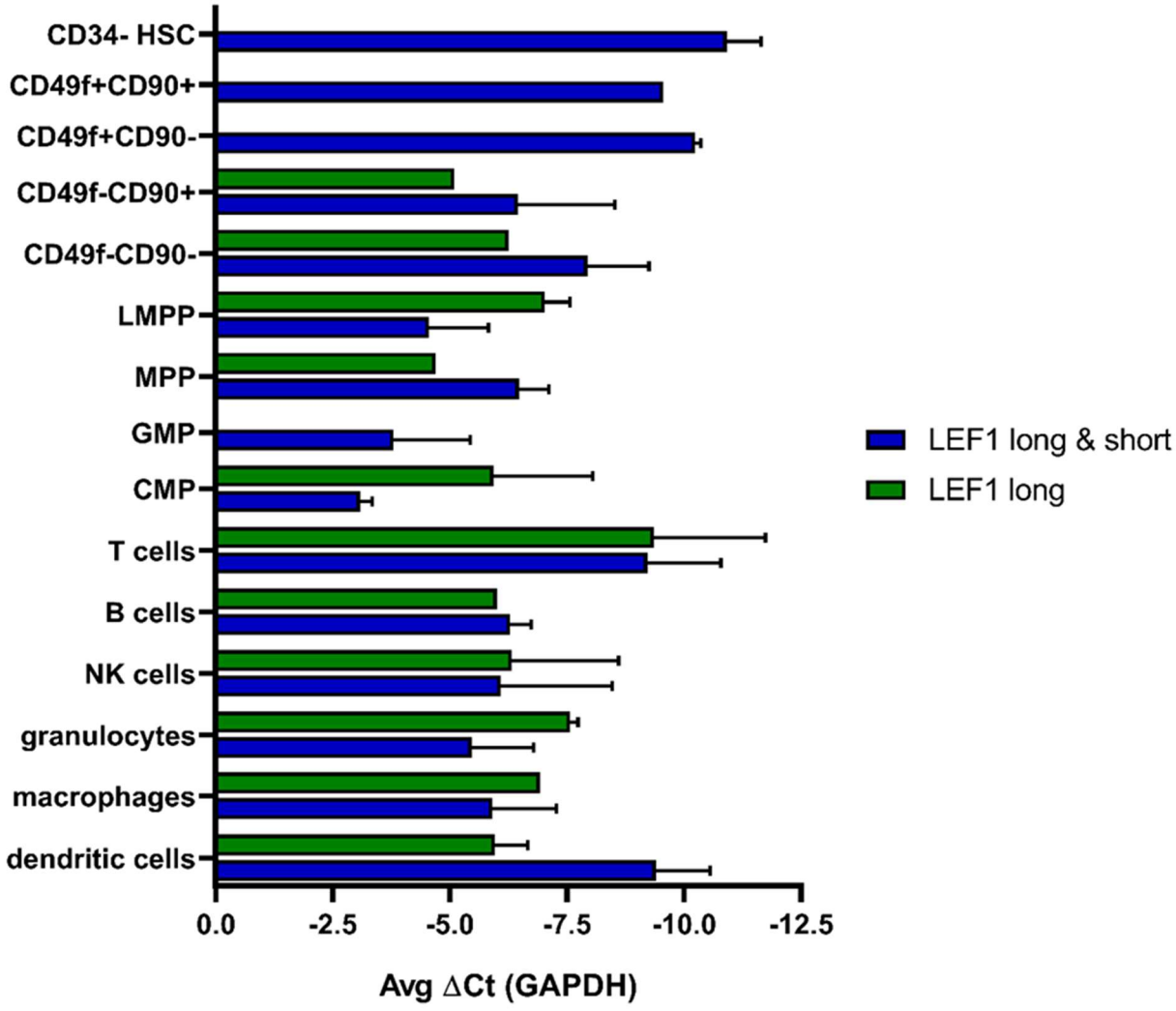

Figure 18: qRT-PCR analysis of the expression of LEF1 isoforms throughout the hematopoietic hierarchy after normalization to the housekeeping gene GAPDH n=3, values shown as mean + SEM (according to [26]). The expression is shown as Avg ΔCt, meaning the higher the value the lower is the expression.

The qRT-PCR analysis revealed exclusive expression of ΔNLEF1 in CD34$^-$ HSCs with emerging expression of the long isoform during HSC "maturation". CD49f was used as a classical stem cell marker, whereas loss indicated a more MPP like cell.

$CD49f^+CD90^+$ stem cells exclusively expressed the short isoform of LEF1, as well as $CD49f^+CD90^-$ cells. The cells lacking the CD49f presence showed emerging expression of the long isoform of LEF1. On the level of progenitor (LMPPs, MPPs, GMPs and CMPs) to terminally differentiated cells, nearly exclusively the long isoform of LEF1 was expressed.

Since malignant cells were found to exclusively express the long isoform of LEF1 and being crucially dependent on its expression, whereas most immature HSCs expressed only the short isoform, there was a clear difference in isoform expression between normal and leukemic AML stem cells. This implicated that AML stem cells are more vulnerable to approaches which impair the interaction between β-catenin and the long LEF1 isoform compared to normal HSCs.

4.3. Disturbance of Wnt Signaling by Inhibiting LEF1-β-Catenin Binding Leads to Impairment of AML Cell Line *in Vitro* Properties

Based on the results of isoform expression in normal versus leukemic stem cells, we tested approaches which target interaction between the long isoform of LEF1 with β-catenin in leukemic cells. The two small-molecule inhibitors Calphostin C and Cercosporin (2003 screen paper) and a synthetic peptide (2016 Hsieh) were tested, all interfering directly with the LEF1-β-catenin binding. Calphostin C and Cercosporin were already shown to effectively disrupt binding of LEF1 and β-catenin binding in CML samples (2011 Kreutzer). The synthetic peptide TAT-NLS-BLBD-6 was used to avoid the problem of off-target effects by the compounds mentioned before, since it consists of a part of the binding sequence of LEF1 to β-catenin and thereby should not show any additional activity. TAT-NLS-BLBD-6 was already tested in breast cancer cells and the ability to effectively disrupt binding of LEF1 to β-catenin was confirmed (Hsieh 2016).

Also in our hands, the disruption of LEF1 and β-catenin binding after application of Calphostin C and Cercosporin was confirmed by Co-Immunoprecipitation in 293T HEK cells (s. Figure 19).

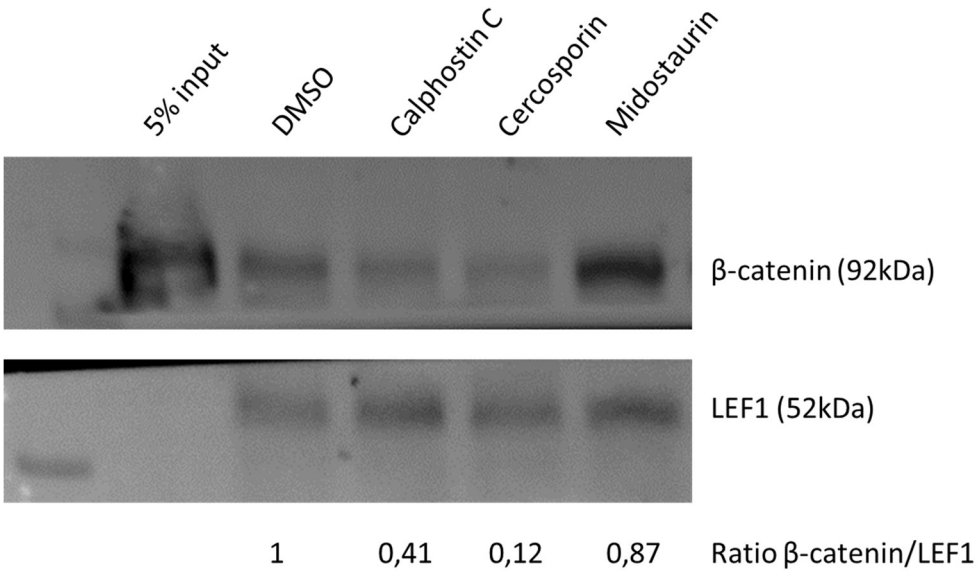

Figure 19: Western Blot of the Co-IP of LEF1 and β-catenin in lysates of 293T HEK cells overexpressing LEF1WT. Treatment with the LEF1-β-catenin inhibitors was performed o/n at 4°C and reduced the intensity of the β-catenin band in contrast to the PKC inhibitor Midostaurin. Band intensity ratios were calculated using the ImageJ software.

Upon treatment with Calphostin C and Cercosporin the ratio of β-catenin to LEF1 was drastically reduced. Since both of the compounds are PKC inhibitors, another PKC inhibitor was tested in addition for its LEF1-β-catenin binding inhibition property. As treatment control the well-known PKC inhibitor Midostaurin was used, which was recently FDA-approved in treatment of FLT3 length mutation positive AML (Döhner 2017 NEJM, 2017 Stone, 2019 Schlenk). Midostaurin did not affect the LEF1-β-catenin binding, confirming that this effect is specific to the other two compounds and not due to a general effect of PKC inhibitors.

Since Calphostin C and Cercosporin effectively reduced binding of LEF1 to β-catenin, we next tested the functional relevance of this pharmacological approach in appropriate assays. DMSO is the solvent of both compound and pure DMSO was used as a solvent control. Additionally, *in vitro* assays were performed after treatment with the TAT-NLS-BLBD-6 active peptide versus the TAT-NLS-BLBD-6m control peptide. These peptides were dissolved in 1X DPBS, which was used as a solvent control.

IC50 calculation was performed after treatment with the inhibitors, confirming a high sensitivity of the cell lines towards the compounds, since all of the IC50 values were within a nano molar range (s. Table 20).

Table 20: IC50 values from OCI-AML3, SKNO1 and THP1 after treatment with the LEF1-β-catenin binding inhibitors Calphostin C or Cercosporin.

	IC50 Calphostin C [nM]	IC50 Cercosporin [nM]
OCI-AML3	111,41	396,35
SKNO1	316,31	201,75
THP1	145,87	269,10

To test the effects of the inhibitors on the proliferative potential, the cell lines were treated with 10nM, 100nM and 1000nM of either of the inhibitors versus DMSO. Application of the compounds reduced the proliferative potential of AML cell lines in a concentration dependent manner (s. Figure 20).

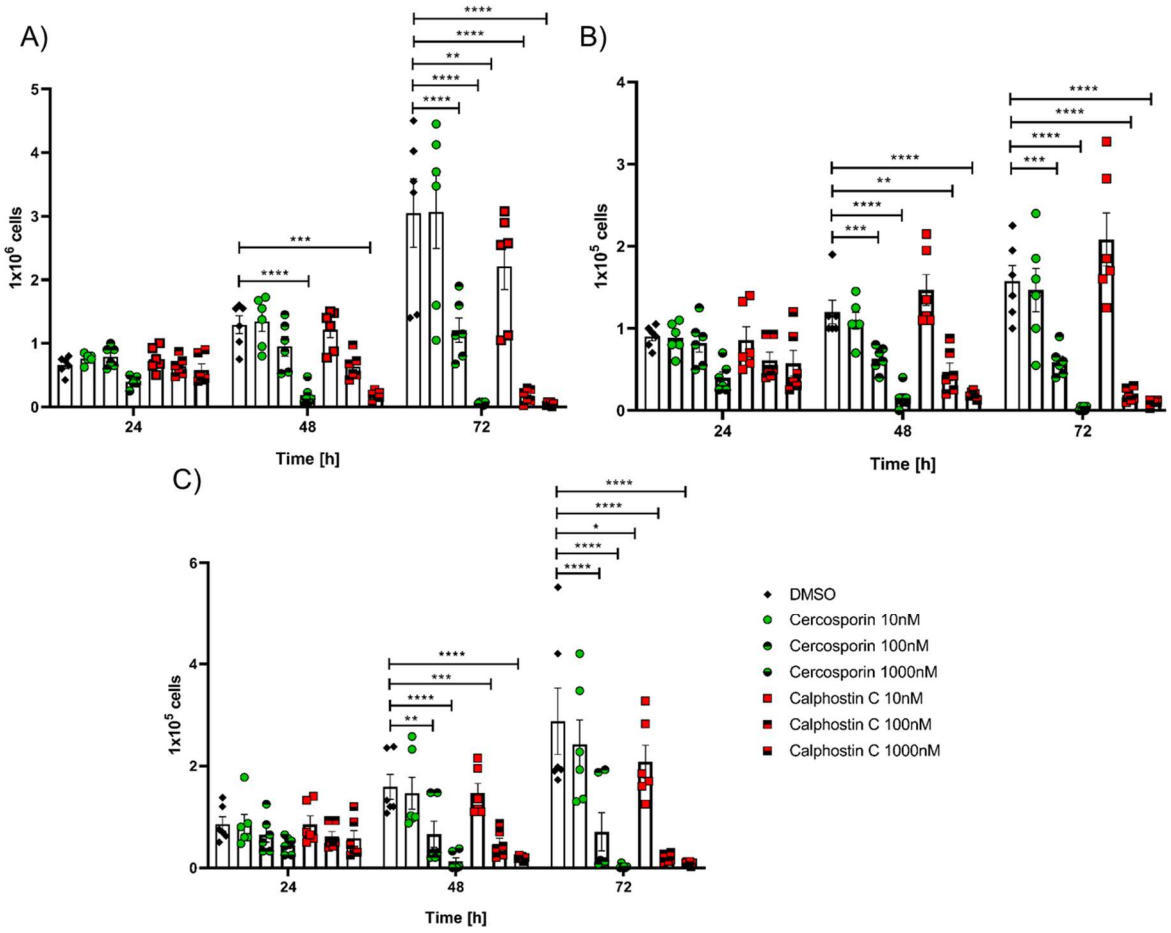

Figure 20: Proliferation of OCI-AML3 (A), SKNO1 (B) and THP1 (C) after application of Calphostin C or Cercosporin in different concentrations, n=3, values shown as mean + SEM (according to [26]). Significances were calculated using Dunnett's multiple comparisons test, p<0,05 = *, p<0,01 = **, p<0,001 = ***, p<0,0001 = ****.

Already after 48h of treatment, the proliferation of all three cell lines was severely and significantly decreased. Application of TAT-NLS-BLBD-6 also effectively reduced the proliferation (s. Figure 21).

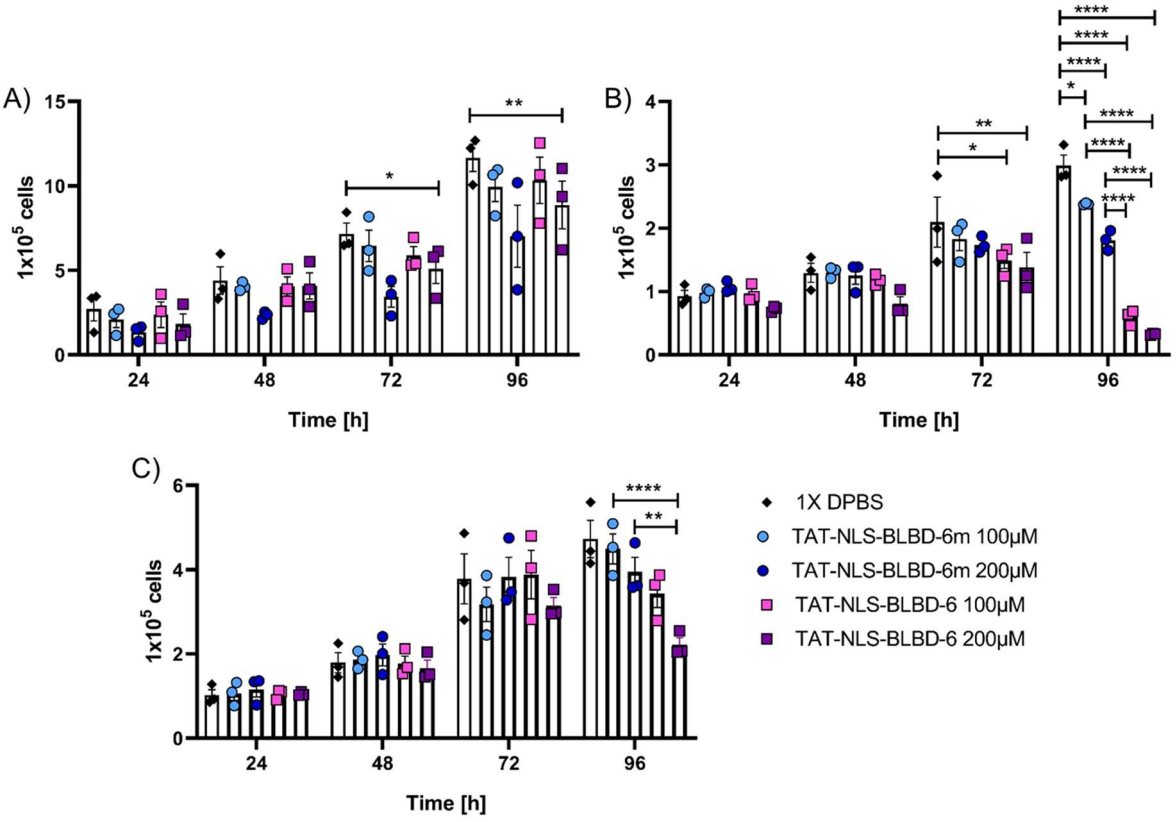

Figure 21: Proliferation of (A) OCI-AML3, (B) SKNO1 and (C) THP1 after application of the active peptide TAT-NLS-BLBD-6, the control peptide TAT-NLS-BLBD-6m or the solvent control 1X DPBS, n=3, values shown as mean + SEM. Significances were calculated using Tukey's multiple comparisons test, p<0,05 = *, p<0,01 = **, p<0,001 = ****, p<0,0001 = ****.

As proliferation of OCI-AML3 cells treated with TAT-NLS-BLBD-6m after 96h significantly decreased when compared to the 1X DPBS control, it seems that the control peptide also had a slight activity in this assay. In case of the SKNO1 and THP1 cell lines, proliferation after treatment with the active peptide TAT-NLS-BLBD-6 was significantly reduced compared to the TAT-NLS-BLBD-6m control after 96h of treatment.

The next step was to assess the effect of all approaches on the colony-forming potential of the cell lines. Both the compounds reduced the colony-forming potential of the cell lines significantly compared to the DMSO control (s. Figure 22).

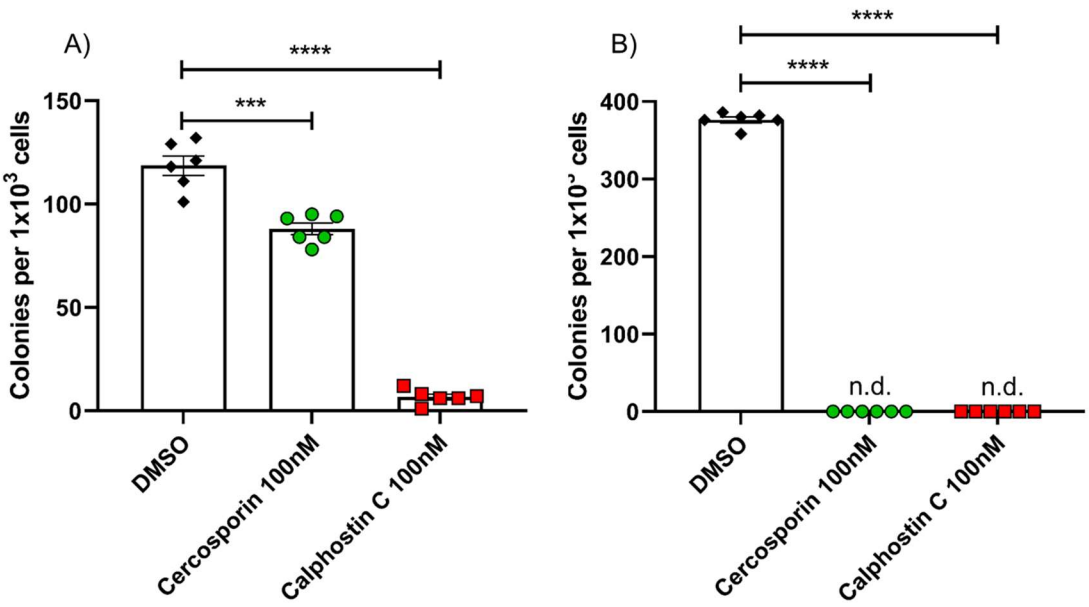

Figure 22: Colony-forming potential of OCI-AML3 (A) and THP1 (B) after application of 100nM Calphostin C or 100nM Cercosporin, n=3, values shown as mean + SEM (according to [26]). In THP1 no colonies could be determined (not determined = n.d.) after treatment. Significances were calculated compared to the DMSO control using Dunnett's multiple comparisons test, p<0,001 = ***, p<0,0001 = ****.

The reduction of colony-forming potential in OCI-AML3 cell line was 25,84% (p<0,001) for 100nM Cercosporin and 94,38% (p<0,0001) in case of 100nM Calphostin C, in THP1 100% (p<0,0001) for both inhibitors. The THP1 cell line completely lost the colony-forming potential (p<0,0001) after treatment with 100nM of either of the compounds.

After treatment of the cell lines with TAT-NLS-BLBD-6 a significant decrease of colony-forming potential was found (s. Figure 23).

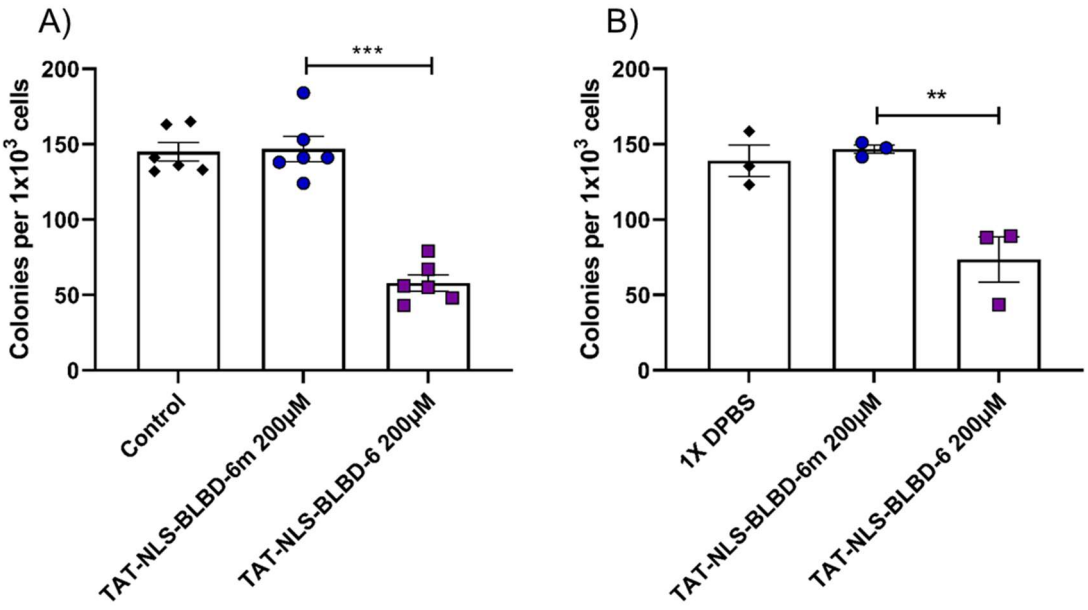

Figure 23: Colony-forming potential of OCI-AML3 (A) and THP1 (B) after application of 200µM of the active peptide TAT-NLS-BLBD-6, 200µM of the control peptide TAT-NLS-BLBD-6m or the 1X DPBS control, n=3, values shown as mean + SEM (according to [26]). Significances were calculated using Tukey's multiple comparisons test, $p<0,01$ = **, $p<0,001$ = ***.

In the CFC assay, the TAT-NLS-BLBD-6m control peptide did not affect the activity of the AML cells at all. The colony forming potential of OCI-AML3 treated with BLBD-6 was reduced by 60,50% ($p<0,001$) compared to the BLBD-6m peptide treated cells. In THP1 cells treatment with the active peptide reduced the colony-forming potential by 48,89% ($p<0,001$) compared to the control peptide.

Even though the number of colonies was decreased, the amount of cells per colony was increased significantly (s. Figure 24) by 81,82% compared to the TAT-NLS-BLBD-6m treatment ($p<0,05$) in the OCI-AML3 cell line. For the THP1 cell line the number of cells per colony is not significantly changed between the experimental arms.

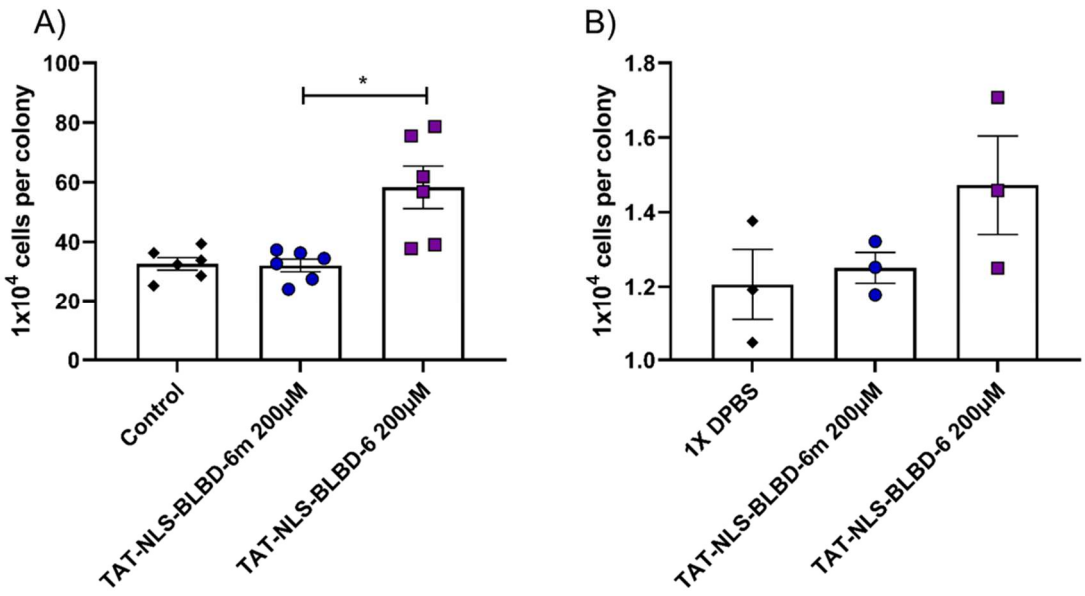

Figure 24: Number of cells per colony in the CFC assay of (A) OCI-AML3 and (B) THP1 after treatment with either the 1X DPBS control, BLBD-6m control peptide or BLBD-6 active peptide, n=3, values shown as mean + SEM. Significances were calculated using Tukey's multiple comparisons test, $p<0,05$ = *.

Taken together, the compounds as well as the peptides effectively reduced proliferative and colony-forming potential of the cells. This further confirms an essential role of orderly LEF1 expression and Wnt signaling for AML cell lines.

4.4. Inhibition of LEF1 Binding to β-Catenin Affects Apoptosis and Cell Cycle of AML Cell Lines

To further investigate whether the loss of proliferative and colony-forming potential after treatment was due to apoptosis or changes in the cell cycle, Annexin V apoptosis staining and BrdU cell cycle staining was performed. First, the effect on apoptosis was analyzed (s. Figure 25).

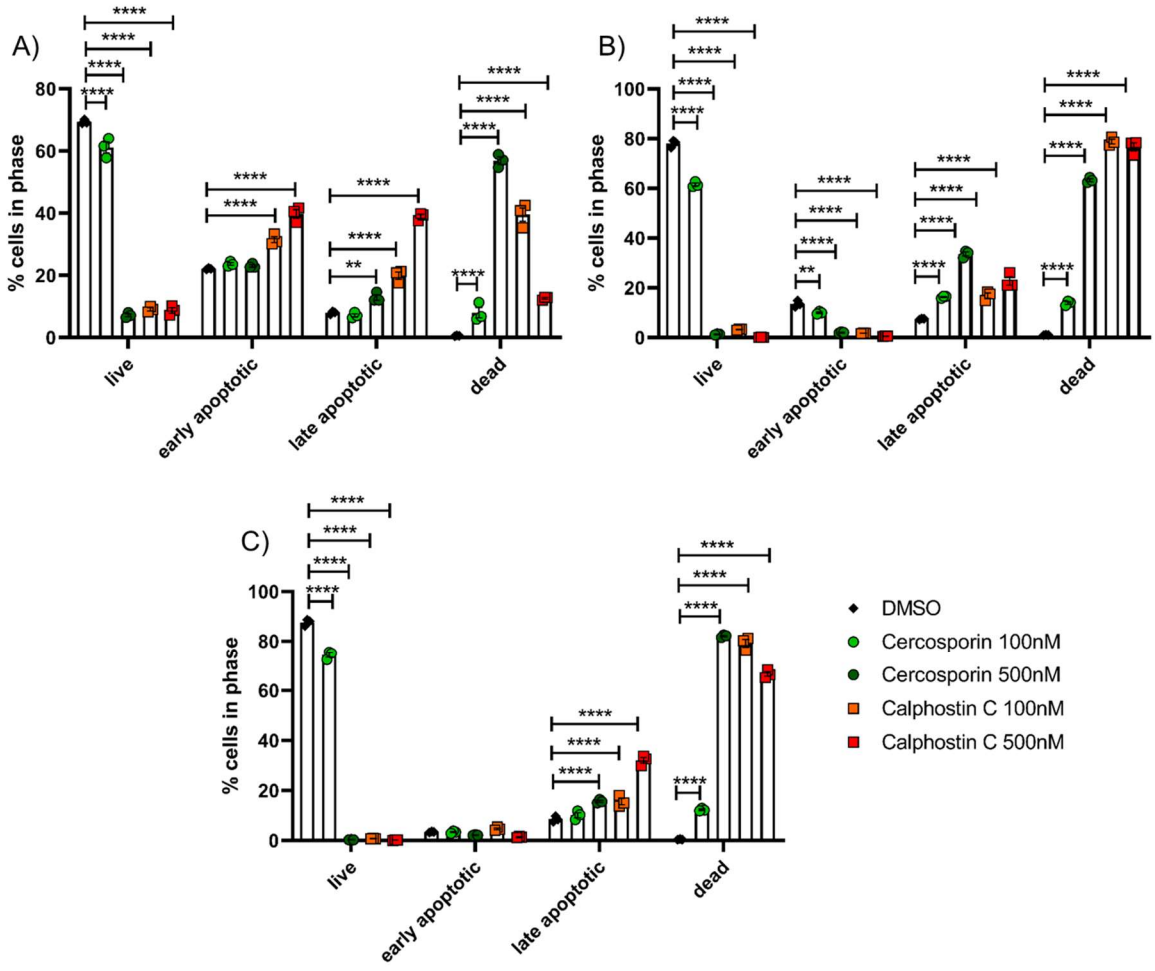

Figure 25: Apoptosis assay of (A) OCI-AML3, (B) SKNO1 and (C) THP1 after treatment with 100nM or 500nM of Calphostin C or Cercosporin versus DMSO, n=3, values shown as mean + SEM (according to [26]). Significances were calculated compared to the DMSO control using Dunnett's multiple comparisons test, p<0,01 = **, p<0,001 = ***, p<0,0001 = ****.

In the Annexin V apoptosis assay it was found, that reduction of the proliferative potential is accompanied by increased apoptosis. Already treatment with a low concentration of 100nM of either of the compounds for 24h significantly increased the number of late apoptotic as well as dead cells. The portion of cells in the early apoptotic stage was not significantly altered, but portion of cells in late apoptotic state and number dead cells were significantly increased. Treatment with 100nM Cercosporin reduced the number of living cells significantly by 8,20% in OCI-AML3, 16,47% in SKNO1 and 13,33% in THP1 compared to DMSO. No significant changes could be found with regard to early and late apoptotic cells, but the number of dead cells was significantly increased. Percentage of dead cells rose by 7,45% in OCI-AML3 (p<0,0001), 11,84% in SKNO1 (p<0,0001) and 12,83% in THP1 (p<0,0001) compared to DMSO.

In case of Calphostin C treatment with 100nM and 500nM concentration and treatment with 500nM Cercosporin, the number of living cells was reduced to ≤10% for all three cell lines ($p<0,0001$). This treatment also led to significant increase of number of cells in late apoptotic state ($p<0,0001$) and dead cells ($p<0,0001$) in all three cell lines.

The effect on apoptosis if the TAT-NLS-BLBD-6 peptide was also determined in the cell lines (s. Figure 26).

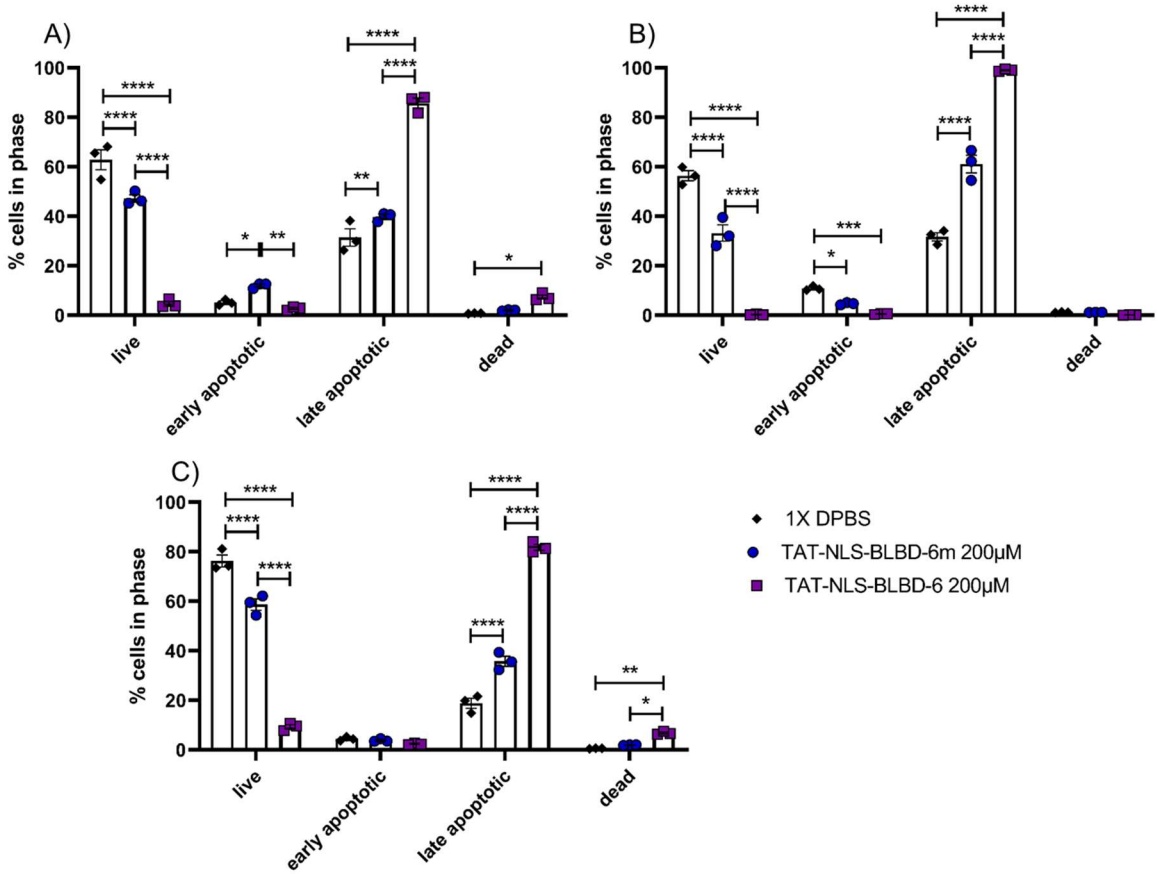

Figure 26: Apoptosis assay of (A) OCI-AML3, (B) SKNO1 and (C) THP1 after treatment with 200µM of TAT-NLS-BLBD-6 or TAT-NLS-BLBD-6m versus 1X DPBS, n=3, values shown as mean + SEM. Significances were calculated using Tukey's multiple comparisons test, $p<0,05$ = *, $p<0,01$ = **, $p<0,001$ = ***, $p<0,0001$ = ****.

In all of the cell lines, the proportion of living cells were significantly reduced not only compared to the 1X DPBS control but also to the TAT-NLS-BLBD-6m, whereas the early and late apoptotic and dead cells were significantly increased. Within the OCI-AML3 cell line, the portion of living cells significantly decreased ($p<0,0001$) from 47,23% (±2,13%) in TAT-NLS-BLBD-6m treated cells to 4,63% (±1,32%) for TAT-NLS-BLBD-6 treated cells, whereas the portion of late apoptotic cells significantly

(p<0,0001) rose from 39,80% (±1,42%) to 85,73% (±2,86%). The same result was obtained after treatment of SKNO1 and THP1 with the control and active peptide. In case of SKNO1, the percentage of living cells was reduced from 33,20% (±4,73%) after treatment with the control peptide to 0,27% (±0,20%) (p<0,0001) after treatment with the active peptide and the percentage of late apoptotic cells increased from 61,10% (±5,00%) to 99,03% (±0,37%) (p<0,0001). For THP1, the portion of late apoptotic cells increased significantly from 35,77% (±2,86%) in TAT-NLS-BLBD-6m treated cells to 81,73% (±1,70%) (p<0,0001) in the TAT-NLS-BLBD-6 treated cells, whereas the percentage of living cells was reduced from 58,67% (±3,20%) to 9,35% (±1,21%).

In addition, cell cycle analysis via FACS BrdU assay was performed with the compounds (s. Figure 27) and peptides (s. Figure 28) after serum starvation for synchronization, followed by 24h of cycling.

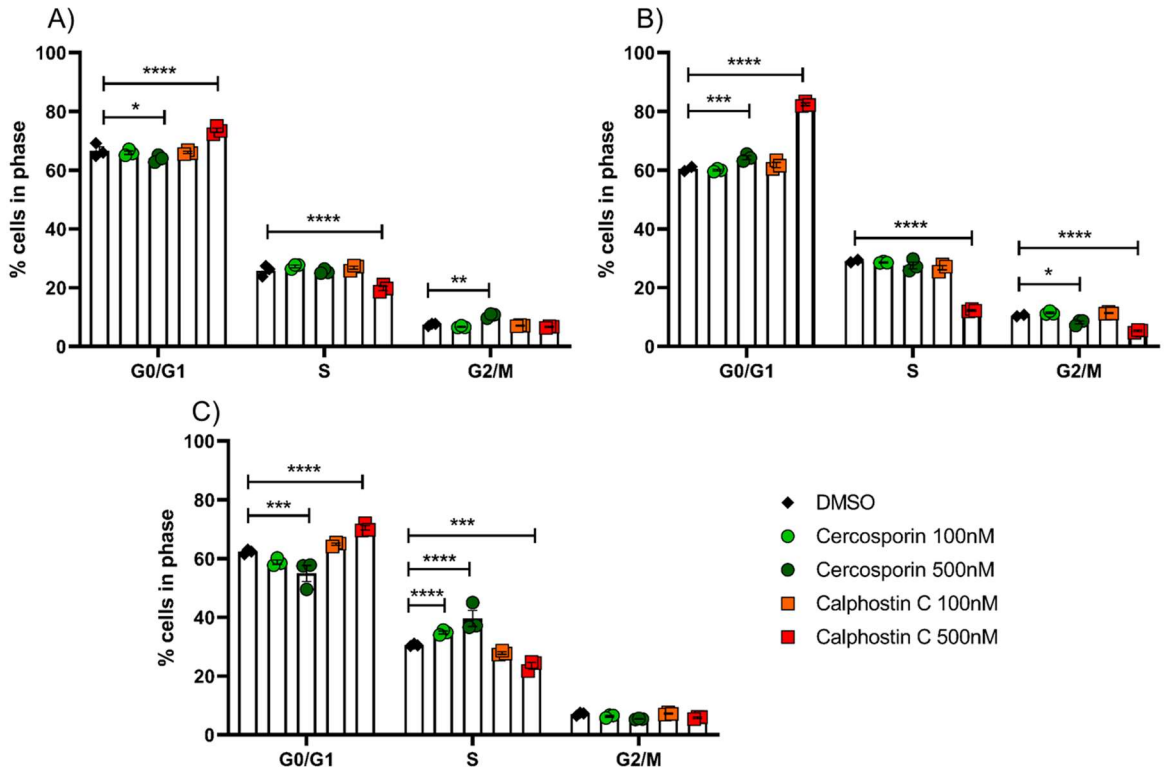

Figure 27: BrdU assay of OCI-AML3 (A), SKNO1 (B) and THP1 (C) after cycling for 24h with compounds, n=3, values shown as mean + SEM. Significances were calculated compared to the DMSO control using Dunnett's multiple comparisons test, p<0,05 = *, p<0,01 = **, p<0,001 = ***, p<0,0001 = ****.

The reduced proliferative and colony-forming potential after compound treatment was accompanied by an increased amount of cells in G0/G1 phase and less cells in

S phase in case of the OCI-AML3 and SKNO1 cells. In the THP1 cells Cercosporin treatment with 500nM significantly reduced the percentage of cells in G0/G1 ($p<0,001$) but increased the number of cells in S phase ($p<0,0001$). On the other hand, after treatment with 500nM Calphostin C the portion of cells in G0/G1 phase was significantly enhanced ($p<0,0001$) and the portion of cells in S phase was significantly reduced ($p<0,001$).

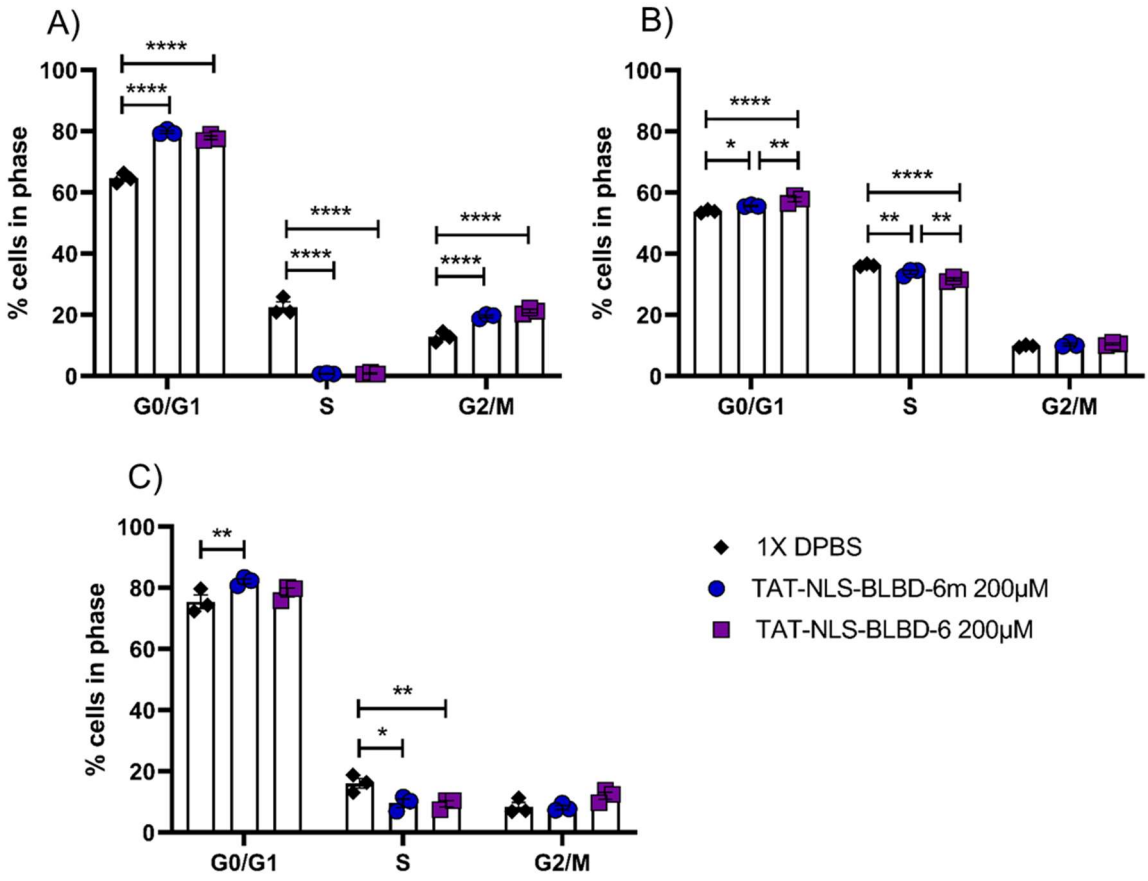

Figure 28: BrdU assay of OCI-AML3 (A), SKNO1 (B) and THP1 (C) after cycling for 24h with peptides, n=3, values shown as mean + SEM. Significant changes in TAT-NLS-BLBD-6 treated samples were calculated compared to the TAT-NLS-BLBD-6m control peptide using Dunnett's multiple comparisons test, $p<0,05$ = *, $p<0,01$ = **, $p<0,0001$ = ****.

The cell lines reacted differently towards peptide treatment. In OCI-AML3, the S phase was not detectable after treatment with control and active peptide, no significant changes between active and control peptide treatment were found. In THP1 a significantly increased G0/G1 phase and significantly reduced S phase was found in the TAT-NLS-BLBD-6 treated experimental arm compared to the TAT-NLS-BLBD-6m control, indicating a reduced cycling of cells. In THP1 no significant change was found between treatment with control and active peptide.

To sum up, treatment with the compounds and the peptide induced apoptosis in all of the cell lines. In addition, in most cases the treatment significantly reduced the portion of cells in S phase, whereas the portion of cells in G0/G1 phase was significantly increased.

4.5. Inhibition of LEF1-β-Catenin Signaling by Compounds Leads to a Reduced Leukemogenic Potential

To further define the changes induced by application of LEF1-β-catenin inhibiting compounds, expression levels of different canonical and non-canonical Wnt genes were determined by qRT-PCR. A significant decrease of the proto-oncogene and direct LEF1 target C-MYC was induced in all cell lines (s. Figure 29).

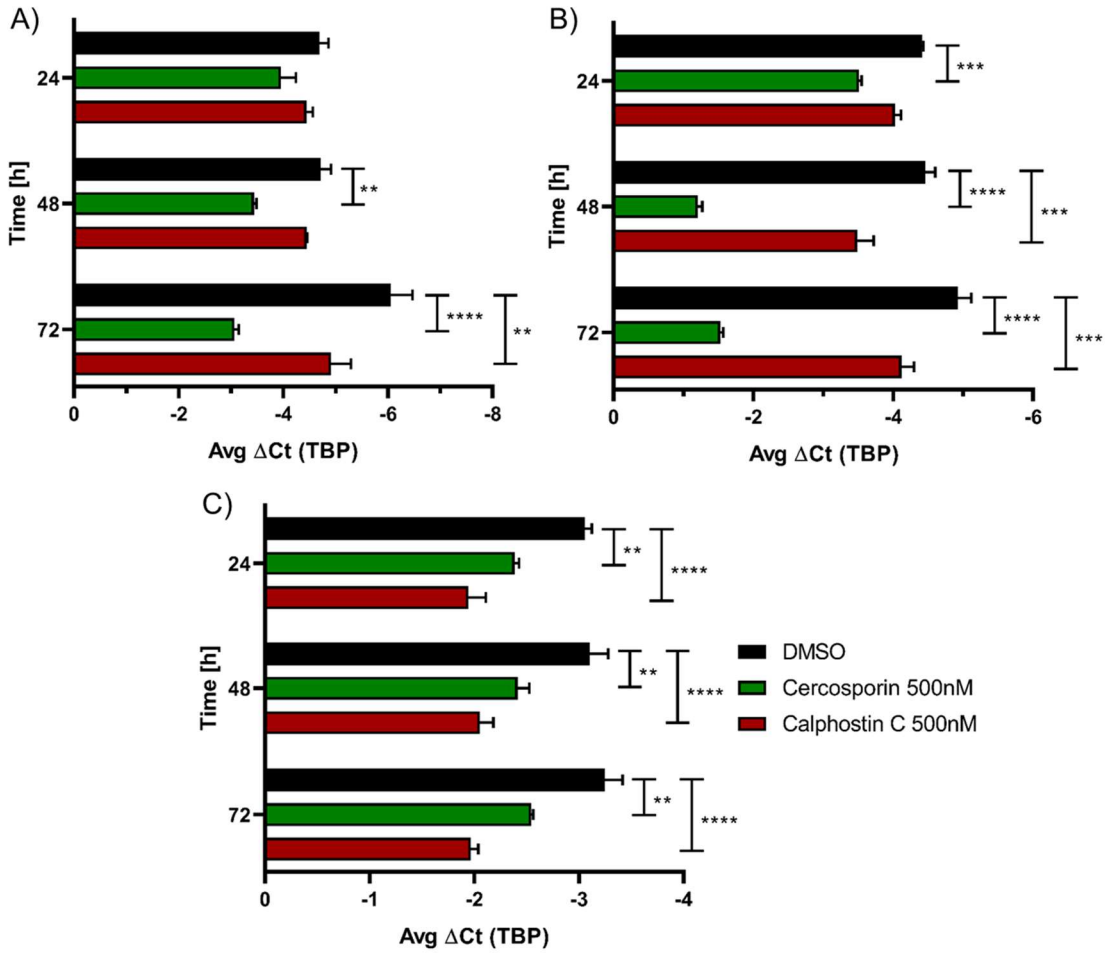

Figure 29: Expression of CCND1 in OCI-AML3 (A), SKNO1 (B) and THP1 (C) after treatment with 500nM Cercosporin or Calphostin C for 24h, 48h or 72h, n=3, values shown as mean + SEM (according to [26]). Significances were calculated compared to the DMSO control using Dunnett's multiple comparisons test, p<0,05 = *, p<0,01 = **, p<0,001 = ****, p<0,0001 = ****.

A comparable effect of TAT-NLS-BLBD-6 was not found. Since the application of Calphostin C and Cercosporin reduced AML cell line growth significantly, paralleled by drop in C-MYC expression, the next step was to examine the impact of the compounds on the leukemogenic potential *in vivo*. THP1 cells, which are known to give a fast readout in the NSG mouse model, were treated *in vitro* for 48h with 100nM or 1µM of the compounds versus the DMSO control and the d0 equivalent was transplanted in sub-lethally irradiated and IvIG treated NSG mice (s. Figure 30).

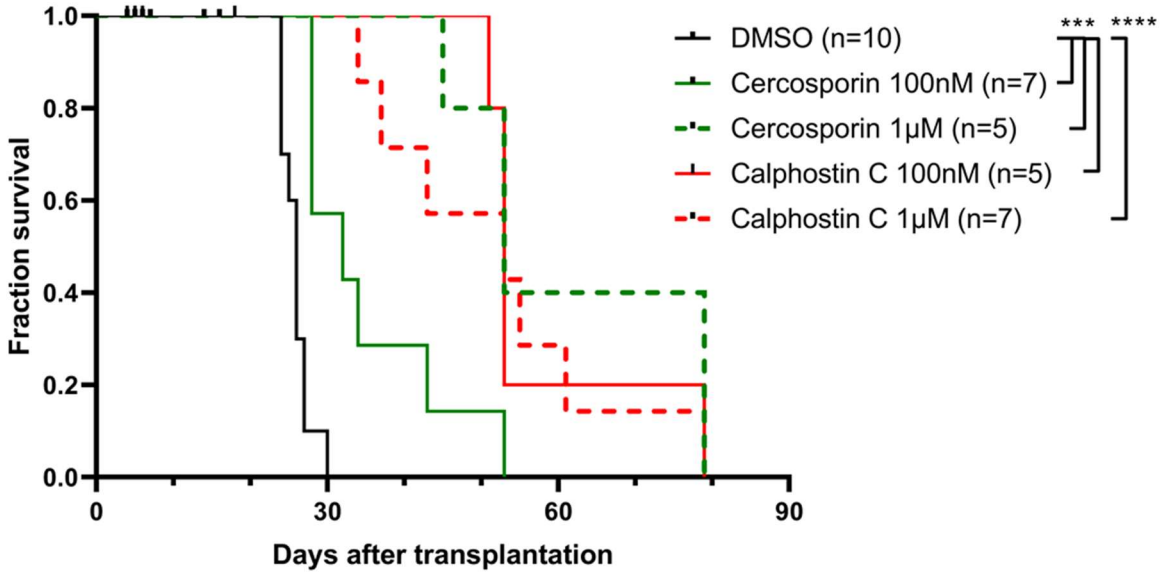

Figure 30: Survival of NSG mice after intravenous injection of THP1 cells treated *in vitro* with DMSO, 100nM or 1000nM of either of the inhibitors, n=5-10 (according to [26]). Mice transplanted with the treated cells survived significantly longer (significances calculated with Log-rank/Mantel-Cox test, p<0,001 = ***, p<0,0001 = ****).

There was a significant delay in disease development in mice transplanted with the compound treated cells compared to the DMSO control. The median of mice transplanted with DMSO treated cells was 26 days, prolonged median survival was 32 days (p<0,001) for Cercosporin 100nM, 53 days (p<0,001) for Cercosporin 1µM, 53 days for Calphostin C (p<0,001) and 53 days (p<0,0001) for Calphostin C 1µM.

4.6. LEF1-β-Catenin Inhibition constraints LSCs derived from Primary AML Samples

The observed growth inhibition of AML cell lines after treatment approaches inhibiting LEF1-β-catenin binding was further confirmed in primary AML samples. In

total 6 different primary CN-AML patient samples were tested for their colony-forming and engraftment potential after treatment with Cercosporin, Calphostin C or the TAT-NLS-BLBD-6 peptide. *In vitro* treatment with the compounds Calphostin C and Cercosporin for 24h significantly reduced the colony-forming potential of primary samples (s. Figure 31).

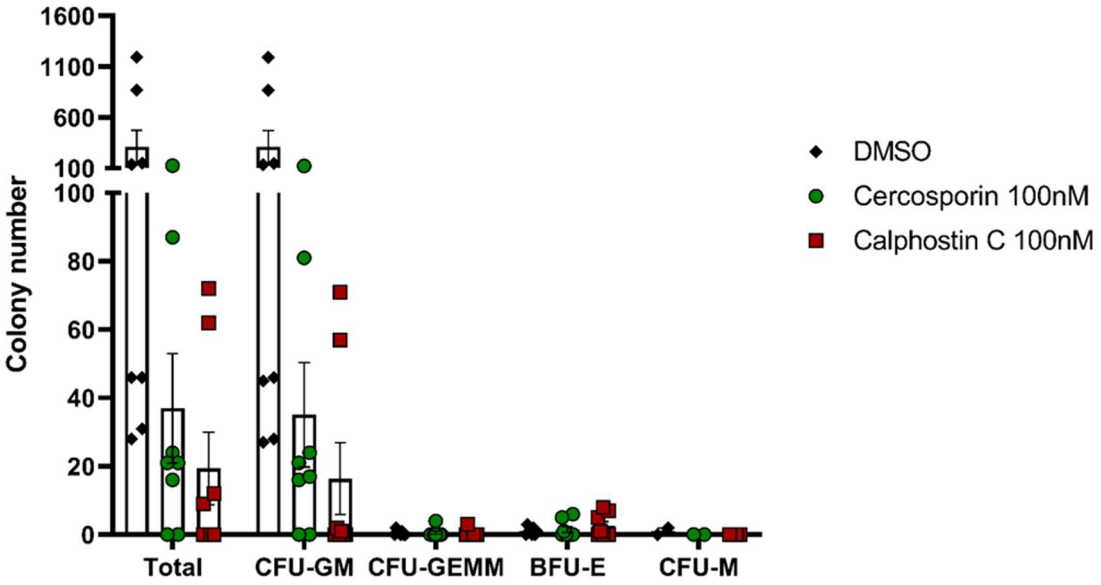

Figure 31: Primary AML samples were treated with DMSO or 100nM Cercosporin for 24h and plated into H4434 methylcellulose, n=3, values shown as mean + SEM (according to [26]). Significances were calculated using Dunnett's multiple comparisons test p<0,01 = **.

Two of the 6 CN-AML samples did not form colonies. For the other samples the colony-forming potential was reduced by 88,17% after Cercosporin treatment (p<0,01) and 93,82% by Calphostin C treatment (p<0,01). Treatment with the active peptide TAT-NLS-BLBD-6 versus the control peptide for 24h did not induce a comparable reduction of colony-forming potential (s. Figure 32).

Figure 32: Primary AML samples were treated with 1X DPBS, 200µM TAT-NLS-BLBD-6m or 200µM TAT-NLS-BLBD-6 for 6h under serum-free conditions and plated into H4434 methylcellulose, n=3, values shown as mean + SEM.

To test the impact of pharmacological inhibition of LEF1-β-catenin binding on normal hematopoietic stem and progenitor cells, $CD34^+$ cord blood cells were used as a healthy control and treated with either of the small-molecule inhibitors versus DMSO (s. Figure 33).

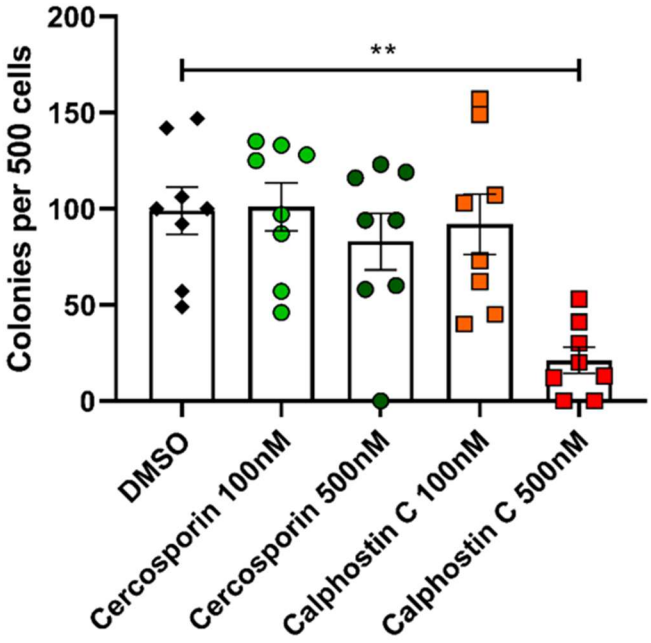

Figure 33: $CD34^+$ cord blood cells were enriched from total cord blood via MACS, treated with DMSO, 100nM or 500nM of either of the compounds for 24h and then plated into H4434 methylcellulose, n=4, values shown as mean + SEM (according to [26]). Significances were calculated using Dunnett's multiple comparisons test $p<0,01$ = **.

Here, no significant effect was found on the colony-forming potential after treatment with 100nM of either of the compounds or 500nM Cercosporin. Only after application of 500nM Calphostin C the colony forming potential was reduced by 78,69% ($p<0,01$).

To test, whether the compounds also have an effect on engraftment, patient samples and healthy $CD34^+$ control cells were treated with 100nM Cercosporin or 100nM Calphostin C for 24h and were transplanted into sub-lethally irradiated and IvIG treated NSG mice (s. Figure 34).

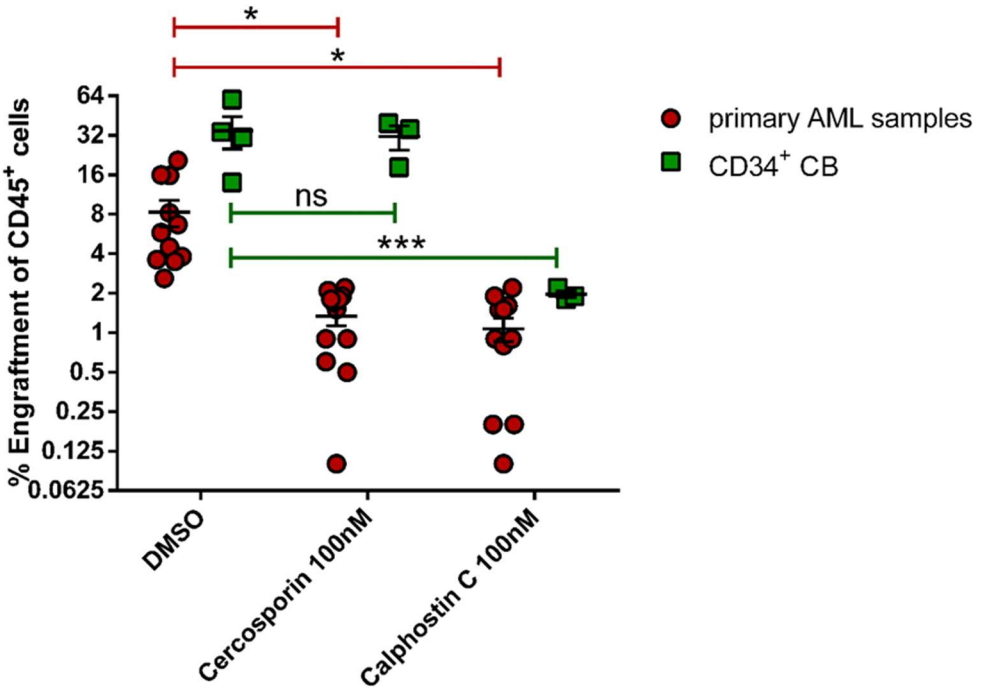

Figure 34: Engraftment of primary patient samples versus $CD34^+$ cord blood cells treated with 100nM Cercosporin or 100nM Calphostin C versus DMSO in the bone marrow of sub-lethally irradiated NSG mice after 14 weeks, values shown as mean ±SEM (according to [26]). Significances were calculated Dunnett's multiple comparisons test, $p<0,05$ = *, $p<0,001$ = ***.

For the patient samples a significant decrease of engraftment was found for both compounds, indicating a role of the LEF1-β-catenin binding inhibition at the level of human LSCs. In clear contrast, $CD34^+$ CB engraftment was not at all affected by treatment with 100nM Cercosporin. Only after treatment with 100nM Calphostin C the engraftment was reduced significantly by 94,33% ($p<0,001$).

In addition, the engraftment of patient samples after peptide treatment was tested. Here, no significant difference in engraftment between the TAT-NLS-BLBD-6m

control peptide and the TAT-NLS-BLBD-6 active peptide was observed (s. Figure 35).

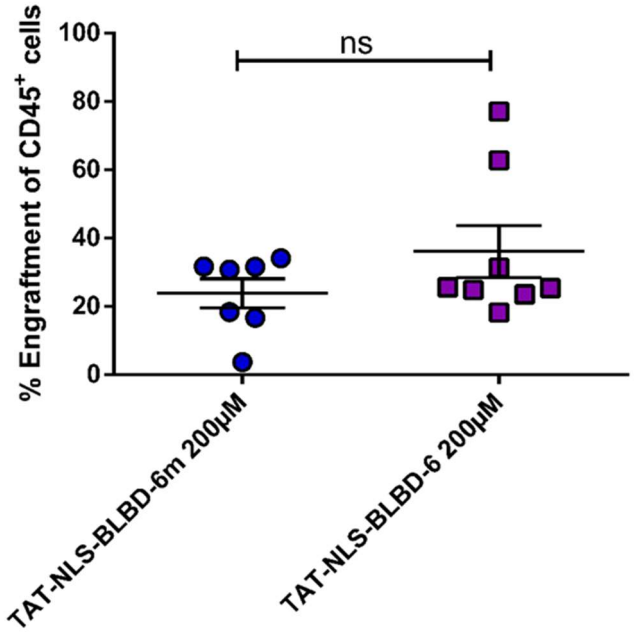

Figure 35: Engraftment of primary patient samples treated with 200µM TAT-NLS-BLBD-6m or 20µM TAT-NLS-BLBD-6 in the bone marrow of sub-lethally irradiated NSG mice after 14 weeks, values shown as mean ±SEM. Significance was calculated using Mann Whitney test.

4.7. Lef1 and AML1-ETO Collaborate in Induction of AML in the BMT Model

It is already known, that aberrant expression of Lef1 induces AML in mice, propagated by a LSC with lymphoid characteristics. The induced AML occurs after a long latency of one year and only in a small sub fraction of mice [80]. This indicates that Lef1 needs additional partners to be able to induce AML more effectively. In *AML1-ETO* positive AML patient samples usually *LEF1* is highly expressed (s. Figure 36). The expression of the *CEBPα* (s. Figure 37), which is able to inhibit LEF1 expression, is lower in t(8;21) AML than in most other AMLs, whereas *PAX5*, known to upregulate *LEF1* expression, is higher expressed (s. Figure 38).

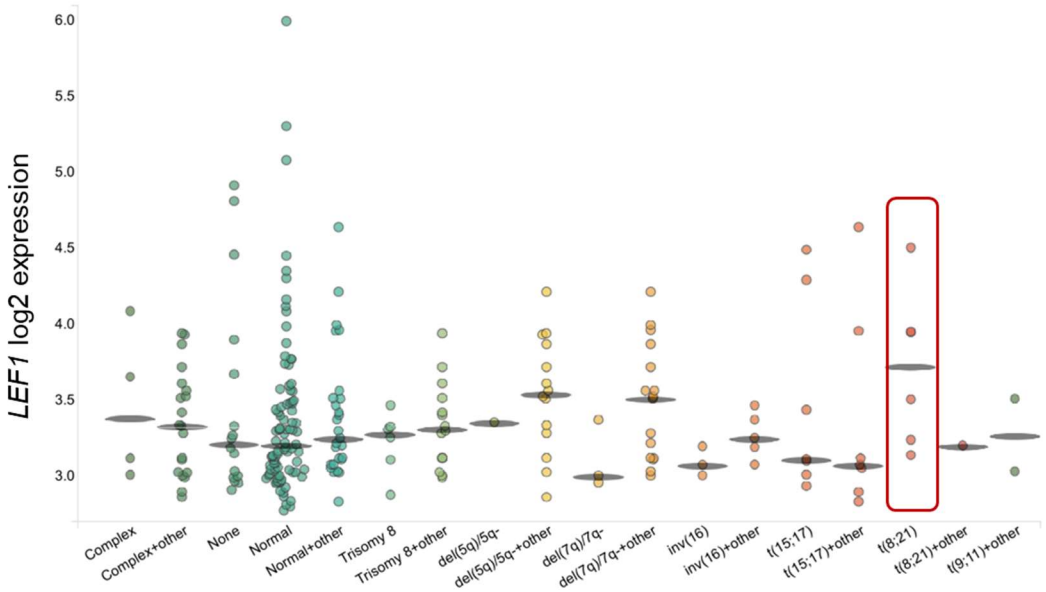

Figure 36: *LEF1* log2 expression in the AML TCGA dataset [8] (BloodSpot, AML TCGA dataset, subset 210948_s_at, accessed on 02.03.2019).

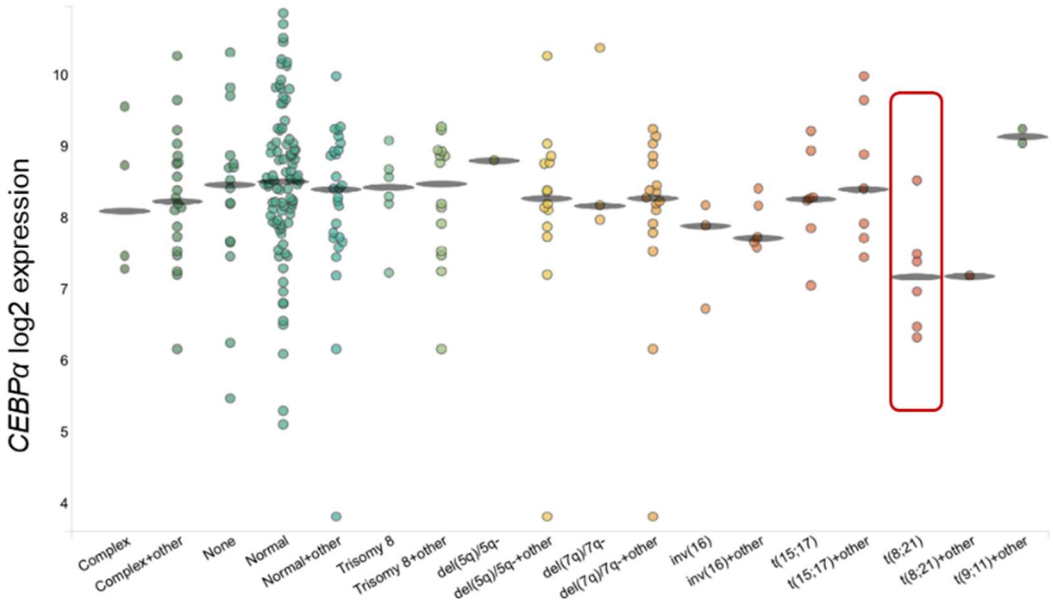

Figure 37: *CEPAα* log2 expression in the AML TCGA dataset [8] (BloodSpot, AML TCGA dataset, subset 204039_s_at. accessed on 02.03.2019).

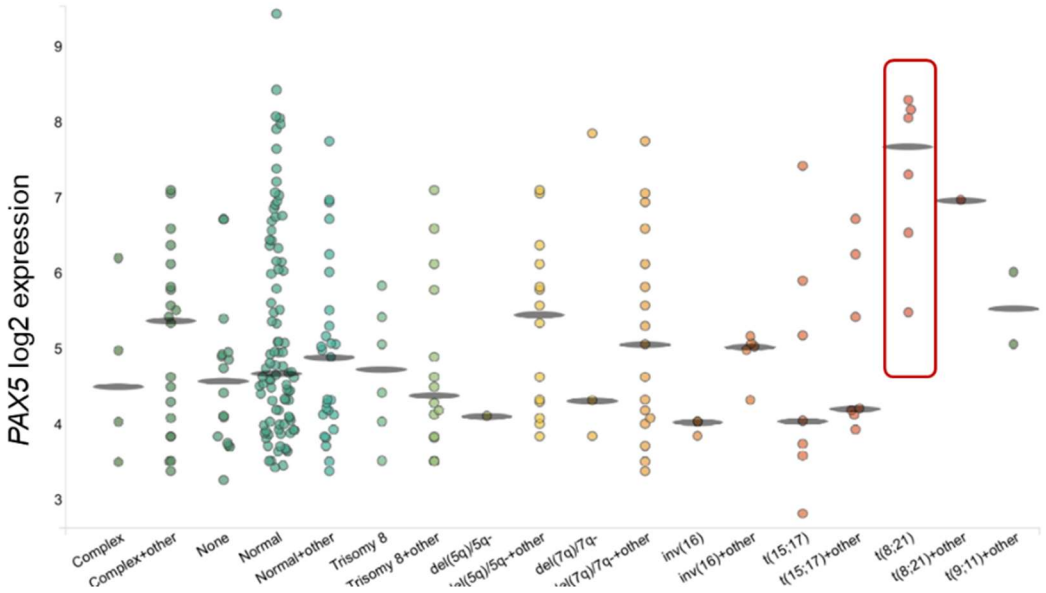

Figure 38: *PAX5* log2 expression in the AML TCGA dataset [8] (BloodSpot, AML TCGA dataset, subset 221969_s_at, accessed on 02.03.2019).

To further dissect this possible collaboration, AML1-ETO and Lef1 were overexpressed in 5-FU stimulated bone marrow (s. Figure 39).

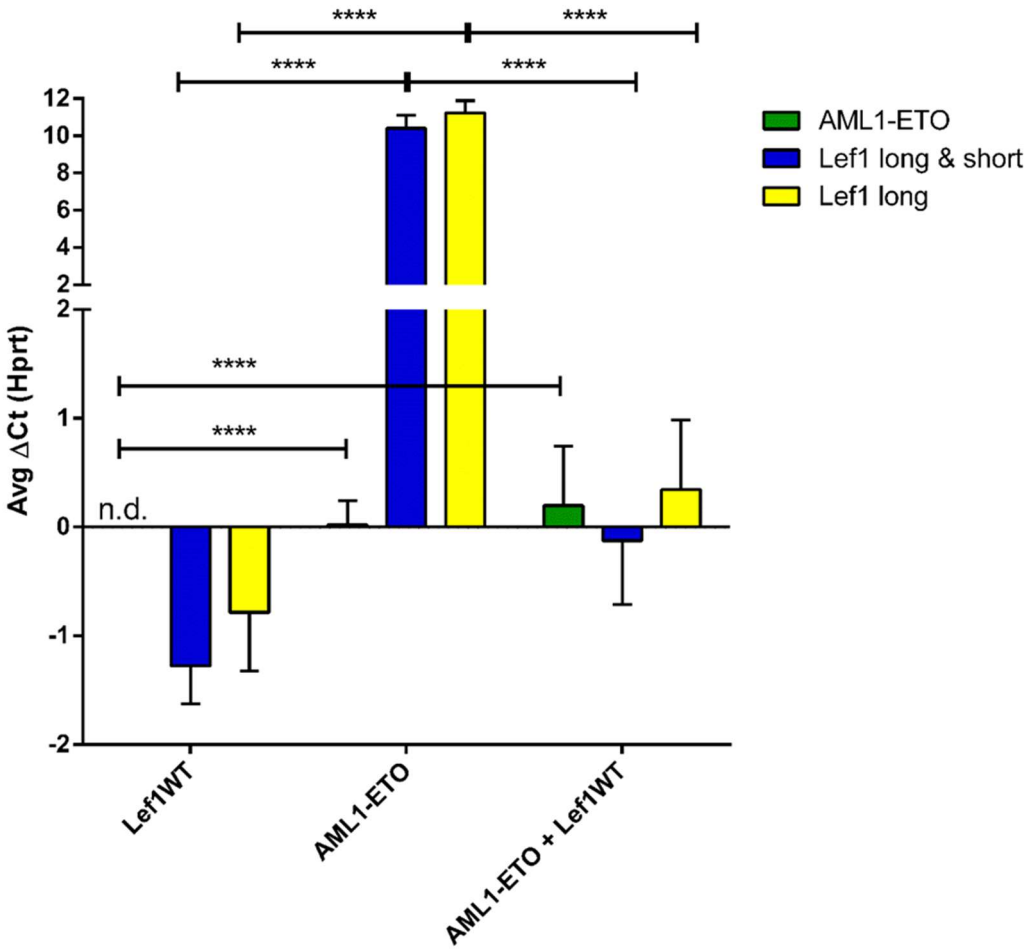

Figure 39: Expression of *AML1-ETO* and *Lef1* isoforms in 5-FU stimulated murine bone marrow cells, which was retrovirally treated to overexpress either *AML1-ETO* or *Lef1WT* or co-expressing *AML1-ETO* and *Lef1WT*, n=3, values shown as mean + SEM. Significances were calculated using Tukey's multiple comparisons test, p<0,0001 = ****.

The positively single and double transduced cells were sorted and analyzed for their *Lef1* and *AML1-ETO* expression levels. As controls, 5FU BM was also transduced with either *AML1-ETO* or *Lef1WT* alone. The overexpression was highly significant in all samples (p<0,0001). The overexpressing cells were plated into CFCs (s. Figure 40) as a first test for collaboration.

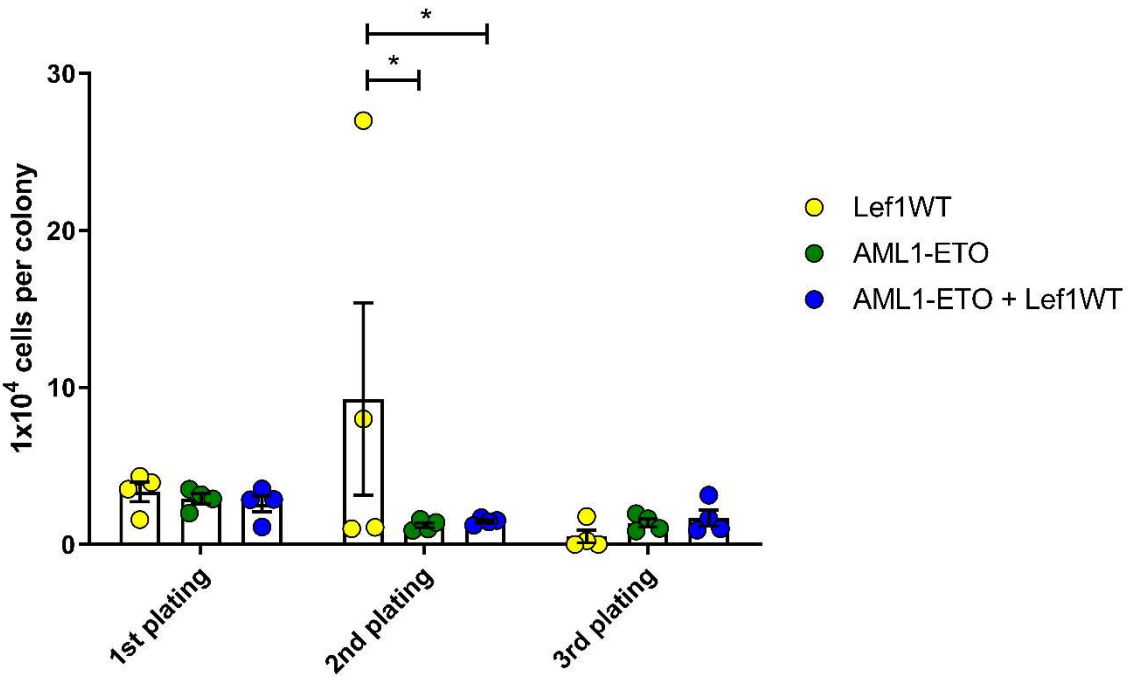

Figure 40: Colony-forming potential of 5-FU stimulated murine bone marrow, which was retrovirally treated to overexpress either *AML1-ETO* or *Lef1WT* or co-expressing *AML1-ETO* and *Lef1WT*, n=3, values shown as mean + SEM. Significances were calculated using Tukey's multiple comparisons test, p<0,05 = *, p<0,001 = ***, p<0,0001 = ****.

Cells transduced with *Lef1* alone lost re-plating capacity already at the 2nd plating, whereas cells transduced with *AML1-ETO* alone were re-platable more often without losing colony-forming potential. The cells overexpressing both *Lef1* and *AML1-ETO* showed a high re-plating capacity especially at the 2nd plating, which indicates a collaborative effect of *Lef1* and *AML1-ETO* expression at the level of CFCs compared to *Lef1* alone.

Next, *AML1-ETO* and *Lef1* were co-overexpressed in 5FU BM and transplanted into mice. As controls, also 5FU BM cells transduced with either *AML1-ETO* or *Lef1WT* were transplanted. Indeed, a strong collaborative effect between *Lef1WT* and *AML1-ETO* was found (s. Figure 41).

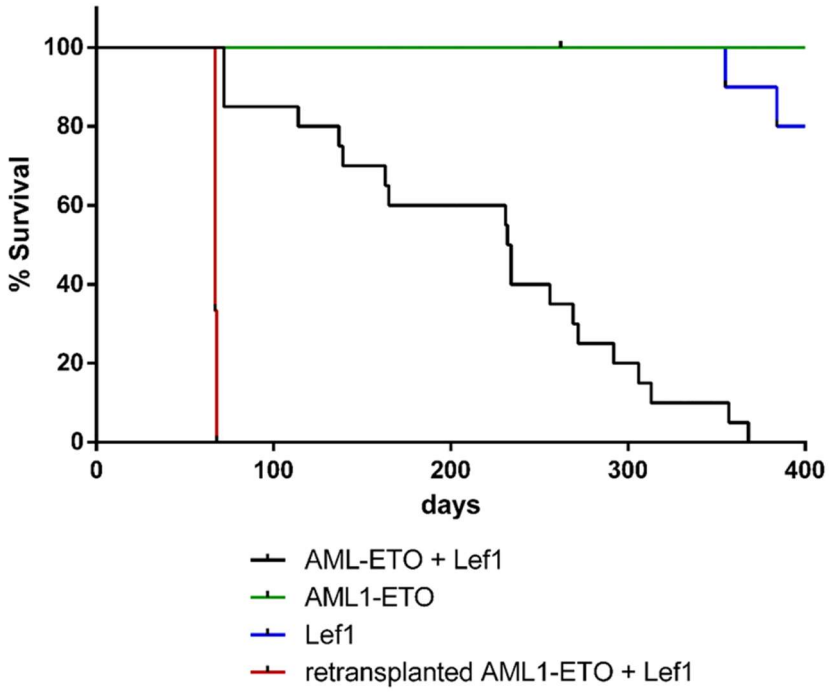

Figure 41: Survival of mice from the BMT. Mice transplanted with *AML1-ETO* and *Lef1* co-transduced BM (black line) diseased after a median of 233 days with AML (n=20). Re-transplantation (red line) led to a decreased survival with a median of 67 days (n=3). *AML1-ETO* control mice (green line) did not disease at all (n=10), out of *Lef1* control mice (blue line) only two diseased until day 384 after transplantation (n=10).

All of the mice transplanted with 5-FU BM co-expressing *Lef1* and *AML1-ETO* diseased with leukemia after a median of 233 days. This disease was also re-transplantable with a latency of 62 days, whereas the mice transplanted with bone marrow overexpressing *AML1-ETO* did not disease at all. The mice transplanted with BM overexpressing *Lef1WT* alone did not develop disease with the exception of 2 mice after a long latency of 354 days and 384 days after transplantation. According to the cytospin analysis, the mice transplanted with 5-FU BM co-expressing *AML1-ETO* and *Lef1* diseased with a leukemia, since the blast counts were 25,96% (±12,48%). The two diseased mice transplanted with 5-FU BM expressing *Lef1* only also were found to be diseased with leukemia, since the cytospin analysis revealed blast counts of 40,8% and 31,5%, respectively.

The size of spleens of diseased *AML1-ETO* + *Lef1WT* mice was severely enlarged to a median of 515mg (±338mg) compared to healthy mouse spleens, which usually reach sizes ranging from 80mg to 100mg [102]. All peripheral blood, bone marrow and spleen samples were analyzed by Hemavet, revealing overall elevated white blood cell counts, decreased red blood cell counts and thrombocytopenia. Within

the peripheral blood, the white blood cell counts were elevated to a median of 26,36x10^6/ml (±29,54x10^6/ml) compared to the normal value of approximately 3mio/ml [102]. The PB red blood cell counts were decreased to a median of 2,68x10^9/ml (±3,87x10^9/ml) compared to the count in healthy mice of around 10x10^9/ml [102] (s. Table 21).

Table 21: Survival, peripheral blood RBC and WBC counts and spleen weight of diseased mice transplanted with AML1-ETO + Lef1WT or a healthy untreated control Bl6 mouse [102], n.a.: not available.

	Day of sacrifice	RBCs in PB [1x10^9/ml]	WBCs in PB [1x10^6/ml]	Spleen [mg]
healthy Bl6 mouse **[102]**	n.a.	10,00	3,00	80-100
AML1-ETO + Lef1 1	137	1,57	4,25	515
AML1-ETO + Lef1 2	162	4,20	10,84	95
AML1-ETO + Lef1 3	72	10,91	13,76	n.a.
AML1-ETO + Lef1 4	72	11,23	37,96	n.a.
AML1-ETO + Lef1 5	72	11,73	22,50	n.a.
AML1-ETO + Lef1 6	269	0,81	55,08	332
AML1-ETO + Lef1 7	368	7,64	7,16	n.a.
AML1-ETO + Lef1 8	292	3,08	6,70	535
AML1-ETO + Lef1 9	272	0,77	73,90	327
AML1-ETO + Lef1 10	357	1,12	3,68	487
AML1-ETO + Lef1 11	256	1,10	60,96	862
AML1-ETO + Lef1 12	231	1,21	10,84	n.a.
AML1-ETO + Lef1 13	165	4,49	96,72	1530
AML1-ETO + Lef1 14	306	2,60	35,42	725
AML1-ETO + Lef1 15	232	1,35	43,50	763
AML1-ETO + Lef1 16	139	0,63	30,28	381
AML1-ETO + Lef1 17	234	0,39	71,36	602
AML1-ETO + Lef1 18	234	10,28	5,60	102
AML1-ETO + Lef1 19	313	4,49	3,68	448
AML1-ETO + Lef1 20	114	2,75	85,22	718

Low platelets counts are also a symptom of leukemia in human; in the peripheral blood of diseased *AML1-ETO* + *Lef1* mice the platelet count was reduced to 183x10^6/ml (±141,28x10^6/ml), whereas in healthy mice the lowest normal value is around 1000x10^6/ml [102]. For the bone marrow samples, already macroscopically the lack of RBCs was obvious, since the bones appeared completely white. Here, the amount of red blood cells was decreased to 0,02x10^9/ml (±0,01x10^9/ml).

To further analyze of the kind of leukemia induced by *AML1-ETO* and *Lef1* co-expression, FACS staining of B220, Gr1, Mac1, CD4 and CD8 was performed, as well as cKit and Sca1 staining (s. Figure 42).

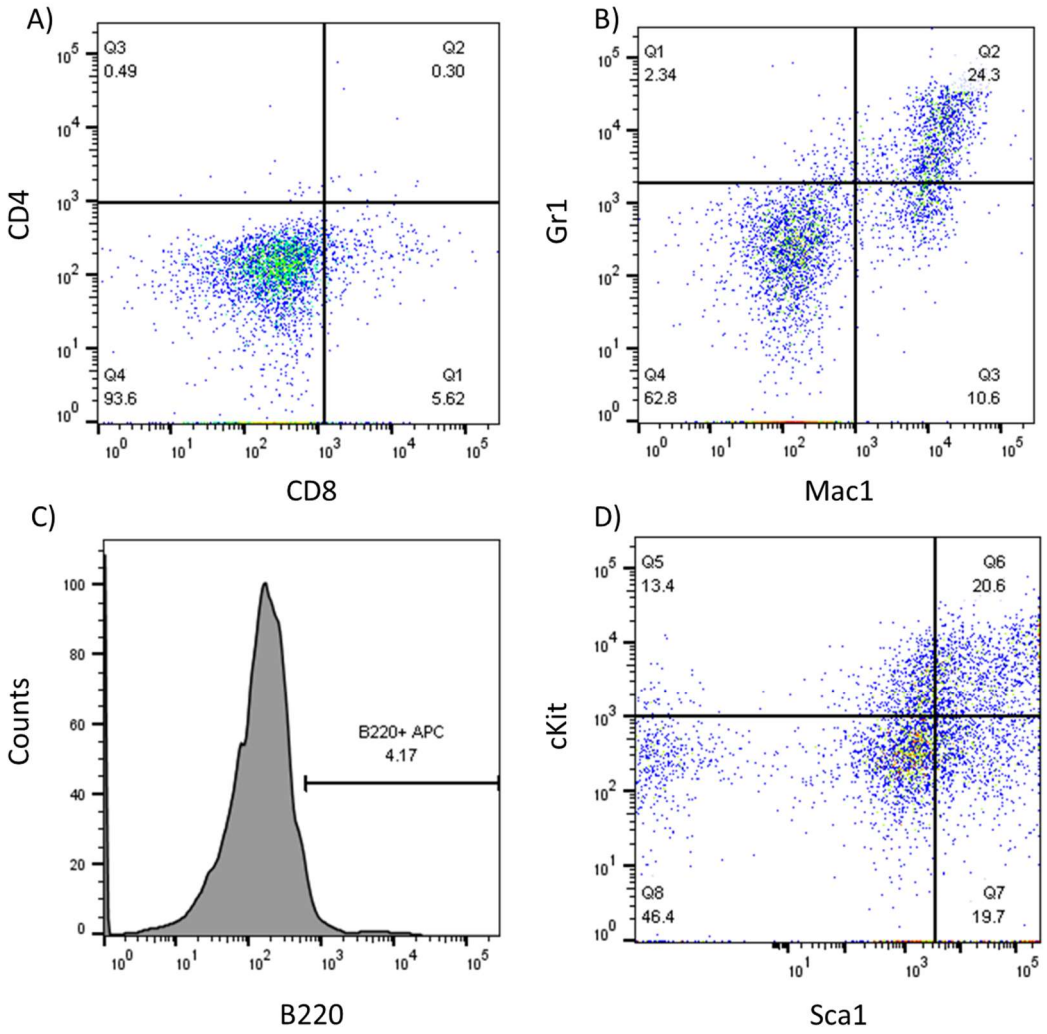

Figure 42: Representative FACS analysis of the overexpressing BM cells for a diseased AML1-ETO+Lef1 mouse for CD4 and CD8 (A), Gr1 and Mac1 (B), B220 (C), cKit and Sca1 (D).

The engraftment of diseased mice with overexpressing cells was quite heterogeneous with a median of 32,91% (±20,30%). Within the overexpressing

cells, the amounts of B220, Gr1, Mac1, CD4 and CD8 positive cells was as follows (s. Table 22):

Table 22: FACS analysis of the diseased *AML1-ETO* + *Lef1WT* transplanted mice.

	Mean (%)	Standard Deviation (%)
CD4+	15,14	15,64
CD8+	0,33	0,35
B220+	8,53	6,39
Gr1+	2,66	1,55
Mac1+	15,20	11,60
Gr1+ Mac1+	16,87	16,05
cKit+	28,54	22,01
Sca1+	14,31	9,15
cKit+ Sca1+	16,22	9,67

In addition, the diseased mice were sent for histopathological analysis, which was performed by the group of Prof. Dr. Quintanilla-Martinez de Fend from the Institute of Pathology in Tübingen. Macroscopically analysis, followed by HE microscopic analysis and B220, CD3, myeloperoxidase (MPO), Ter119 and ASDCL staining were performed in all animals. Different tissues were analyzed, including brain, skin, bone marrow, lung, spleen, liver, thymus, kidney, heart, lymph nodes, adrenal, thyroid and salivary glands, esophagus, trachea, small and big intestine, stomach, pancreas, bladder and sexual organs. The characterized mice were found to be diseased with AML with (s. Figures 45 and 46) and without (s. Figures 43 and 44) maturation according to the Bethesda classification for non-lymphoid neoplasms [53].

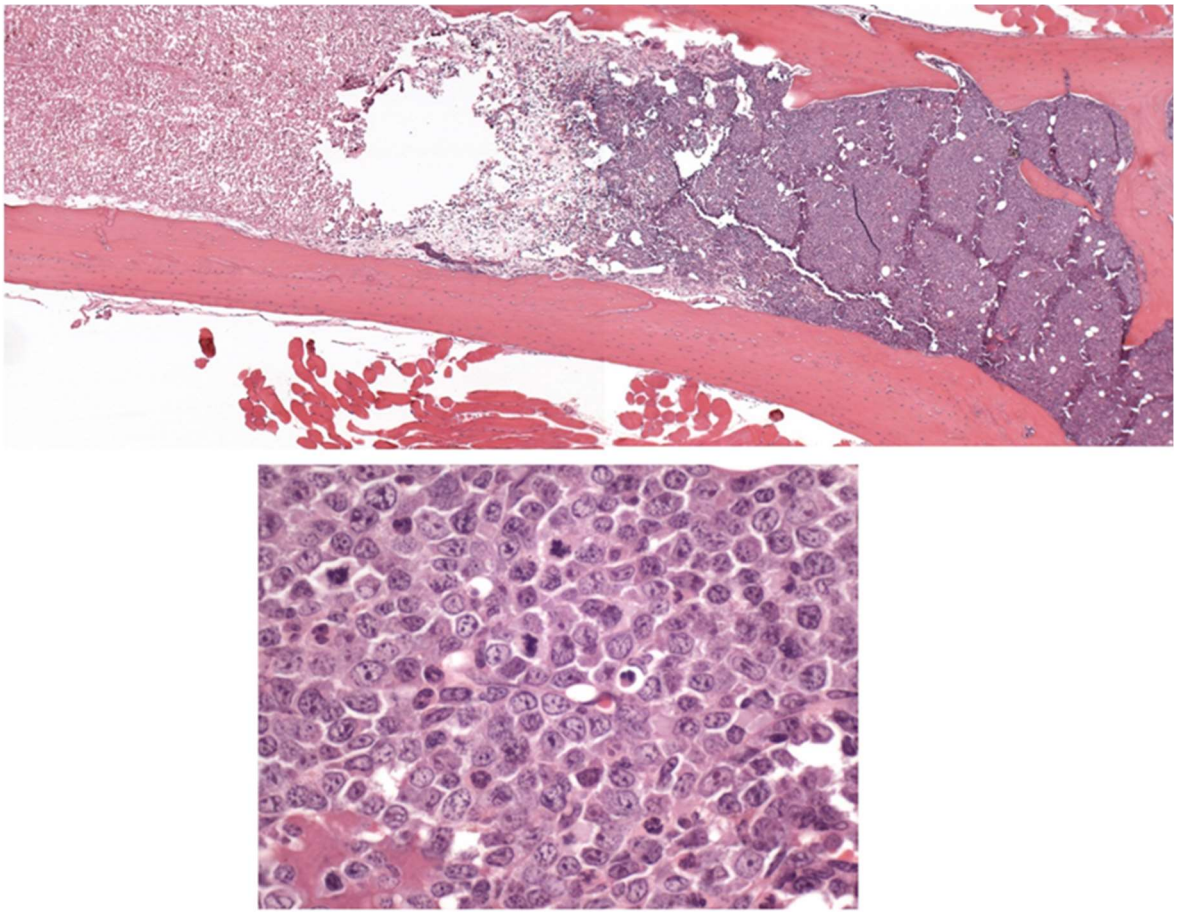

Figure 43: Representative histopathological analysis of the bone marrow of a mouse diseased with AML without maturation.

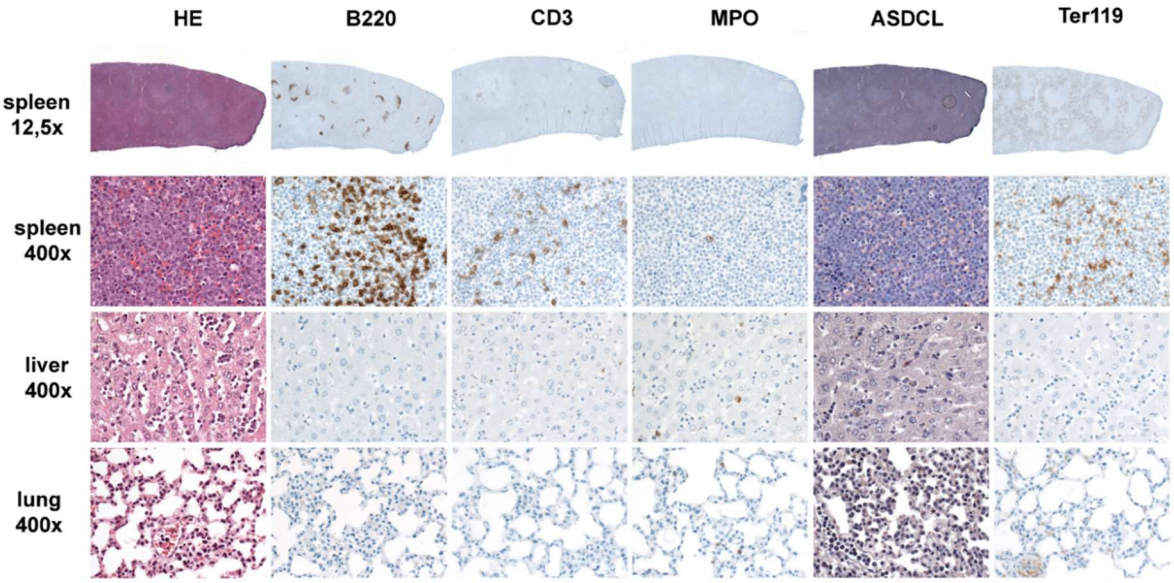

Figure 44: Representative histopathological analysis of the spleen, liver and lung of a mouse diseased with AML without maturation.

Mice diseased with AML without maturation were all found to have enlarged spleens, that showed an expanded red pulp with atrophy of the white pulp. The

staining for CD3 and B220 showed only the residual normal lymphoid cells in the white pulp, confirming the atrophy of the white pulp. The red pulp was diffusely infiltrated by medium to large blasts with open chromatin, prominent nucleoli and expanded cytoplasm. Practically no neutrophil granulocytes or myeloid precursors were observed. MPO and ASDCL was positive cells in rare cells scattered in the red pulp (<3%), indicating the diagnosis of AML without maturation. Morphologically, the liver showed leukemic infiltrate both in the portal trials and in the sinusoids. The lung showed infiltration in the alveolar walls. Ter119 immunohistochemistry revealed the normal presence of erythropoiesis. Additional infiltrations in heart and brain tissues were found.

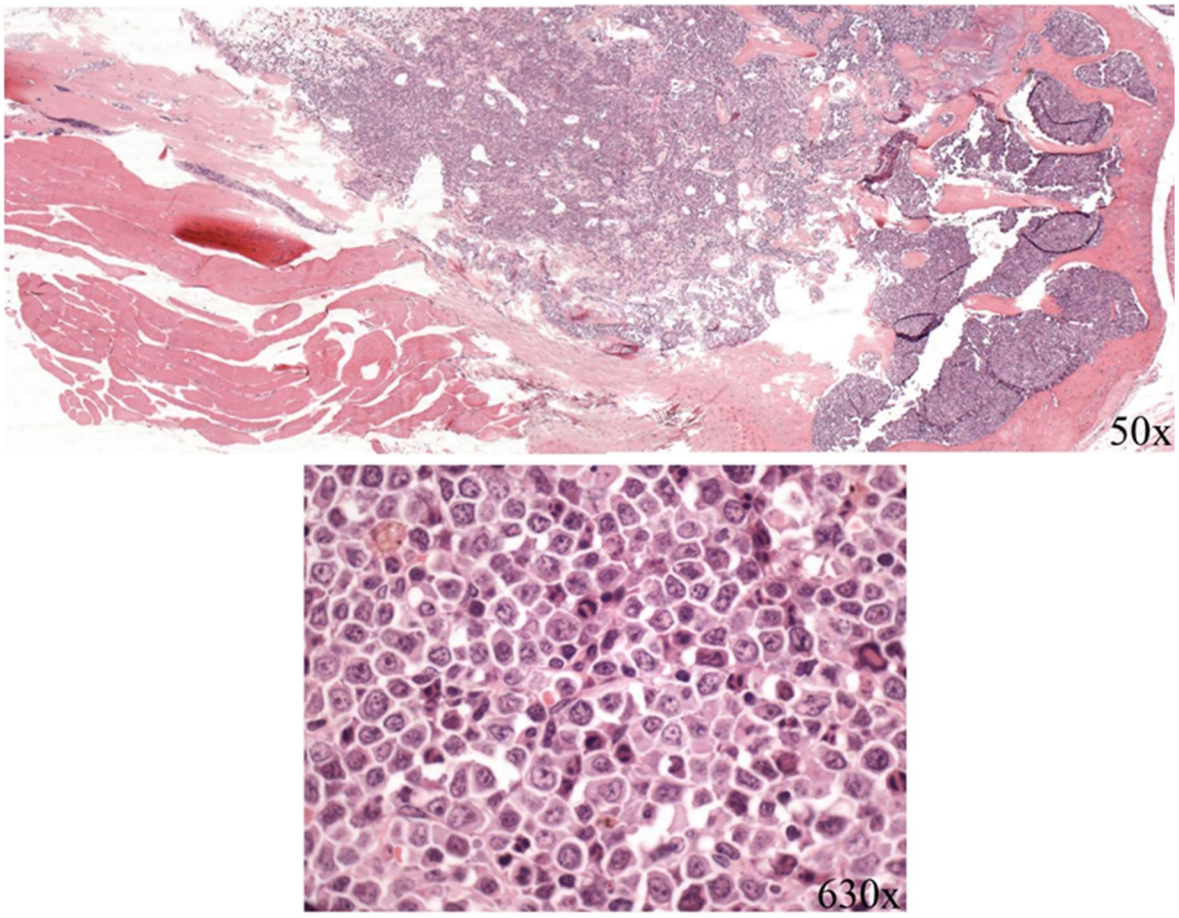

Figure 45: Representative histopathological analysis of the bone marrow of a mouse diseased with AML with maturation.

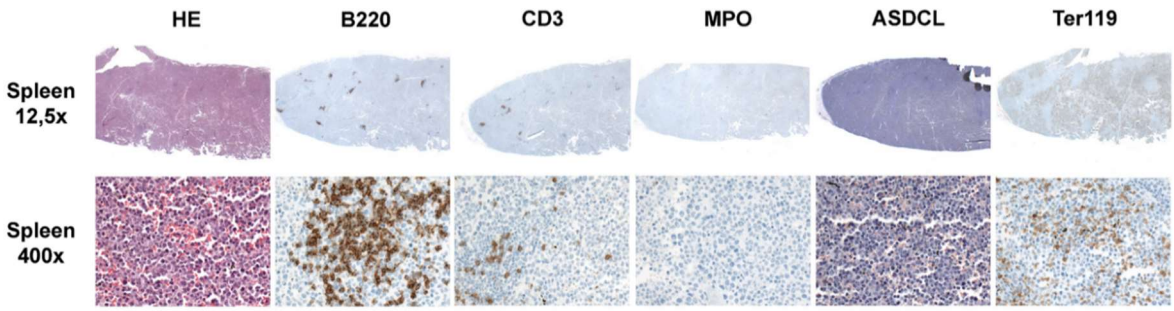

Figure 46: Representative histopathological analysis of the spleen, liver and lung of a mouse diseased with AML with maturation.

The mice diseased with AML with maturation showed enlarged spleens with expansion of the red pulp with atrophy of the white pulp. The staining for CD3 and B220 showed only the residual normal lymphoid cells in the white pulp. The expanded red pulp was infiltrated by medium to large blast cells with open chromatin, prominent nucleoli and relatively abundant cytoplasm corresponding to myeloblasts with signs of maturation. The MPO stain was positive in >3% of the myeloid precursors corresponding to the diagnosis of AML with maturation. Further infiltrations were found in liver, lung and heart.

Taken together, *Lef1* was identified as a strong collaborator for *AML1-ETO* positive AML, inducing reliably AML in the BMT model. This indicates a crucial role for *Lef1* expression in *AML1-ETO* positive leukemia.

5. Discussion

In this thesis, the differential expression of LEF1 isoforms between healthy and malignant samples was revealed, opening a potential therapeutic window for the treatment of AML. This therapeutic window was further investigated by use of different methods to inhibit specifically the action of the long isoform of LEF1, including two small molecule inhibitors and a synthetic peptide. The therapeutic effect of the methods was further investigated in several *in vitro* and *in vivo* assays, including cell lines as well as primary samples. In addition, a collaboration of the most recurrent fusion protein in AML, AML1-ETO, and the canonical LEF1 was identified using appropriate *in vitro* and *in vivo* modelling.

5.1. The role of LEF1 isoforms in healthy and malignant hematopoiesis

LEF1 is a major transcription factor of the canonical Wnt signaling pathway. Deregulated Wnt signaling is found in leukemia, but also in many other types of cancer. Since it is mediating the very last step of the Wnt signaling cascade, it is a very attractive target to inhibit Wnt signaling. Here we were able to show, that malignant samples exclusively express the long, canonical isoform of LEF1, already indicating by its expression pattern that leukemic cells depend on its expression. Knockdown of *LEF1* in AML cell lines was performed to test the dependency of the malignant cells on this isoform. The shRNA mediated knockdown could successfully show the importance of *LEF1* expression for proper leukemic growth of SKNO1 and THP1 cells. In this analysis, OCI-AML3 as a cell line with normal karyotype behaved completely opposite, which was not reported so far. Here, proliferation was enhanced after knockdown, the portion of apoptotic cells decreased and the cell cycle was not perturbed at all. Usually, repression of *LEF1* expression was shown to be anti-proliferative due to decreased expression of the downstream target *C-MYC* [117]. Possibly, the effect of LEF1 knockdown depends on the genetic background: our institute could demonstrate, that high expression of *LEF1* in CN-AML is a favorable prognostic factor, which is associated with better overall survival, relapse-free survival and event-free survival [69]. Thus, it is intriguing to speculate that LEF1 does not act as a pro-survival signal in normal karyotype AML.

As mentioned, AML cells are dependent on the long isoform of LEF1, harboring the ability to bind to β-catenin and being responsible for Wnt signaling. In most primitive human $CD34^{-}CD38^{-}CD93^{high}$ stem cells, which are at the very top of the hematopoietic hierarchy, exclusively the short isoform was found to be expressed [4]. This result was confirmed in our hands and the *LEF1* isoform expression analysis was as well extended down the hematopoietic hierarchy including progenitor and terminally differentiated cells. Along HSC maturation to progenitor cells, increasing expression of the long isoform of *LEF1* was found. In progenitor to terminally differentiated cells, *LEF1* was exclusively expressed as the long isoform. This suggests independence of the most immature $CD34^{-}$ stem cells of the canonical Wnt signaling and with this opening the possibility of targeting AML cells but sparing most immature HSCs.

Theoretically, there are many ways to target Wnt signaling at different positions in the signaling cascade with small-molecule inhibitors and antibodies. Since the Wnt pathway is very complex, specific targeting more downstream seems the most promising method to effectively inhibit the signal transduction.

A small molecule inhibitor, which is currently tested by Novartis in preclinical studies [55] is PKF115-584, also known as Cercosporin. Cercosporin was shown to be effectively inhibiting the binding of LEF1 and β-catenin just as CGP049090, also called Calphostin C [31, 61, 74]. These small-molecule inhibitors were identified by screening of libraries of natural compounds by a high-throughput assay [61]. Both compounds were already tested for their anti-proliferative effect in the AML cell lines HL60 and Kasumi1, as well as primary AML samples [74]. They induced apoptosis by Caspase 3/7 activation, leading to decreased ATP levels after treatment. A decrease of C-MYC protein levels was confirmed, which is a direct LEF1 downstream target. Protein levels of β-catenin were also shown to be reduced as a result of Caspase 3/7 activation [74]. The effect of Calphostin C and Cercosporin was further confirmed in chronic lymphoid leukemia cells [31]. The inhibition of LEF1-β-catenin binding was confirmed by co-immunoprecipitation after treatment of protein lysates. However, treatment was performed on the lysates instead of living cells to avoid β-catenin degradation through caspase activation. For this reason, also in this thesis treatment was performed on protein lysates instead of living cells to show the dissociation of LEF1 and β-catenin. In the CLL xenograft model [31], subcutaneous injection of a CLL cell line was performed, leading to the formation of

tumors. Significant cessation of tumor and increased median survival was found after i.p. treatment with either of the compounds.

Both Cercosporin and Calphostin C are protein kinase C (PKC) inhibitors. PKCs are classical downstream targets of non-canonical Wnt signaling, in particular the Wnt/Ca^{2+} pathway [57]. With regards to Wnt signaling, PKCδ was shown to promote β-catenin stabilization via interaction with the APC complex, leading to enhanced canonical Wnt signaling [40] and also PKCζ is regulating canonical Wnt by enhancing the nuclear localization of β-catenin [66]. PKCα regulates cell proliferation by *Cyclin D1* repression [41]. PKCβ, having two splice variants with opposing activity, is involved in proliferation and differentiation. PKCβI is responsible for differentiation and was found to be downregulated in colon cancer [16], while PKCβII leads to hyper-proliferation and increased carcinogenesis [34, 78]. The "PKC with the greatest potential in carcinogenesis" [65] is PKCε, as overexpression was found to be implicated in several types of cancer by malignant transformation of cells via Ras/Raf/mitogen-activated protein kinase (MAPK) pathway [103]. Due to the multitude of PKC functions, the use of PKC inhibitors in this thesis may also affect other pathways than LEF1-β-catenin signaling, but some of these effects may act synergistically and lead to even better pharmacological activity than the pure LEF1-β-catenin inhibition.

Another method to specifically target LEF1-β-catenin binding was also tested. Here, a synthetic peptide was used, which was already shown to inhibit the binding of LEF1 to β-catenin in a co-immunoprecipitation assay [46]. The peptide consists of a part of the TAT protein for cellular import, a NLS for nuclear import and a part of the binding sequence of LEF1 to β-catenin. The protein harboring the BLBD-6 sequence was found to have the best effect on LEF1-β-catenin binding inhibition. The effects of this peptide together with its control peptide TAT-NLS-BLBD-6m were tested in this thesis. The TAT-NLS-BLBD-6m consists of the same TAT and NLS sequence as the active peptide, but the BLBD-6 sequence was mutated, so that it should have no effect. The benefit of using a synthetic peptide to inhibit LEF1-β-catenin binding is the exclusion of off-target effects in contrast to PKC inhibitors. The downside of peptides, which need to be taken up by the cell and need to be imported in the nucleus is the fast degradation. The peptides used in this thesis were analyzed with the ProtParam tool from the ExPASy website for their half-life in *in vitro* assays, which is shorter than 3 hours at normal cell culture condition. Probably

for this reason, high concentrations of 100µM and 200µM had to be used in order to see an effect in the different assays. In addition, incubation of cells with the peptides usually had to be performed in serum-free medium, since serum may contain proteases, which could lead to faster degradation of the peptide, and albumin, which is known to be “sticky” and bind to free peptides and proteins [27].

So far, the differential expression of the *LEF1* isoforms in normal versus leukemic cells has not been exploited conceptually by using compounds inhibiting LEF1-β-catenin binding. Treatment with the compounds Calphostin C and Cercosporin as well as the synthetic peptide TAT-NLS-BLBD-6 led to reduced proliferative and colony-forming potential in the AML cell lines OCI-AML3, SKNO1 and THP1. Apoptosis was significantly enhanced after treatment with either Calphostin C or Cercosporin. This effect was also seen in TAT-NLS-BLBD-6 treated cells versus TAT-NLS-BLBD-6m treated cells. Cycling of the cells was also found to be affected, in most samples a significantly decreased portion of cells in S phase and increased number of cells in G0/G1 phase was observed.

Since the changes in cell cycle behavior of the cells may have been due to decreased *Cyclin D1* (CCND1) expression, which is a LEF1-β-catenin downstream target [89], qRT-PCR analysis was performed. *CCND1* expression is necessary for transition from G0/G1 to S phase [9] and is directly regulated by LEF1 [89]. Significantly decreased levels of *CCND1* were found in OCI-AML3 after 72h of incubation with 500nM Calphostin C or Cercosporin ($p<0,01$, data not shown), expression in SKNO1 already after 24h treatment was significantly decreased for Calphostin C 500nM ($p<0,0001$, data not shown) and Cercosporin ($p<0,001$, data not shown). In case of THP1, changes in cell cycling could not be explained by altered expression of *CCND1* after treatment, since the expression was not significantly decreased (data not shown).

It was shown before, that application of LEF1-β-catenin binding inhibitors would also affect *C-MYC* expression [74]. This effect was also found after treatment of the cell lines used in this thesis. This significantly reduced *C-MYC* expression was accompanied by loss in leukemogenic growth potential. THP1 cells were treated *in vitro* for 48h with 100nM or 1000nM of the compounds versus DMSO and the d0 equivalent of the cells were transplanted. A significantly increased survival of mice transplanted with the treated cells was found. This assay, however, measured

efficacy of the compound *in vitro* and further experiments, applying the drug *in vivo* in THP1 engrafted mice are necessary to further confirm the activity of this treatment approach.

After promising effects of Calphostin C, Cercosporin and TAT-NLS-BLBD-6 were seen on cell lines in *in vitro* and *in vivo* assays, primary AML patient samples were tested. Here, primary samples were treated for 24h with 100nM of either of the compounds versus DMSO or 200µM of either of the peptides versus 1X DPBS and plated into CFCs or transplanted into sub-lethally irradiated NSG mice. The colony-forming potential of primary samples treated with the compounds was significantly reduced. Treatment with Calphostin C as well as Cercosporin also significantly reduced the engraftment of primary patient samples, suggesting that both compounds act at the level of AML LSCs. The treatment with TAT-NLS-BLBD-6 did not lead to significantly reduced colony-forming or engraftment potential of the primary samples. This indicates, that the peptide needs to be further improved, possibly stabilized, before its application would result in reduction of primary AML cell growth.

After obtaining the confirmation, that Calphostin C and Cercosporin effectively inhibit AML cell lines and primary AML samples, the effect on healthy cells was investigated. For the healthy counterpart, $CD34^+$ cells were enriched from cord blood using MACS. $CD34^+$ CB cells were treated with 100nM of either of the compounds versus DMSO as the primary samples. In addition, a higher concentration of 500nM was tested to analyze, whether there would be a higher tolerance of inhibitor treatment in healthy cells. Indeed, the colony-forming potential of $CD34^+$ CB cells was not reduced by Cercosporin with 100nM or 500nM concentration or 100nM Calphostin C. Only after 500nM Calphostin C treatment a significant decrease was found. Treated $CD34^+$ CB were also transplanted into sub-lethally irradiated NSG mice. Here, there was no effect on engraftment found after treatment with 100nM Cercosporin, but for 100nM Calphostin C.

This data demonstrates, that low-dose Cercosporin is able to target AML LSCs, but spares normal HSCs.

The reason why Cercosporin and Calphostin C have comparable activity on malignant samples but different activity on healthy HSCs cannot be explained so far. Both compounds are naturally occurring small molecule inhibitors, are light-

sensitive compounds, show activity as selective PKC inhibitors, effectively inhibit LEF1 binding to β-catenin and have comparable IC50 values after application to AML cell lines. Further investigation of the compounds to elaborate the exact mechanism of action and the effect on the different PKCs may lead to improvement of the chemical structure of the inhibitors and an improved ability to preferentially target AML LSCs.

5.2. The collaborative effect of Lef1 and AML1-ETO

The most common fusion gene in AML is *AML1-ETO*, arising from the t(8;21) translocation. On its own, *AML1-ETO* has not been shown to induce a disease so far, so there is a requirement for additional hits for leukemia induction [56]. One of the already identified collaborators in leukemia induction is the Flt3 length mutation (LM) [86]. Both *AML1-ETO* and *FLT3-LM* are amongst the most frequent genetic alterations in AML, on their own these are not able to induce diseases, only upon co-overexpression an acute leukemia was induced. Another collaborator of the t(8;21) fusion gene in AML induction is *MEIS2* [108]. *MEIS2* was found to be highly expressed in AML harboring the t(8;21) translocation. MEIS2 directly binds to AML-ETO and changes the target gene binding of the fusion protein, thereby inducing the disease.

It could be shown, that in *AML1-ETO* positive AML *LEF1* expression is usually highly expressed [30]. The finding, that many pathways link AML1-ETO activity to increased *LEF1* expression further strengthens the hypothesis, that expression of *LEF1* might contribute to t(8;21) AML (s. Figure 47).

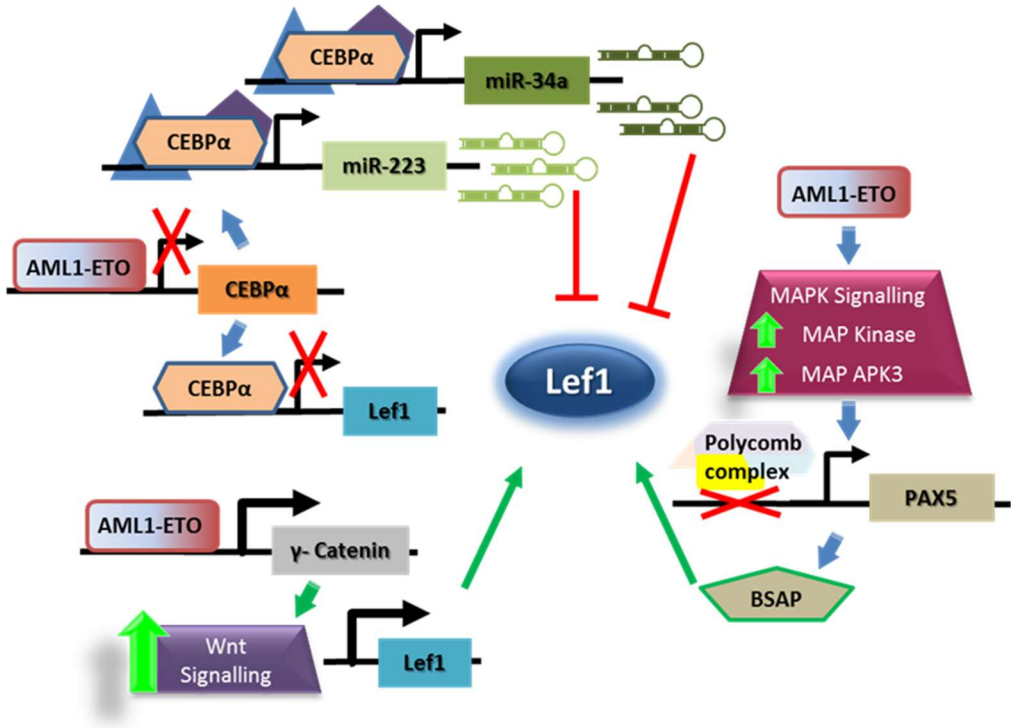

Figure 47: Model of regulation of LEF1 expression by the fusion gene AML1-ETO.

This upregulation occurs through epigenetic silencing of *CEBPα* [118], leading to decreased expression of two *LEF1*-downregulating micro RNAs miR223 and miR34a [83]. In addition, AML1-ETO enhances MAPK signaling [109] and γ-catenin expression [77]. Both factors lead to higher *LEF1* expression, in case of the MAPK pathway through elevated *PAX5* expression. In t(8;21) AMLs, *CEBPα* was found to be lower expressed than in most other AMLs. High *PAX5* expression also is typical for *AML1-ETO* positive AML [81]. Furthermore, AML1-ETO was shown to recruit the co-activator p300, which upregulates expression of the early growth response gene I (*EGR1*), leading higher expression of the *EGR1* downstream target *LEF1* [29].

The effect of *Lef1* on leukemia induction was already investigated and it was found, that aberrant *Lef1* expression leads to AML induction in the BMT model, but only in a small fraction of transplanted mice and with a long latency of around one year [80]. It seems that not only AML1-ETO but also Lef1 needs a collaborative partner to reliably induce AML.

AML1-ETO and *Lef1* were co-expressed in 5-FU stimulated murine bone marrow cells, the successfully transduced single and double positive cells were sorted and plated into CFCs. A collaborative effect of the *AML1-ETO* + *Lef1* co-expressing cells, leading to an increased clonogenic potential, could be found at the 2nd plating

compared to the *Lef1* transduced cells. Next, *AML1-ETO* and *Lef1* were co-expressed in 5-FU BM and the collaboration was analyzed in the BMT model. Indeed, a collaborative effect was found, leading to induction of AML in all transplanted mice with a median latency of 233 days. Cytospin analysis revealed an average blast count of approximately 25%, indicating the induction of acute leukemia. This finding was confirmed by Hemavet analysis of peripheral blood, bone marrow and spleen, revealing severely elevated white blood cell counts, low red blood cell counts and thrombocytopenia. The control mice transplanted with 5-FU BM expressing only AML1-ETO did not disease so far, but the WBC and RBC counts as well as spleen weights can be compared to other AML1-ETO control mice data available in our institute [108]. Here, the median peripheral RBC count was $4{,}50x10^9$/ml (±$2{,}97x10^9$/ml), median WBC was $14{,}50x10^6$/ml (±$6{,}39x10^6$/ml) and median spleen weight was 265mg (±66,85mg). Even though WBC counts and spleen weights were slightly elevated, no disease was induced in these mice. To exclude that these effects are due to the transduction process, an additional control was included and mice were transplanted with a vector only leading to expression of GFP in the transduced cells [108]. In this experiment, the median RBC count was found to be $5{,}20x10^9$/ml (±$0{,}42x10^9$/ml), the median WBC count was $7{,}00x10^6$/ml (±$2{,}49x10^6$/ml) and spleen weight was 135mg (±48,37mg). Taking these control mice into account, still the changes in RBC count, WBC count and spleen weight obtained from diseased *AML1-ETO* + *Lef1* mice are drastic and definitely due to the co-expression.

To further determine the kind of leukemia induced in this experiment, FACS analysis of diseased mice was performed by bone marrow staining for CD4, CD8, B220, Gr1, Mac1, cKit and Sca1. As part of a cooperation, a representative portion of diseased mice was sent for histopathological analysis to the group of Prof. Dr. Quintanilla-Martinez de Fend (Department of Pathology, University of Tübingen). Histologically, AML with or without maturation could be confirmed in all mice.

To further determine the changes induced by co-expression of *AML1-ETO* and *Lef1*, DNA of 3 diseased *AML1-ETO* + *Lef1* mice as well as of 3 *AML1-ETO* control mice was extracted and “Whole Exome Sequencing” was performed. This analysis is ongoing and will help to identify mutational changes in the leukemic mice compared to *AML1-ETO* engrafted mice.

Taken together, we could show for the first time that there is a collaborative effect of *Lef1* and *AML1-ETO* in induction of AML in the BMT. Further investigation of this model may give further insight in the mechanisms of t(8;21) AMLs and reveal new targets to effectively treat this disease.

6. Summary

In this thesis differential expression of LEF1 isoforms between healthy HSCs, progenitor and terminally differentiated cells compared to AML could be demonstrated. Based on this differential expression of the LEF1 isoforms, targeting LEF1-β-catenin binding both pharmacologically via two small-molecule inhibitors and molecularly using a synthetic peptide was performed, following the hypothesis that such an approach would preferentially target AML cells but spare normal HSCs.

The results gained after treatment with the small-molecule inhibitors Calphostin C and Cercosporin were promising. Here, already in the *in vitro* readout drastic effects were found consistently with all cell lines. Application of the compounds to primary AML samples significantly reduced their clonogenic potential and also the potential to engraft, indicating an effect on AML LSCs. The effects of both compounds were also tested on healthy HSCs. The clonogenic potential was not reduced by 100nM or 500nM Cercosporin or 100nM Calphostin C, only after application of 500nM Calphostin C there was a significant reduction. Engraftment of $CD34^+$ cord blood cells was not affected at all after treatment with 100nM Cercosporin, but after treatment with 100nM Calphostin C. To the end, these data demonstrate that it is in principle possible to preferentially target AML stem cells by using compounds which impair binding of the long LEF1 isoform to β-catenin.

Also the TAT-NLS-BLBD-6 showed some effect with regards to proliferation, colony-forming potential, apoptosis and cell cycle of the cell lines, but no effect on colony-forming potential and engraftment of primary AML samples compared to the TAT-NLS-BLBD-6m, probably due to its short half-life. The concept of using a synthetic peptide to target LEF1-β-catenin binding without any off-target effect is intriguing, but definitely needs further peptide optimization for efficient treatment.

Further studies have to define to which extent the anti-leukemogenic effect of the small-molecule inhibitors Calphostin C and Cercosporin are depending on their other multiple effects on PKCs.

Targeting of LEF1-β-catenin binding may also be interesting in the future for AMLs harboring the (8;21) translocation. Here, we could show for the first time via *in vitro* and *in vivo* assays, that there is a collaborative effect of *Lef1* and *AML1-ETO* in the

BMT model. We were able to induce reliably an AML with and without maturation in mice, which was confirmed by histopathological analysis. To understand the mechanism underlying this leukemogenic collaboration whole exome sequencing is ongoing from bulk bone marrow samples from diseased *AML1-ETO* + *Lef1* mice versus healthy *AML1-ETO* control mice.

7. Bibliography

1. Allsopp, R.C., et al., *Telomere shortening is associated with cell division in vitro and in vivo.* Exp Cell Res, 1995. **220**(1): p. 194-200.
2. American Cancer Society. Available from: https://www.cancer.org/cancer/acute-myeloid-leukemia/detection-diagnosis-staging/how-classified.html, accessed on 12.03.2019.
3. Angers, S. and R.T. Moon, *Proximal events in Wnt signal transduction.* Nat Rev Mol Cell Biol, 2009. **10**(7): p. 468-77.
4. Anjos-Afonso, F., et al., *CD34(-) cells at the apex of the human hematopoietic stem cell hierarchy have distinctive cellular and molecular signatures.* Cell Stem Cell, 2013. **13**(2): p. 161-74.
5. Aronson, B.D., et al., *Groucho-dependent and -independent repression activities of Runt domain proteins.* Mol Cell Biol, 1997. **17**(9): p. 5581-7.
6. Atcha, F.A., et al., *A unique DNA binding domain converts T-cell factors into strong Wnt effectors.* Mol Cell Biol, 2007. **27**(23): p. 8352-63.
7. Austin, G.E., et al., *Identification of an upstream enhancer containing an AML1 site in the human myeloperoxidase (MPO) gene.* Leuk Res, 1998. **22**(11): p. 1037-48.
8. Bagger, F.O., S. Kinalis, and N. Rapin, *BloodSpot: a database of healthy and malignant haematopoiesis updated with purified and single cell mRNA sequencing profiles.* Nucleic Acids Res, 2019. **47**(D1): p. D881-d885.
9. Baldin, V., et al., *Cyclin D1 is a nuclear protein required for cell cycle progression in G1.* Genes Dev, 1993. **7**(5): p. 812-21.
10. Banziger, C., et al., *Wntless, a conserved membrane protein dedicated to the secretion of Wnt proteins from signaling cells.* Cell, 2006. **125**(3): p. 509-22.
11. Bartscherer, K., et al., *Secretion of Wnt ligands requires Evi, a conserved transmembrane protein.* Cell, 2006. **125**(3): p. 523-33.
12. Behrens, J., et al., *Functional interaction of beta-catenin with the transcription factor LEF-1.* Nature, 1996. **382**(6592): p. 638-42.
13. Behrmann, L., J. Wellbrock, and W. Fiedler, *Acute Myeloid Leukemia and the Bone Marrow Niche-Take a Closer Look.* Front Oncol, 2018. **8**: p. 444.

14. Bennett, J.M., et al., *Proposals for the classification of the acute leukaemias. French-American-British (FAB) co-operative group.* Br J Haematol, 1976. **33**(4): p. 451-8.
15. Berga-Bolanos, R., et al., *Cell-autonomous requirement for TCF1 and LEF1 in the development of Natural Killer T cells.* Mol Immunol, 2015. **68**(2 Pt B): p. 484-9.
16. Black, J.D., *Protein kinase C-mediated regulation of the cell cycle.* Front Biosci, 2000. **5**: p. D406-23.
17. Bruhn, L., A. Munnerlyn, and R. Grosschedl, *ALY, a context-dependent coactivator of LEF-1 and AML-1, is required for TCRalpha enhancer function.* Genes Dev, 1997. **11**(5): p. 640-53.
18. Chen, J.D. and R.M. Evans, *A transcriptional co-repressor that interacts with nuclear hormone receptors.* Nature, 1995. **377**(6548): p. 454-7.
19. Davis, J.N., L. McGhee, and S. Meyers, *The ETO (MTG8) gene family.* Gene, 2003. **303**: p. 1-10.
20. Döhner, H., et al., *Diagnosis and management of acute myeloid leukemia in adults: recommendations from an international expert panel, on behalf of the European LeukemiaNet.* Blood, 2010. **115**(3): p. 453-74.
21. Edmaier, K.E., et al., *Expression of the lymphoid enhancer factor 1 is required for normal hematopoietic stem and progenitor cell function.* Leukemia, 2014. **28**(1): p. 227-30.
22. Elagib, K.E. and A.N. Goldfarb, *Oncogenic pathways of AML1-ETO in acute myeloid leukemia: multifaceted manipulation of marrow maturation.* Cancer Lett, 2007. **251**(2): p. 179-86.
23. Erdfelder, F., et al., *High lymphoid enhancer-binding factor-1 expression is associated with disease progression and poor prognosis in chronic lymphocytic leukemia.* Hematol Rep, 2010. **2**(1): p. e3.
24. Erickson, P., et al., *Identification of breakpoints in t(8;21) acute myelogenous leukemia and isolation of a fusion transcript, AML1/ETO, with similarity to Drosophila segmentation gene, runt.* Blood, 1992. **80**(7): p. 1825-31.
25. Erickson, P.F., et al., *ETO and AML1 phosphoproteins are expressed in CD34+ hematopoietic progenitors: implications for t(8;21) leukemogenesis and monitoring residual disease.* Blood, 1996. **88**(5): p. 1813-23.

26. Feder, K., et al., *Differences in expression and function of LEF1 isoforms in normal versus leukemic hematopoiesis.* Leukemia, 2019, accepted for publication on 06.08.2019.
27. Finn, T.E., et al., *Serum albumin prevents protein aggregation and amyloid formation and retains chaperone-like activity in the presence of physiological ligands.* J Biol Chem, 2012. **287**(25): p. 21530-40.
28. Frank, R., et al., *The AML1/ETO fusion protein blocks transactivation of the GM-CSF promoter by AML1B.* Oncogene, 1995. **11**(12): p. 2667-74.
29. Fu, L., et al., *AML1-ETO triggers epigenetic activation of early growth response gene l, inducing apoptosis in t(8;21) acute myeloid leukemia.* Febs j, 2014. **281**(4): p. 1123-31.
30. Fu, Y., et al., *Clinical significance of lymphoid enhancer-binding factor 1 expression in acute myeloid leukemia.* Leuk Lymphoma, 2014. **55**(2): p. 371-7.
31. Gandhirajan, R.K., et al., *Small molecule inhibitors of Wnt/beta-catenin/lef-1 signaling induces apoptosis in chronic lymphocytic leukemia cells in vitro and in vivo.* Neoplasia, 2010. **12**(4): p. 326-35.
32. Geering, B., et al., *Living and dying for inflammation: neutrophils, eosinophils, basophils.* Trends Immunol, 2013. **34**(8): p. 398-409.
33. Giese, K., et al., *Assembly and function of a TCR alpha enhancer complex is dependent on LEF-1-induced DNA bending and multiple protein-protein interactions.* Genes Dev, 1995. **9**(8): p. 995-1008.
34. Gokmen-Polar, Y., et al., *Elevated protein kinase C betaII is an early promotive event in colon carcinogenesis.* Cancer Res, 2001. **61**(4): p. 1375-81.
35. Golling, G., et al., *Drosophila homologs of the proto-oncogene product PEBP2/CBF beta regulate the DNA-binding properties of Runt.* Mol Cell Biol, 1996. **16**(3): p. 932-42.
36. Goodman, R.M., et al., *Sprinter: a novel transmembrane protein required for Wg secretion and signaling.* Development, 2006. **133**(24): p. 4901-11.
37. Gordon, M.D. and R. Nusse, *Wnt signaling: multiple pathways, multiple receptors, and multiple transcription factors.* J Biol Chem, 2006. **281**(32): p. 22429-33.

38. Green, J.L., S.G. Kuntz, and P.W. Sternberg, *Ror receptor tyrosine kinases: orphans no more.* Trends Cell Biol, 2008. **18**(11): p. 536-44.
39. Gutierrez, A., Jr., et al., *LEF-1 is a prosurvival factor in chronic lymphocytic leukemia and is expressed in the preleukemic state of monoclonal B-cell lymphocytosis.* Blood, 2010. **116**(16): p. 2975-83.
40. Hernandez-Maqueda, J.G., et al., *Protein kinase C delta negatively modulates canonical Wnt pathway and cell proliferation in colon tumor cell lines.* PLoS One, 2013. **8**(3): p. e58540.
41. Hizli, A.A., et al., *Protein kinase C alpha signaling inhibits cyclin D1 translation in intestinal epithelial cells.* J Biol Chem, 2006. **281**(21): p. 14596-603.
42. Hoeppner, L.H., et al., *Runx2 and bone morphogenic protein 2 regulate the expression of an alternative Lef1 transcript during osteoblast maturation.* J Cell Physiol, 2009. **221**(2): p. 480-9.
43. Hoeppner, L.H., et al., *Lef1DeltaN binds beta-catenin and increases osteoblast activity and trabecular bone mass.* J Biol Chem, 2011. **286**(13): p. 10950-9.
44. Hope, K.J., L. Jin, and J.E. Dick, *Acute myeloid leukemia originates from a hierarchy of leukemic stem cell classes that differ in self-renewal capacity.* Nat Immunol, 2004. **5**(7): p. 738-43.
45. Hovanes, K., et al., *Beta-catenin-sensitive isoforms of lymphoid enhancer factor-1 are selectively expressed in colon cancer.* Nat Genet, 2001. **28**(1): p. 53-7.
46. Hsieh, T.H., et al., *A novel cell-penetrating peptide suppresses breast tumorigenesis by inhibiting beta-catenin/LEF-1 signaling.* Sci Rep, 2016. **6**: p. 19156.
47. Imai, Y., et al., *TLE, the human homolog of groucho, interacts with AML1 and acts as a repressor of AML1-induced transactivation.* Biochem Biophys Res Commun, 1998. **252**(3): p. 582-9.
48. Jia, M., et al., *Overexpression of lymphoid enhancer-binding factor-1 (LEF1) is a novel favorable prognostic factor in childhood acute lymphoblastic leukemia.* Int J Lab Hematol, 2015. **37**(5): p. 631-40.
49. Kagoshima, H., et al., *The Runt domain identifies a new family of heteromeric transcriptional regulators.* Trends Genet, 1993. **9**(10): p. 338-41.

50. Kahler, R.A. and J.J. Westendorf, *Lymphoid enhancer factor-1 and beta-catenin inhibit Runx2-dependent transcriptional activation of the osteocalcin promoter.* J Biol Chem, 2003. **278**(14): p. 11937-44.
51. Karasawa, T., et al., *Frizzled-9 is activated by Wnt-2 and functions in Wnt/beta -catenin signaling.* J Biol Chem, 2002. **277**(40): p. 37479-86.
52. Kim, W.Y., et al., *Mutual activation of Ets-1 and AML1 DNA binding by direct interaction of their autoinhibitory domains.* Embo j, 1999. **18**(6): p. 1609-20.
53. Kogan, S.C., et al., *Bethesda proposals for classification of nonlymphoid hematopoietic neoplasms in mice.* Blood, 2002. **100**(1): p. 238-45.
54. Kompetenznetz Leukämie. Available from: https://www.kompetenznetz-leukaemie.de/content/patienten/leukaemien/aml/, accessed on 28.01.2019.
55. Krishnamurthy, N. and R. Kurzrock, *Targeting the Wnt/beta-catenin pathway in cancer: Update on effectors and inhibitors.* Cancer Treat Rev, 2018. **62**: p. 50-60.
56. Kuchenbauer, F., M. Feuring-Buske, and C. Buske, *AML1-ETO needs a partner: new insights into the pathogenesis of t(8;21) leukemia.* Cell Cycle, 2005. **4**(12): p. 1716-8.
57. Kuhl, M., et al., *The Wnt/Ca2+ pathway: a new vertebrate Wnt signaling pathway takes shape.* Trends Genet, 2000. **16**(7): p. 279-83.
58. Kuhn, V., et al., *Red Blood Cell Function and Dysfunction: Redox Regulation, Nitric Oxide Metabolism, Anemia.* Antioxid Redox Signal, 2017. **26**(13): p. 718-742.
59. Kuhnl, A., et al., *Overexpression of LEF1 predicts unfavorable outcome in adult patients with B-precursor acute lymphoblastic leukemia.* Blood, 2011. **118**(24): p. 6362-7.
60. Lareau, C., J. Ulirsch, and E. Bao. *The hematopoietic system, designed with R package gchromVAR*. Available from: https://caleblareau.github.io/gchromVAR/articles/gchromVAR_vignette.html, accessed on 10.03.2019.
61. Lepourcelet, M., et al., *Small-molecule antagonists of the oncogenic Tcf/beta-catenin protein complex.* Cancer Cell, 2004. **5**(1): p. 91-102.
62. Li, T.W., et al., *Wnt activation and alternative promoter repression of LEF1 in colon cancer.* Mol Cell Biol, 2006. **26**(14): p. 5284-99.

63. Licht, J.D., *AML1 and the AML1-ETO fusion protein in the pathogenesis of t(8;21) AML.* Oncogene, 2001. **20**(40): p. 5660-79.
64. Lu, J., et al., *Subcellular localization of the alpha and beta subunits of the acute myeloid leukemia-linked transcription factor PEBP2/CBF.* Mol Cell Biol, 1995. **15**(3): p. 1651-61.
65. Luna-Ulloa, L.B., et al., *Protein kinase C in Wnt signaling: implications in cancer initiation and progression.* IUBMB Life, 2011. **63**(10): p. 915-21.
66. Luna-Ulloa, L.B., et al., *Protein kinase C zeta is a positive modulator of canonical Wnt signaling pathway in tumoral colon cell lines.* Carcinogenesis, 2011. **32**(11): p. 1615-24.
67. MacDonald, B.T., K. Tamai, and X. He, *Wnt/beta-catenin signaling: components, mechanisms, and diseases.* Dev Cell, 2009. **17**(1): p. 9-26.
68. Mao, S., et al., *Functional and physical interactions between AML1 proteins and an ETS protein, MEF: implications for the pathogenesis of t(8;21)-positive leukemias.* Mol Cell Biol, 1999. **19**(5): p. 3635-44.
69. Metzeler, K.H., et al., *High expression of lymphoid enhancer-binding factor-1 (LEF1) is a novel favorable prognostic factor in cytogenetically normal acute myeloid leukemia.* Blood, 2012. **120**(10): p. 2118-26.
70. Meyers, S., J.R. Downing, and S.W. Hiebert, *Identification of AML-1 and the (8;21) translocation protein (AML-1/ETO) as sequence-specific DNA-binding proteins: the runt homology domain is required for DNA binding and protein-protein interactions.* Mol Cell Biol, 1993. **13**(10): p. 6336-45.
71. Meyers, S., N. Lenny, and S.W. Hiebert, *The t(8;21) fusion protein interferes with AML-1B-dependent transcriptional activation.* Mol Cell Biol, 1995. **15**(4): p. 1974-82.
72. Mikels, A.J. and R. Nusse, *Wnts as ligands: processing, secretion and reception.* Oncogene, 2006. **25**(57): p. 7461-8.
73. Miller, J.R. and R.T. Moon, *Analysis of the signaling activities of localization mutants of beta-catenin during axis specification in Xenopus.* J Cell Biol, 1997. **139**(1): p. 229-43.
74. Minke, K.S., et al., *Small molecule inhibitors of WNT signaling effectively induce apoptosis in acute myeloid leukemia cells.* Eur J Haematol, 2009. **82**(3): p. 165-75.

75. Morgan, R.G., et al., *LEF-1 drives aberrant beta-catenin nuclear localization in myeloid leukemia cells.* Haematologica, 2019.
76. Morrison, S.J., et al., *Identification of a lineage of multipotent hematopoietic progenitors.* Development, 1997. **124**(10): p. 1929-39.
77. Muller-Tidow, C., et al., *Translocation products in acute myeloid leukemia activate the Wnt signaling pathway in hematopoietic cells.* Mol Cell Biol, 2004. **24**(7): p. 2890-904.
78. Murray, N.R., et al., *Overexpression of protein kinase C betaII induces colonic hyperproliferation and increased sensitivity to colon carcinogenesis.* J Cell Biol, 1999. **145**(4): p. 699-711.
79. Ogawa, M., *Differentiation and proliferation of hematopoietic stem cells.* Blood, 1993. **81**(11): p. 2844-53.
80. Petropoulos, K., et al., *A novel role for Lef-1, a central transcription mediator of Wnt signaling, in leukemogenesis.* J Exp Med, 2008. **205**(3): p. 515-22.
81. Ray, D., et al., *Lineage-inappropriate PAX5 expression in t(8;21) acute myeloid leukemia requires signaling-mediated abrogation of polycomb repression.* Blood, 2013. **122**(5): p. 759-69.
82. Reya, T., et al., *Wnt signaling regulates B lymphocyte proliferation through a LEF-1 dependent mechanism.* Immunity, 2000. **13**(1): p. 15-24.
83. Rodriguez-Ubreva, J., et al., *C/EBPa-mediated activation of microRNAs 34a and 223 inhibits Lef1 expression to achieve efficient reprogramming into macrophages.* Mol Cell Biol, 2014. **34**(6): p. 1145-57.
84. Roman-Gomez, J., et al., *Epigenetic regulation of Wnt-signaling pathway in acute lymphoblastic leukemia.* Blood, 2007. **109**(8): p. 3462-9.
85. Sacchi, N., et al., *Detection and subcellular localization of an AML1 chimeric protein in the t(8;21) positive acute myeloid leukemia.* Oncogene, 1996. **12**(2): p. 437-44.
86. Schessl, C., et al., *The AML1-ETO fusion gene and the FLT3 length mutation collaborate in inducing acute leukemia in mice.* J Clin Invest, 2005. **115**(8): p. 2159-68.
87. Sengupta, A., et al., *Deregulation and cross talk among Sonic hedgehog, Wnt, Hox and Notch signaling in chronic myeloid leukemia progression.* Leukemia, 2007. **21**(5): p. 949-55.

88. Shi, J., et al., *Emerging Role and Therapeutic Implication of Wnt Signaling Pathways in Autoimmune Diseases.* J Immunol Res, 2016. **2016**: p. 9392132.
89. Shtutman, M., et al., *The cyclin D1 gene is a target of the beta-catenin/LEF-1 pathway.* Proc Natl Acad Sci U S A, 1999. **96**(10): p. 5522-7.
90. Skokowa, J., et al., *LEF-1 is crucial for neutrophil granulocytopoiesis and its expression is severely reduced in congenital neutropenia.* Nat Med, 2006. **12**(10): p. 1191-7.
91. Skokowa, J., et al., *Interactions among HCLS1, HAX1 and LEF-1 proteins are essential for G-CSF-triggered granulopoiesis.* Nat Med, 2012. **18**(10): p. 1550-9.
92. Stamos, J.L. and W.I. Weis, *The beta-catenin destruction complex.* Cold Spring Harb Perspect Biol, 2013. **5**(1): p. a007898.
93. Steinke, F.C., et al., *TCF-1 and LEF-1 act upstream of Th-POK to promote the CD4(+) T cell fate and interact with Runx3 to silence Cd4 in CD8(+) T cells.* Nat Immunol, 2014. **15**(7): p. 646-656.
94. Stone, R.M., R.A. Larson, and H. Dohner, *Midostaurin in FLT3-Mutated Acute Myeloid Leukemia.* N Engl J Med, 2017. **377**(19): p. 1903.
95. Stone, R.M., et al., *Midostaurin plus Chemotherapy for Acute Myeloid Leukemia with a FLT3 Mutation.* N Engl J Med, 2017. **377**(5): p. 454-464.
96. Takada, R., et al., *Monounsaturated fatty acid modification of Wnt protein: its role in Wnt secretion.* Dev Cell, 2006. **11**(6): p. 791-801.
97. Takahashi, A., et al., *Positive and negative regulation of granulocyte-macrophage colony-stimulating factor promoter activity by AML1-related transcription factor, PEBP2.* Blood, 1995. **86**(2): p. 607-16.
98. Tanaka, K., Y. Kitagawa, and T. Kadowaki, *Drosophila segment polarity gene product porcupine stimulates the posttranslational N-glycosylation of wingless in the endoplasmic reticulum.* J Biol Chem, 2002. **277**(15): p. 12816-23.
99. Tanaka, K., et al., *The AML1/ETO(MTG8) and AML1/Evi-1 leukemia-associated chimeric oncoproteins accumulate PEBP2beta(CBFbeta) in the nucleus more efficiently than wild-type AML1.* Blood, 1998. **91**(5): p. 1688-99.
100. Tanaka, T., et al., *The extracellular signal-regulated kinase pathway phosphorylates AML1, an acute myeloid leukemia gene product, and*

potentially regulates its transactivation ability. Mol Cell Biol, 1996. **16**(7): p. 3967-79.

101. Tandon, B., et al., *Nuclear overexpression of lymphoid-enhancer-binding factor 1 identifies chronic lymphocytic leukemia/small lymphocytic lymphoma in small B-cell lymphomas.* Mod Pathol, 2011. **24**(11): p. 1433-43.
102. The Jackson Laboratory. Available from: http://jackson.jax.org/rs/444-BUH-304/images/physiological_data_000664.pdf, accessed on 16.04.2019.
103. Toton, E., et al., *Protein kinase Cepsilon as a cancer marker and target for anticancer therapy.* Pharmacol Rep, 2011. **63**(1): p. 19-29.
104. Valencia, A., et al., *Wnt signaling pathway is epigenetically regulated by methylation of Wnt antagonists in acute myeloid leukemia.* Leukemia, 2009. **23**(9): p. 1658-66.
105. van de Wetering, M., et al., *Armadillo coactivates transcription driven by the product of the Drosophila segment polarity gene dTCF.* Cell, 1997. **88**(6): p. 789-99.
106. Vardiman, J.W., et al., *The 2008 revision of the World Health Organization (WHO) classification of myeloid neoplasms and acute leukemia: rationale and important changes.* Blood, 2009. **114**(5): p. 937-51.
107. Vaziri, H., et al., *Evidence for a mitotic clock in human hematopoietic stem cells: loss of telomeric DNA with age.* Proc Natl Acad Sci U S A, 1994. **91**(21): p. 9857-60.
108. Vegi, N.M., et al., *MEIS2 Is an Oncogenic Partner in AML1-ETO-Positive AML.* Cell Rep, 2016. **16**(2): p. 498-507.
109. Wajapeyee, N., et al., *Senescence induction in human fibroblasts and hematopoietic progenitors by leukemogenic fusion proteins.* Blood, 2010. **115**(24): p. 5057-60.
110. Wang, J., et al., *ETO, fusion partner in t(8;21) acute myeloid leukemia, represses transcription by interaction with the human N-CoR/mSin3/HDAC1 complex.* Proc Natl Acad Sci U S A, 1998. **95**(18): p. 10860-5.
111. Wang, S.H., et al., *The balance between two isoforms of LEF-1 regulates colon carcinoma growth.* BMC Gastroenterol, 2012. **12**: p. 53.
112. Wang, W., et al., *Alterations of lymphoid enhancer factor-1 isoform expression in solid tumors and acute leukemias.* Acta Biochim Biophys Sin (Shanghai), 2005. **37**(3): p. 173-80.

113. Willert, K., et al., *Wnt proteins are lipid-modified and can act as stem cell growth factors.* Nature, 2003. **423**(6938): p. 448-52.
114. Wu, W., et al., *High LEF1 expression predicts adverse prognosis in chronic lymphocytic leukemia and may be targeted by ethacrynic acid.* Oncotarget, 2016. **7**(16): p. 21631-43.
115. Yamaguchi, T.P., et al., *A Wnt5a pathway underlies outgrowth of multiple structures in the vertebrate embryo.* Development, 1999. **126**(6): p. 1211-23.
116. Zhan, T., N. Rindtorff, and M. Boutros, *Wnt signaling in cancer.* Oncogene, 2017. **36**(11): p. 1461-1473.
117. Zhang, Z., et al., *MicroRNA-26b represses colon cancer cell proliferation by inhibiting lymphoid enhancer factor 1 expression.* Mol Cancer Ther, 2014. **13**(7): p. 1942-51.
118. Zhuang, W.Y., et al., *Epigenetic silencing of Bcl-2, CEBPA and p14(ARF) by the AML1-ETO oncoprotein contributing to growth arrest and differentiation block in the U937 cell line.* Oncol Rep, 2013. **30**(1): p. 185-92.

Acknowledgement

I wish to express my sincere appreciation and gratitude to all of you who have contributed to the completion of this thesis. In particular, I would like to acknowledge:

Prof. Dr. Christian Buske, for giving me the opportunity to pursue my PhD in the Institute for Experimental Cancer Research. Thank you for your support and trust, and for being truly inspiring and motivating.

Dr. Nicole Kirsten, Linda Geisdorf and Julia Rappold for their support at any time, with any issue and for helpful discussion. We had a great time working together and this really pushed me forward.

All recent and former co-workers from the Institute for Experimental Cancer Research, for your assistance and advice during the daily lab work and for the great time together.

The members of IGradU, CEMMA training group and SFB1074 for support and fruitful discussions.

Prof. Dr. Lars Bullinger and Prof. Dr. Michael Fiegl for supporting me by being part of my TAC committee.

My parents, my sister and my friends, for having faith in me and my dreams and supporting me to be as ambitious as I wanted. Without you, I wouldn't stand near where I am now.

Per aspera ad astra.

Statutory declaration

I hereby declare that I prepared the present dissertation with the topic:

Dissecting the Role of Lymphoid Enhancer Factor 1 (LEF1) in Acute Myeloid Leukemia

independently and used no other references than those cited. In each individual case, I have clearly identified the source of the passages that are taken word for word or paraphrased.

I hereby declare that I have carried out my scientific work according to the principles of good scientific practice in accordance with the current „Satzung der Universität Ulm zur Sicherung guter wissenschaftlicher Praxis “[Rules of the University of Ulm for Assuring Good Scientific Practice].

Ulm, _____ _____

Date Signature